AN ABSTRACT OF THE DISSERTATION OF

Shumpei Maruyama for the degree of Doctor of Philosophy in Integrative Biology presented on June 9, 2022.

Title: The Role of Algal Cellular Physiology on the Onset and Maintenance of a Model Cnidarian-Algal Symbiosis.

Abstract approved: _____

Virginia M. Weis

Coral reefs form vast ecosystems in tropical oceans that are hotspots for biodiversity and are economically valuable. The ecological success of coral reefs is made possible by the symbiotic relationship between corals and dinoflagellate algae from the family Symbiodiniaceae. In this symbiosis, the algae are found within host gastrodermal cells in a membrane-bound organelle called the symbiosome. The success of this symbiosis relies upon an exchange of information between the algal symbiont and coral host. The partners must recognize each other, initiate symbiosis, and homeostatically maintain and regulate the partnership. In this dissertation, I used the sea anemone *Exaiptasia diaphana* (commonly called Aiptasia), a model system for the study of coral-algal symbiosis, and its symbiont, *Breviolum minutum*, and explored how algal cell physiology changes with and affects each step of cnidarian-algal symbiosis. In Chapter 2, I characterized how heat stress affects the *B. minutum* glycome, cell-surface ligands hypothesized to be involved in interpartner recognition. I found that heat-stress of the algal symbiont hindered the establishment of symbiosis and altered the algal glycome to become more like that of non-symbiotic species of Symbiodiniaceae. In Chapters 3 and 4, I described several limitations of using cultured algae to represent algae in the free-living state and studied how expelled algae from Aiptasia in the form of discrete pellets could be a more robust representation of the free-living state in Symbiodiniaceae. I found that algae from egesta are viable and competent symbionts, but are short-lived outside the host. In addition, I

determined that algae from egesta had a similar nutritional status to that of algae in the host by studying the expression of several nutrient-related algal genes. These results confirmed my hypothesis that including expelled algae in studies can strengthen the comparison between the symbiotic and free-living states of Symbiodiniaceae and provide new insights into the mechanisms governing cnidarian-algal symbiosis. Finally, in Chapter 5, I developed an aptamer Cell-SELEX (Selective Evolution of Ligands by EXponential enrichment) protocol to characterize symbiotic-state specific cell-surface molecules in *B. minutum*. Aptamer Cell-SELEX is a promising technology that can enable the discovery of molecules specific to cell phenotypes. In this work, although I could not identify symbiotic-state specific aptamers, I made substantial progress in protocol development and identified critical modifications to improve the chances of success in future attempts. In summary, findings from this work emphasize the role of algal cellular physiology in the success of the cnidarian-algal symbiosis and contribute to a greater understanding of the cellular underpinnings of the cnidarian-dinoflagellate mutualism.

The Role of Algal Cellular Physiology on the Onset and Maintenance of a Model Cnidarian-Algal Symbiosis

by
Shumpei Maruyama

A DISSERTATION

submitted to

Oregon State University

in partial fulfillment of
the requirements for the
degree of

Doctor of Philosophy

Presented June 9, 2022
Commencement June 2023

Doctor of Philosophy dissertation of Shumpei Maruyama presented on June 9, 2022

APPROVED:

Major Professor, representing Integrative Biology

Head of the Department of Integrative Biology

Dean of the Graduate School

I understand that my dissertation will become part of the permanent collection of Oregon State University libraries. My signature below authorizes release of my dissertation to any reader upon request.

Shumpei Maruyama, Author

ACKNOWLEDGEMENTS

I thank eminent and distinguished professor, Virginia Weis. Ever since I first met her, she was kind and welcoming. What I appreciate most about her is that she values the well being of her students and respects work-life balance. And of course, she is a brilliant scientist and I thank her for her amazing mentorship over the years. Most of all, thank you for making my PhD one of the most fun experiences of my life.

Thank you to my committee members, Nate Kirk, Allen Milligan, Jeff Anderson, and Andy Karplus. They have all provided me with great mentorship and have helped me improve my science. Thank you, Nate Kirk, for trusting me with the development and execution of multiple CUREs for your labs, it has been a great experience working with you.

I thank current and previous Weis lab members, John Parkinson, Jason Presnell (and honorary Weis member, Allie Graham), Trevor Tivey, Jack Koch, Valeri Sawiccy, Erick White, Jun Chua, Keyla Plichon, and Sam Bedgood. Thank you to John Parkinson, whom I consider my shadow advisor. During the first few years of my PhD, I would bother him with all the questions I was too afraid to ask Virginia, and I consider him a critical figure for my growth as a scientist. I thank Jason Presnell, for the mentorship he has provided in my middle years of my PhD and for being a fantastic dungeon master. I thank Allie Graham for her friendship, and mentorship. I thank Trevor Tivey for making me feel welcome in the lab, for answering all my questions, and for his friendshipI thank Jack Koch for being a bright figure in the lab, pushing all of us to excellence, also for answering all my questions and for his friendship. I thank Valeri Sawiccy for being an amazing office mate, a true friend and confidant. I will miss our gossiping. I thank Erick White for being a great friend and mahjong player. I thank Jun Chua for his friendship, taking care of Ami, and for a great hotpot experience. I thank Keyla for her friendship and excellent crepes. And I thank Sam Bedgood for his friendship and optimistic attitude.

I thank my colleague and friends, Silke Bachhuber, Heather Fulton-Bennett, Dan Schneck, and Andrea Burton. Thanks for all the game nights, floats, laughs, and dinners together as we made our way through graduate school. I also thank the rest of the

graduate student IB department, past and present, for their comradery and for making the department a better place. Especially thank you to the CGE and all those who fight for fairness in graduate education.

Thank you to instructors Devon Quick and Lindsay Biga, you have made teaching a joy over the many years.

I thank my dear friends Gaku Kelliher, Zoey Towner, and Eli Schwartz for being great friends despite our distance. You've been great anchors that I can depend on for companionship throughout my PhD. And thank you to Umi Hoshijima for being an inspirational scientist and dear friend. Drift in peace.

Thank you to the teachers I've had over the many years. Thank you, Lee Decker, for your mentorship during my formative years. I learned more about marine science from my time with you than any other point in my life. Thank you, Mr. Decker! I thank Ian Tibbetts and John Hall for their mentorship during my time in Australia. They taught me the joys of research and science and solidified my passion for it. Thank you to my karate teachers, Shihan Alfonso Gomez Sr, Sensei Alfonso Gomez Jr, Sensei Ophira Bergman, and Kyoshi Tomohiro Arashiro. You have all formed me into the person that I am now, and I thank you for that.

Thank you to my dad for his financial support and for the phone calls we had when my PCR kept failing. It's nice to have a family member I can talk shop with, even if his advice didn't end up working most of the time.

Thank you to my partners, former and current, Morgan Chapleau-Stein, Emily Carlson, and Kyra Duffy (and son, Stephen Colbert). You've all kept me sane and have filled my life with joy and laughter through the years.

Thank you to my love, Ami. You are the best dog. Thank you taking me on daily walks and humping my leg every evening.

And thank you for reading my dissertation!

CONTRIBUTION OF AUTHORS

Chapter 2: Paige E. Mandelare-Ruiz, Mark McCauley, Wenjing Peng, Byeong Gwan Cho, and Junyao Wang helped with experiments. Wenjing Peng, Yehia Mechref, Sandra Loesgen, and Virginia M. Weis designed experiments and provided significant contributions to chapter revisions. Mark McCauley also provided significant contributions to chapter revisions.

Chapter 3: Virginia M. Weis helped with conceptualization and provided significant contribution to chapter revisions.

Chapter 4: Virginia M. Weis helped with conceptualization and provided significant contribution to chapter revisions. Valeri Sawiccy, Julia Unsworth, and Students of Oregon State University's Z362 Spring 2021 helped with experiments.

Chapter 5: Virginia M. Weis helped with methodology and provided significant contribution to chapter revisions.

TABLE OF CONTENTS

TABLE OF CONTENTS (Continued)

Page

TABLE OF CONTENTS (Continued)

Page

LIST OF FIGURES

LIST OF TABLES

LIST OF APPENDIX FIGURES

LIST OF APPENDIX TABLES

The Role of Algal Cellular Physiology on the Onset and Maintenance of a Model Cnidarian-Algal Symbiosis

1. Introduction

Mutualistic symbioses are formally defined as the close living together of two or more species. From fungal-algal associations in lichens so abundant in the Pacific Northwest, to deep-sea giant tube worms harboring chemosynthetic bacteria, mutualistic symbioses are key players to the success of many ecosystems. In tropical oceans, a prominent mutualism is that of the intimate, intracellular symbiosis between cnidarians and their single-celled dinoflagellate partners from the family Symbiodiniaceae (Figure 1.1). The cnidarian-algal symbiosis is the cornerstone to the success of tropical coral reef ecosystems. Corals form massive three-dimensional structures, providing critical ecological goods and services for an immense diversity of organisms (Roberts et al. 2002). In this partnership, the dinoflagellate symbiont resides within the host cnidarian cell, where the algae photosynthesize and translocate sugars to the host. In exchange, the symbiont is provided protection from the environment, a modulated light environment, and access to host waste-products (Davy et al. 2012). The holobiont (the host and all its microbial symbionts) also includes beneficial and commensal bacteria, fungi, viruses and other protists (Hernandez-Agreda et al. 2017).

The breakdown of symbiosis, known as dysbiosis, leads to the loss of algae from the cnidarian host. The coral left without its photosynthetic partner, will eventually starve to death if the association does not recover. Coral bleaching, as this dysbiosis is aptly named, happens easily through a variety of anthropogenic stressors, but is primarily induced by heat stress from global climate change (Hughes et al. 2018). These global bleaching events are increasing in frequency and the widespread loss of coral reefs is predicted if climate change is not mitigated (van Oppen and Lough 2018). Despite the massive loss of coral reefs, the threat of extinction of some coral species, and the decline of a key marine biome on which the lives of 500 million people rely (Hoegh-Guldberg et al. 2017), the cellular and molecular mechanisms involved in cnidarian-algal symbiosis maintenance and in dysbiosis are not well understood.

1.1 Onset of symbiosis

The primary acquisition of symbionts occurs either vertically or horizontally. In vertical transmission, the parent cnidarian host inoculates its offspring directly with symbionts during gametogenesis or during brooding of larvae. Most corals (approximately 85% of species) are horizontal transmitters, where the recruits must acquire their symbionts from the surrounding environment (Fadlallah 1983). It is unclear where environmental Symbiodiniaceae originate, but evidence suggests that symbiotic species are transient in the environment and are actively released from their hosts (Thornhill et al. 2017, Fujise et al. 2021). Therefore, while horizontal transmitters are not provided symbionts directly by their parents, they may indirectly acquire symbionts from nearby adult hosts (Ali et al. 2019).

Key events in the onset of symbiosis have been described (Davy et al. 2012). First, the host and symbiont must initiate contact. There are several putative mechanisms for horizontal transmitters that allow the symbiont to find the host or *vice versa* (Schwarz et al. 2002, Pasternak et al. 2004, Takeuchi et al. 2017). Second, the host and symbiont must recognize each other once contact is initiated, in which host pattern recognition receptors (PRRs) detect symbiont microbe associated molecular patterns (MAMPs) (Rosset et al. 2021).

Host PRRs, putatively present on nutritive phagocytes lining the gastric cavity, are part of the highly conserved innate immune system, shared across the Metazoa. As such, it is useful to ask questions about symbiosis based on our understanding of innate immunity and host-microbe interactions in higher animals. Cnidarian host PRRs include Toll-like receptors (Williams et al. 2018), glycan-binding lectins (Wood-Charlson et al. 2006, Kvennefors et al. 2008, Kuniya et al. 2015), and scavenger receptors (Neubauer et al. 2016). Comparatively, we have a very limited understanding of Symbiodiniaceae MAMPs that are detected by the host. After the symbiont is successfully recognized, the host cell phagocytizes the symbiont where further events occur to regulate and maintain the symbiosis.

1.2 Maintenance of symbiosis

Once inside of the host cell, the symbiont must avoid host-destruction (Davy et al. 2012). Evidence suggests that the symbiont prevents phagosomal maturation, thereby preventing lysosomal digestion (Hohman et al. 1982, Chen et al. 2003, 2005, Hong et al. 2009). There is also ample evidence that the symbiont modulates host immunity, suppressing apoptosis, autophagy, and vomocytic (non-lytic) expulsion (Kitchen et al. 2017, Mansfield et al. 2017, Matthews et al. 2017, Merselis et al. 2018, Jacobovitz et al. 2021). A recent study compared transcriptomes of the model system sea anemone Aiptasia (*Exaiptasia pallida*) when colonized by two different symbiont species and found an elevated immune response when the host was invaded by the unnatural (non-homologous) species, while the natural (homologous) association had a modulated immune response (Matthews et al. 2017).

Within the host, *in hospite*, the algal symbiont resides within a host-derived membrane-bound organelle called the symbiosome (Davy et al. 2012). The symbiont also routinely sheds layers of plasma membrane underneath the symbiosome, creating a symbiosome membrane complex (Wakefield et al. 2000). Inside the symbiosome, host and symbiont ATPases are hypothesized to maintain an acidic environment, which has been measured down to ~pH 4 (Bertucci et al. 2010, Barott et al. 2015). The acidic environment is hypothesized to play a role in facilitating the translocation of sugars to the host and may act as a carbon concentrating mechanism by increasing inorganic carbon availability to the symbiont (Barott et al. 2015).

1.3 Symbiodiniaceae biology and diversity

Dinoflagellates in the family Symbiodiniaceae are unicellular, photosynthetic protists in the Kingdom Alveolata. Like most dinoflagellates, they are surrounded by a cell wall, harbor three-membrane chloroplasts (Durnford et al. 1999), use form II Rubisco derived from proteobacteria (Rowan et al. 1996), and have seemingly abandoned the use of histones in favor of virus-derived nucleoproteins to package genetic material (Irwin et al. 2018). The genome size of Symbiodiniaceae, while smaller than that of other dinoflagellates, is still immense at 1-5 Gb (Aranda et al. 2016). Due to their unusual cellular, molecular and genomic properties, conventional toolkits such as gene-editing

tools are not available and their study is difficult (Leggat et al. 2011, Meyer and Weis 2012).

Symbiodiniaceae are an evolutionarily diverse taxon comprised of symbiotic and free-living members, with ten formally described genera (LaJeunesse et al. 2018, Nitschke et al. 2020, Pochon and LaJeunesse 2021). Members of the genera *Symbiodinium*, *Breviolum*, *Cladocopium*, and *Durusdinium* are most commonly found in association with cnidarians and other metazoan hosts (Pochon and Gates 2010), and others are present in cnidarian hosts at background levels, form symbioses with other metazoans, or are entirely free-living (LaJeunesse et al. 2018, Nitschke et al. 2020, Pochon and LaJeunesse 2021). Some Symbiodiniaceae species, such as most *Cladocopium* spp., are suggested to be highly obligate symbionts inferred in part by the difficulty in rearing them in culture (Krueger and Gates 2012), while others are easily cultured and/or are thought to be entirely free-living (Thornhill et al. 2017, Fujise et al. 2021). Furthermore, there are physiological differences (such as thermal tolerance) between different symbiotic species and populations within a single species (Suggett et al. 2008, Hawkins et al. 2016, Levin et al. 2016, Chakravarti et al. 2017, Buerger et al. 2020).

1.4 The Aiptasia-Symbiodiniaceae model system

Our understanding of cnidarian-algal symbiosis has benefited from the use of model systems. These model systems include a hydrozoan *Hydra viridis*, the upside-down jellyfish (*Cassiopeia xamachana*), the aggregating sea anemone (*Anthopleura elegantissima*), a temperature coral (*Astrangia poculata*) and the sea anemone Aiptasia (*Exaiptasia diaphana*) (Neff 2020). Of these, Aiptasia is the best studied model for cnidarian-algal symbiosis. There are several advantages to the use of Aiptasia: anemones are more closely related to corals compared to some other model systems (Baumgarten et al. 2015), their symbionts are similar to those found in corals (Weis et al. 2008), numerous clonal lines have been produced (Weis et al. 2008), they can be chemically bleached (Matthews et al. 2016), kept aposymbiotic indefinitely, repopulated by algae from culture, induced to sexually reproduce in the laboratory (Grawunder et al. 2015), and can be housed in simple aquaria. Among the models, Aiptasia and its symbionts have

the largest number of molecular resources with numerous transcriptomes, a few proteomes, draft genomes, and metabolomes for both partners (Stochaj and Grossman 1997, Sunagawa et al. 2009, Meyer and Weis 2012, Shoguchi et al. 2013, Lehnert et al. 2014, Baumgarten et al. 2015, Pasaribu et al. 2015, Oakley et al. 2016, 2017, 2022, Matthews et al. 2017, Cziesielski et al. 2018, Cleves et al. 2020, Xiang et al. 2020).

Aiptasia is found in tropical and subtropical regions around the world (Thornhill et al. 2013). There are two recognized genetic networks, the global and Atlantic networks. Aiptasia in the global network is primarily symbiotic with *Breviolum minutum*, while Aiptasia in the Atlantic network harbors *Breviolum minutum* and *Symbiodinium linucheae* (Thornhill et al. 2013) and occasionally a cold-water-adapted species, *Breviolum psygmophilum* (Parkinson, pers comm). However, in laboratory settings, Aiptasia will accept many non-homologous species to varying degrees of success (Hambleton et al. 2014, Biquand et al. 2017, Matthews et al. 2017, Gabay et al. 2018, Herrera et al. 2021).

Many putative symbiosis-related genes and proteins have been identified using the Aiptasia model system (Detournay et al. 2012, Barott et al. 2015, Poole et al. 2016, Kitchen and Weis 2017, Mansfield et al. 2017, Neubaeur et al. 2017). Comparatively, we have a poor understanding of the role that algal cellular physiology plays in symbiosis with any cnidarian (Stochaj and Grossman 1997, Bertucci et al. 2010, Bay et al. 2011, Pasaribu et al. 2015, Parkinson et al. 2018). To address this gap in our understanding of cnidarian-algal symbiosis, I used the Aiptasia-Symbiodiniaceae model system to characterize the role of algal cellular physiology during the onset and maintenance of symbiosis. In Chapter 2, I first describe how heat stress of the algal partner affects the algal cell-surface glycome and simultaneously decreases colonization success of host Aiptasia. In Chapter 3, I discuss the limitations of using cultured algae to study cnidarian-algal symbiosis and follow-up this perspective in Chapter 4 by examining the physiology of expelled algae from Aiptasia egesta and explore its use as a study system in contrast to cultured algae. Finally, in Chapter 5 I describe a methodology to characterize novel symbiosis-specific proteins in the algal symbiont by using aptamer cell-SELEX that I developed.

1.5 References

Ali, A., Kriefall, N.G., Emery, L.E., Kenkel, C.D., Matz, M.V. & Davies, S.W. 2019. Recruit symbiosis establishment and Symbiodiniaceae composition influenced by adult corals and reef sediment. *Coral Reefs*. 38:405–15.

Aranda, M., Li, Y., Liew, Y.J., Baumgarten, S., Simakov, O., Wilson, M.C., Piel, J. et al. 2016. Genomes of coral dinoflagellate symbionts highlight evolutionary adaptations conducive to a symbiotic lifestyle. *Sci. Rep.* 6:1–15.

Barott, K.L., Venn, A.A., Perez, S.O., Tambutté, S. & Tresguerres, M. 2015. Coral host cells acidify symbiotic algal microenvironment to promote photosynthesis. *Proc. Natl. Acad. Sci. U. S. A.* 112:607–12.

Baumgarten, S., Simakov, O., Esherick, L.Y., Liew, Y.J., Lehnert, E.M., Michell, C.T., Li, Y. et al. 2015. The genome of *Aiptasia*, a sea anemone model for coral symbiosis. *Proc. Natl. Acad. Sci. U. S. A.* 112:11893–8.

Bay, L.K., Cumbo, V.R., Abrego, D., Kool, J.T., Ainsworth, T.D. & Willis, B.L. 2011. Infection dynamics vary between *Symbiodinium* types and cell surface treatments during establishment of endosymbiosis with coral larvae. *Diversity* . 3:356–74.

Bertucci, A., Tambutte, E., Tambutte, S., Allemand, D. & Zoccola, D. 2010. Symbiosis-dependent gene expression in coral-dinoflagellate association: cloning and characterization of a P-type H+-ATPase gene. *Proc. R. Soc. Lond. B Biol. Sci.* 277:87–95.

Biquand, E., Okubo, N., Aihara, Y., Rolland, V., Hayward, D.C., Hatta, M., Minagawa, J. et al. 2017. Acceptable symbiont cell size differs among cnidarian species and may limit symbiont diversity. *ISME J.* 11:1702–12.

Buerger, P., Alvarez-Roa, C., Coppin, C.W., Pearce, S.L., Chakravarti, L.J., Oakeshott, J.G., Edwards, O.R. et al. 2020. Heat-evolved microalgal symbionts increase coral bleaching tolerance. *Sci Adv*. 6:eaba2498.

Chakravarti, L.J., Beltran, V.H. & van Oppen, M.J.H. 2017. Rapid thermal adaptation in photosymbionts of reef-building corals. *Glob. Chang. Biol.* 23:4675–88.

Chen, C.-S., Lin, H.-P., Yeh, C.-C. & Fang, L.-S. 2005. Use of a fluorescent membrane probe to identify zooxanthellae in hospite among dissociated endoderm cell culture from coral. *Protoplasma*. 226:175–9.

Chen, M.-C., Cheng, Y.-M., Sung, P.-J., Kuo, C.-E. & Fang, L.-S. 2003. Molecular identification of Rab7 (ApRab7) in *Aiptasia pulchella* and its exclusion from phagosomes harboring zooxanthellae. *Biochem. Biophys. Res. Commun.* 308:586–95.

Cleves, P.A., Krediet, C.J., Lehnert, E.M., Onishi, M. & Pringle, J.R. 2020. Insights into coral bleaching under heat stress from analysis of gene expression in a sea anemone model system. *Proc. Natl. Acad. Sci. U. S. A.* 117:28906–17.

Cziesielski, M.J., Liew, Y.J., Cui, G., Schmidt-roach, S., Campana, S., Marondedze, C. & Aranda, M. 2018. Multi-omics analysis of thermal stress response in a zooxanthellate cnidarian reveals the importance of associating with thermotolerant symbionts. *Proceedings of Royal Society B*. 285:20172654.

Davy, S.K., Allemand, D. & Weis, V.M. 2012. Cell biology of cnidarian-dinoflagellate symbiosis. *Microbiol. Mol. Biol. Rev.* 76:229–61.

Detournay, O., Schnitzler, C.E., Poole, A. & Weis, V.M. 2012. Regulation of cnidarian-dinoflagellate mutualisms: evidence that activation of a host TGFβ innate immune pathway promotes tolerance of the symbiont. *Dev. Comp. Immunol.* 38:525–37.

Durnford, D.G., Deane, J.A., Tan, S., McFadden, G.I., Gantt, E. & Green, B.R. 1999. A phylogenetic assessment of the eukaryotic light-harvesting antenna proteins, with implications for plastid evolution. *J. Mol. Evol.* 48:59–68.

Fadlallah, Y.H. 1983. Sexual reproduction, development and larval biology in scleractinian corals. *Coral Reefs*. 2:129–50.

Fujise, L., Suggett, D.J., Stat, M., Kahlke, T., Bunce, M., Gardner, S.G., Goyen, S. et al. 2021. Unlocking the phylogenetic diversity, primary habitats, and abundances of free-living Symbiodiniaceae on a coral reef. *Mol. Ecol.* 30:343–60.

Gabay, Y., Weis, V.M. & Davy, S.K. 2018. Symbiont identity influences patterns of symbiosis establishment, host growth, and asexual reproduction in a model cnidarian-dinoflagellate symbiosis. *Biol. Bull.* 234:1–10.

Grawunder, D., Hambleton, E.A., Bucher, M., Wolfowicz, I., Bechtoldt, N. & Guse, A. 2015. Induction of gametogenesis in the cnidarian endosymbiosis model *Aiptasia* sp. *Sci. Rep.* 5:15677.

Hambleton, E.A., Guse, A. & Pringle, J.R. 2014. Similar specificities of symbiont uptake by adults and larvae in an anemone model system for coral biology. *J. Exp. Biol.* 217:1613–9.

Hawkins, T.D., Hagemeyer, J.C.G. & Warner, M.E. 2016. Temperature moderates the infectiousness of two conspecific *Symbiodinium* strains isolated from the same host population. *Environ. Microbiol.* 18:5204–17.

Hernandez-Agreda, A., Gates, R.D. & Ainsworth, T.D. 2017. Defining the core microbiome in corals' microbial soup. *Trends Microbiol.* 25:125–40.

Herrera, M., Klein, S.G., Campana, S., Chen, J.E., Prasanna, A., Duarte, C.M. & Aranda, M. 2021. Temperature transcends partner specificity in the symbiosis establishment of a cnidarian. *ISME J.* 15:141–53.

Hoegh-Guldberg, O., Poloczanska, E.S., Skirving, W. & Dove, S. 2017. Coral reef ecosystems under climate change and ocean acidification. *Frontiers in Marine Science*. 4:158.

Hohman, T.C., McNeil, P.L. & Muscatine, L. 1982. Phagosome-lysosome fusion inhibited by algal symbionts of *Hydra viridis*. *J. Cell Biol.* 94:56–63.

Hong, M.C., Huang, Y.S., Song, P.C., Lin, W.W., Fang, L.S. & Chen, M.C. 2009. Cloning and characterization of ApRab4, a recycling rab protein of *Aiptasia pulchella*, and its implication in the symbiosome biogenesis. *Mar. Biotechnol.* 11:771–85.

Hughes, T.P., Anderson, K.D., Connolly, S.R., Heron, S.F., Kerry, J.T., Lough, J.M., Baird, A.H. et al. 2018. Spatial and temporal patterns of mass bleaching of corals in the Anthropocene. *Science*. 359:80–3.

Irwin, N.A.T., Martin, B.J.E., Young, B.P., Browne, M.J.G., Flaus, A., Loewen, C.J.R., Keeling, P.J. et al. 2018. Viral proteins as a potential driver of histone depletion in dinoflagellates. *Nat. Commun.* 9:1535.

Jacobovitz, M.R., Rupp, S., Voss, P.A., Maegele, I., Gornik, S.G. & Guse, A. 2021. Dinoflagellate symbionts escape vomocytosis by host cell immune suppression. *Nat Microbiol*. 6:769–82.

Kitchen, S.A., Poole, A.Z. & Weis, V.M. 2017. Sphingolipid metabolism of a sea anemone is altered by the presence of dinoflagellate symbionts. *Biol. Bull.* 233.

Kitchen, S.A. & Weis, V.M. 2017. The sphingosine rheostat is involved in the cnidarian heat stress response but not necessarily in bleaching. *J. Exp. Biol.* 220:1709–20.

Krueger, T. & Gates, R.D. 2012. Cultivating endosymbionts - Host environmental mimics support the survival of *Symbiodinium* C15 ex hospite. *Journal of Experimental Marine Biology and Ecology*. 413:169–76.

Kuniya, N., Jimbo, M., Tanimoto, F., Yamashita, H., Koike, K., Harii, S., Nakano, Y. et al. 2015. Possible involvement of Tachylectin-2-like lectin from *Acropora tenuis* in the process of *Symbiodinium* acquisition. *Fish. Sci.* 81:473–83.

Kvennefors, E.C.E., Leggat, W., Hoegh-Guldberg, O., Degnan, B.M. & Barnes, A.C. 2008. An ancient and variable mannose-binding lectin from the coral *Acropora millepora* binds both pathogens and symbionts. *Dev. Comp. Immunol.* 32:1582–92.

LaJeunesse, T.C., Parkinson, J.E., Gabrielson, P.W., Jeong, H.J., Reimer, J.D., Voolstra, C.R. & Santos, S.R. 2018. Systematic revision of Symbiodiniaceae highlights the antiquity and diversity of coral endosymbionts. *Curr. Biol.* 28:2570-2580.e6.

Leggat, W., Yellowlees, D. & Medina, M. 2011. Recent progress in *Symbiodinium* transcriptomics. *J. Exp. Mar. Bio. Ecol.* 408:120–5.

Lehnert, E.M., Mouchka, M.E., Burriesci, M.S., Gallo, N.D., Schwarz, J.A. & Pringle, J.R. 2014. Extensive differences in gene expression between symbiotic and aposymbiotic cnidarians. 4:277–95.

Levin, R.A., Beltran, V.H., Hill, R., Kjelleberg, S., McDougald, D., Steinberg, P.D. & van Oppen, M.J.H. 2016. Sex, scavengers, and chaperones: Transcriptome secrets of divergent *Symbiodinium* thermal tolerances. *Mol. Biol. Evol.* 33:2201–15.

Mansfield, K.M., Carter, N.M., Nguyen, L., Cleves, P.A., Alshanbayeva, A., Williams, L.M., Crowder, C. et al. 2017. Transcription factor NF-κB is modulated by symbiotic status in a sea anemone model of cnidarian bleaching. *Sci. Rep.* 7:16025.

Matthews, J.L., Crowder, C.M., Oakley, C.A., Lutz, A., Roessner, U., Meyer, E., Grossman, A.R. et al. 2017. Optimal nutrient exchange and immune responses operate in partner specificity in the cnidarian-dinoflagellate symbiosis. *Proc. Natl. Acad. Sci. U.S.A.* 114:13194–9.

Matthews, J.L., Sproles, A.E., Oakley, C.A., Grossman, A.R., Weis, V.M. & Davy, S.K. 2016. Menthol-induced bleaching rapidly and effectively provides experimental aposymbiotic sea anemones (*Aiptasia* sp.) for symbiosis investigations. *J. Exp. Biol.* 219:306–10.

Merselis, D.G., Lirman, D. & Rodriguez-Lanetty, M. 2018. Symbiotic immuno-suppression: is disease susceptibility the price of bleaching resistance? *PeerJ.* 6:e4494.

Meyer, E. & Weis, V.M. 2012. Study of cnidarian-algal symbiosis in the "omics" age. *Biol. Bull.* 223:44–65.

Neff, E.P. 2020. The quest for an animal model of coral health and disease. *Lab Anim.* 49:37–41.

Neubaeur, E.-F., Poole, A.Z., Neubauer, P., Detournay, O., Tan, K., Davy, S.K. & Weis, V.M. 2017. A diverse host thrombospondin-type-1 repeat protein repertoire

promotes symbiont colonization during establishment of cnidarian-dinoflagellate symbiosis. *Elife*. 6:e24494.

Neubauer, E.F., Poole, A.Z., Weis, V.M. & Davy, S.K. 2016. The scavenger receptor repertoire in six cnidarian species and its putative role in cnidarian-dinoflagellate symbiosis. *PeerJ*. 4:e2692.

Nitschke, M.R., Craveiro, S.C., Brandão, C., Fidalgo, C., Serôdio, J., Calado, A.J. & Frommlet, J.C. 2020. Description of *Freudenthalidium* gen. nov. and *Halluxium* gen. nov. to formally recognize clades Fr3 and H as genera in the family Symbiodiniaceae (Dinophyceae). *J. Phycol.* 56:923–40.

Oakley, C.A., Ameismeier, M.F., Peng, L., Weis, V.M., Grossman, A.R. & Davy, S.K. 2016. Symbiosis induces widespread changes in the proteome of the model cnidarian Aiptasia. *Cell. Microbiol.* 18:1009–23.

Oakley, C.A., Durand, E., Wilkinson, S.P., Peng, L., Weis, V.M., Grossman, A.R. & Davy, S.K. 2017. Thermal shock induces host proteostasis disruption and endoplasmic reticulum stress in the model symbiotic cnidarian Aiptasia. *J. Proteome Res.* 16:2121–34.

Oakley, C.A., Pontasch, S., Fisher, P.L., Wilkinson, S.P., Keyzers, R.A., Krueger, T., Dove, S. et al. 2022. Thylakoid fatty acid composition and response to short-term cold and heat stress in high-latitude Symbiodiniaceae. *Coral Reefs*.

Parkinson, J.E., Tivey, T.R., Mandelare, P.E., Adpressa, D.A., Loesgen, S. & Weis, V.M. 2018. Subtle differences in symbiont cell surface glycan profiles do not explain species-specific colonization rates in a model cnidarian-algal symbiosis. *Front. Microbiol.* 9:1–12.

Pasaribu, B., Weng, L.-C., Lin, I.-P., Camargo, E., Tzen, J.T.C., Tsai, H., Ho, S.-L. et al. 2015. Morphological variability and distinct protein profiles of cultured and endosymbiotic *Symbiodinium* cells isolated from *Exaiptasia pulchella*. *Sci. Rep.* 5:15353.

Pasternak, Z., Bachar, A., Abelson, A. & Achituv, Y. 2004. Initiation of symbiosis between the soft coral *Heteroxenia fuscescens* and its zooxanthellae. *Mar. Ecol. Prog. Ser.* 279:113–6.

Pochon, X. & Gates, R.D. 2010. A new *Symbiodinium* clade (Dinophyceae) from soritid foraminifera in Hawai'i. *Mol. Phylogenet. Evol.* 56:492–7.

Pochon, X. & LaJeunesse, T.C. 2021. *Miliolidium* n. gen, a new Symbiodiniacean genus whose members associate with soritid foraminifera or are free-living. *J. Eukaryot. Microbiol.* e12856.

Poole, A.Z., Kitchen, S.A. & Weis, V.M. 2016. The role of complement in cnidarian-dinoflagellate symbiosis and immune challenge in the sea anemone *Aiptasia pallida*. *Front. Microbiol.* 7.

Roberts, C.M., McClean, C.J., Veron, J.E.N., Hawkins, J.P., Allen, G.R., McAllister, D.E., Mittermeier, C.G. et al. 2002. Marine biodiversity hotspots and conservation priorities for tropical reefs. *Science*. 295:1280–4.

Rosset, S.L., Oakley, C.A., Ferrier-Pagès, C., Suggett, D.J., Weis, V.M. & Davy, S.K. 2021. The molecular language of the cnidarian-dinoflagellate symbiosis. *Trends Microbiol.* 29:320–33.

Rowan, R., Whitney, S.M., Fowler, A. & Yellowlees, D. 1996. Rubisco in marine symbiotic dinoflagellates: form II enzymes in eukaryotic oxygenic phototrophs encoded by a nuclear multigene family. *Plant Cell*. 8:539–53.

Schwarz, J.A., Weis, V.M. & Potts, D.C. 2002. Feeding behavior and acquisition of zooxanthellae by planula larvae of the sea anemone *Anthopleura elegantissima*. *Mar. biol.* 140:471–8.

Shoguchi, E., Shinzato, C., Kawashima, T., Gyoja, F., Mungpakdee, S., Koyanagi, R., Takeuchi, T. et al. 2013. Draft assembly of the *Symbiodinium minutum* nuclear genome reveals dinoflagellate gene structure. *Curr. Biol.* 23:1399–408.

Stochaj, W.R. & Grossman, A.R. 1997. Differences in the protein profiles of cultured and endosymbiotic *Symbiodinium* sp. (Pyrrophyta) from the anemone *Aiptasia pallida* (Anthozoa). *J. Phycol.* 33:44–53.

Suggett, D.J., Warner, M.E., Smith, D.J., Davey, P., Hennige, S. & Baker, N.R. 2008. Photosynthesis and production of hydrogen peroxide by *Symbiodinium* (Pyrrhophyta) phylotypes with different thermal tolerances. *J. Phycol.* 44:948–56.

Sunagawa, S., Wilson, E.C., Thaler, M., Smith, M.L., Caruso, C., Pringle, J.R., Weis, V.M. et al. 2009. Generation and analysis of transcriptomic resources for a model system on the rise: The sea anemone *Aiptasia pallida* and its dinoflagellate endosymbiont. *BMC Genomics*. 10:1–10.

Takeuchi, R., Jimbo, M., Tanimoto, F., Tanaka, C., Harii, S., Nakano, Y., Yasumoto, K. et al. 2017. Establishment of a model for chemoattraction of *Symbiodinium* and characterization of chemotactic compounds in *Acropora tenuis*. *Fish. Sci.*

Thornhill, D.J., Howells, E.J., Wham, D.C., Steury, T.D. & Santos, S.R. 2017. Population genetics of reef coral endosymbionts (*Symbiodinium*, Dinophyceae). *Mol. Ecol.* 26:2640–59.

Thornhill, D.J., Xiang, Y., Pettay, D.T., Zhong, M. & Santos, S.R. 2013. Population genetic data of a model symbiotic cnidarian system reveal remarkable symbiotic specificity and vectored introductions across ocean basins. *Mol. Ecol.* 22:4499–515.

van Oppen, M.J.H. & Lough, J.M. (Eds.) 2018. Coral Bleaching: Patterns, Processes, Causes and Consequences. Springer, Cham.

Wakefield, T.S., Farmer, M.A. & Kempf, S.C. 2000. Revised description of the fine structure of *in situ* zooxanthellae genus *Symbiodinium*. *Biological Bulletin*. 199:76–84.

Weis, V.M., Davy, S.K., Hoegh-guldberg, O., Rodriguez-lanetty, M. & Pringle, J.R. 2008. Cell biology in model systems as the key to understanding corals. *Trends Ecol. Evol.* 23:369–76.

Williams, L.M., Fuess, L.E., Brennan, J.J., Mansfield, K.M., Salas-Rodriguez, E., Welsh, J., Awtry, J. et al. 2018. A conserved Toll-like receptor-to-NF-κB signaling pathway in the endangered coral *Orbicella faveolata*. *Dev. Comp. Immunol.* 79:128–36.

Wood-Charlson, E.M., Hollingsworth, L.L., Krupp, D.A. & Weis, V.M. 2006. Lectin/glycan interactions play a role in recognition in a coral/dinoflagellate symbiosis. *Cell. Microbiol.* 8:1985–93.

Xiang, T., Lehnert, E., Jinkerson, R.E., Clowez, S., Kim, R.G., DeNofrio, J.C., Pringle, J.R. et al. 2020. Symbiont population control by host-symbiont metabolic interaction in Symbiodiniaceae-cnidarian associations. *Nat. Commun.* 11:108.

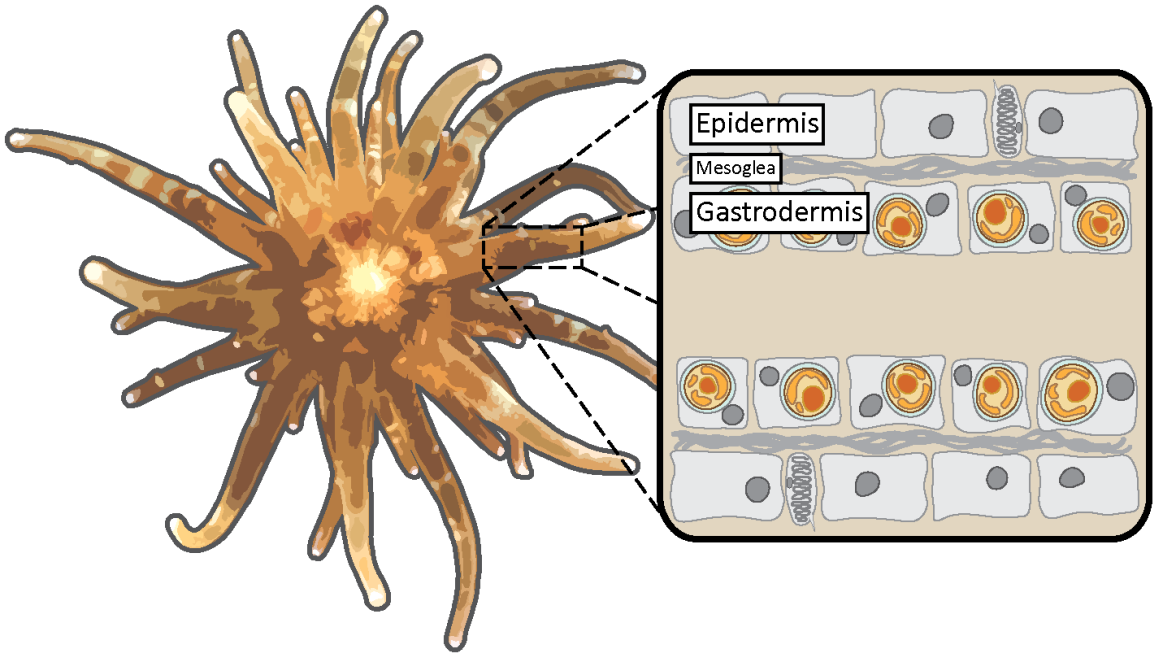

Figure 1.1 – The anatomy of cnidarian-algal symbiosis.
Pictured on the left is an individual Aiptasia. Inset: the tissue layers of Aiptasia and other symbiotic cnidarians. The brown, algal symbionts are housed intracellularly in host gastrodermal cells within a symbiosome membrane. The mesoglea is a thin protein matrix and the epidermis is free of symbionts and contain stinging cells.

2. Heat stress of algal partner hinders colonization success and alters the algal cell surface glycome in a cnidarian-algal symbiosis

Shumpei Maruyama
Paige E. Mandelare-Ruiz
Mark McCauley
Wenjing Peng
Byeong Gwan Cho
Junyao Wang
Yehia Mechref
Sandra Loesgen
Virginia M. Weis

Published in *Microbiology Spectrum*
American Society for Microbiology
1752 N St. NW
Washington, DC 20036, USA
https://doi.org/10.1128/spectrum.01567-22

2.1 Abstract

Corals owe their ecological success to their symbiotic relationship with dinoflagellate algae (Family Symbiodiniaceae). While the negative effects of heat stress on this symbiosis are well studied, how heat stress affects the onset of symbiosis and symbiont specificity is less explored. In this work, we used the model sea anemone, *Exaiptasia diaphana*, and its native symbiont, *Breviolum minutum,* to study the effects of heat stress on the colonization of Aiptasia by algae and the algal cell-surface glycome. Heat stress caused a decrease in the colonization of Aiptasia by algae that was not due to confounding variables such as algal motility or oxidative stress. With mass spectrometric analysis and lectin staining, a thermally induced enrichment of glycans previously found to be associated with free-living strains of algae (high-mannoside glycans) and a concomitant reduction in glycans putatively associated with symbiotic strains of algae (galactosylated glycans) were identified. Differential enrichment of specific sialic acid glycans was also identified, although their role in this symbiosis remains unclear. We also discuss the methods used to analyze the cell-surface glycome of algae, evaluate current limitations, and provide suggestions for future work in algal-coral glycobiology. Overall, this study provides insight into how stress may affect the symbiosis between cnidarians and their algal symbionts by altering the glycome of the symbiodinian partner.

2.2 Introduction

Coral reefs are amongst the most vulnerable ecosystems in the current climate crisis (van Oppen and Lough 2018). As average global temperatures continue to increase, corals are more frequently exposed to their thermal maxima and, as a result, increasingly expel their photosynthetic dinoflagellate partners (Family Symbiodiniaceae) in a process known as coral bleaching (Oakley and Davy 2018, van Oppen and Lough 2018). The loss of their algal symbiont population can leave corals vulnerable to decreased fitness, starvation, disease, and death (Oakley and Davy 2018, van Oppen and Lough 2018). Heat stress is the primary driver of coral bleaching, and lowering the emission of greenhouse gases is the best way to mitigate coral decline globally (Weis 2019). Nonetheless, a deeper understanding of the molecular mechanisms involved in coral-algal dysbiosis and interpartner signaling is critical in predicting the fate of corals and for the rapid development of solutions that could prolong the survival of coral reefs on a warming planet (Weis 2019).

While many studies have investigated the effects of heat stress on coral health and coral bleaching, we still lack a clear understanding of how heat stress affects the colonization of hosts by algae and interpartner specificity during the onset of symbiosis. In experiments using the model sea anemone, *Exaiptasia diaphana* (herein referred to as Aiptasia), heat stress can differentially affect the colonization capacity of symbiodiniaceans native to Aiptasia. Elevated temperatures decrease the colonization capacity of thermally sensitive *Breviolum minutum*, but not of thermally tolerant *B. psygmophilum* (Kishimoto et al. 2020). Heat stress can also cause Aiptasia to preferentially take up thermally tolerant native species of Symbiodiniaceae over sensitive ones (Herrera et al. 2021). Further investigation of how heat affects interpartner signaling mechanisms is critical to understanding how symbiont communities may change within hosts on a warming planet and to predicting the capacity of corals to resist thermal stress.

To date, the potential influence of heat stress on glycan-lectin interactions between algal symbionts and hosts remains unexplored. Glycans are diverse carbohydrates attached to other larger biomolecules such as proteins, lipids, and RNAs (Varki 2017, Flynn et al. 2021). There are O- and N-linked glycans in glycoproteins, with O-glycans attached to serine or threonine amino acid residues and N-linked glycans

attached to asparagine residues. Glycans have many biological roles, such as aiding in protein folding, cell adhesion, and changing protein function (for review, see Varki 2017). One important role of glyco-conjugates is their function as molecular markers on cell surfaces in host-microbe interactions (Varki 2017). Cell surface glycans from one partner are recognized by lectins from the other partner, allowing microbes to invade hosts, modulate immunity, or evade host detection altogether (Varki 2017). In cnidarian-algal symbiosis, molecular manipulation of Symbiodiniaceae glycans or host lectins alters colonization dynamics, suggesting that glycan-lectin interactions are critical for interpartner recognition during the onset of symbiosis (Lin et al. 2000, Wood-Charlson et al. 2006, Bay et al. 2011, Parkinson et al. 2018, Tivey et al. 2020, Tortorelli et al. 2021). Glycan lectin interactions may be involved in interpartner specificity, as different Symbiodiniaceae species maintain distinct surface glycomes (Logan et al. 2010, Parkinson et al. 2018, Tortorelli et al. 2021). In addition, glycan-lectin signaling may also play a role in maintaining symbiosis, as both lectins and glycans are present within the symbiosome even after initial colonization (Jimbo et al. 2000, Vidal-Dupiol et al. 2009, Markell and Wood-Charlson 2010). Furthermore, host lectin gene expression is influenced by heat stress, suggesting that lectins are associated with dysbiosis (Rodriguez-Lanetty et al. 2009, Vidal-Dupiol et al. 2009, Seneca et al. 2010, Bellantuono et al. 2012, Maor-Landaw et al. 2014, Zhou et al. 2017, 2018). Finally, heat stress has been found to alter the cell surface proteome in *B. psygmophilum*, which likely changes its cell surface glycome (Ricci et al. 2020).

Several specific glycan moieties have been characterized in the Symbiodiniaceae. High-mannoside glycans are the most abundant type of N-glycan in *B. minutum*, but increasing the abundance of high-mannoside glycans with inhibitors for glycan maturation pathways can decrease the colonization capacity of *B. minutum* (Tivey et al. 2020). Similarly, Tortorelli et al. (2021) found higher abundances of high-mannoside glycans as measured by lectin array in non-native species of algae, *Cladocopium goreaui* and *Fugacium kawagutii,* compared to *B. minutum*, suggesting that an overabundance of high-mannoside glycans can inhibit symbiosis. The second-most abundant group of N-glycans in *B. minutum* are galactosylated glycans (Tivey et al. 2020). These glycans are less abundant in non-native species of algae, *Symbiodinium pilosum, C. goreaui,* and *F.*

kawagutii, as measured by lectin array when compared to *B. minutum* (Parkinson et al. 2018, Tortorelli et al. 2021). This supports the hypothesis that galactosylation is a marker for a compatible symbiont in Aiptasia (Parkinson et al. 2018, Tortorelli et al. 2021). Sialylated glycans have also been detected in Symbiodiniaceae in several recent studies, but their role in symbiosis remains unclear, and their abundance is low (Parkinson et al. 2018, Tivey et al. 2020, Tortorelli et al. 2021). While sialylation has numerous biological roles in the deuterostomes, its presence in other eukaryotic lineages has only recently been acknowledged (Séveno et al. 2004, Zeleny et al. 2006, Ghosh 2020). Crucially, genes involved in sialylation have been found in Symbiodiniaceae and cnidarians, including scleractinian corals and Aiptasia, suggesting that sialylated glycans play a role in symbiotic interactions (Petit et al. 2018, Tivey et al. 2020).

In this study, we explored how heat stress affects the ability of *B. minutum* to colonize its native host Aiptasia and its effects on the cell-surface algal N-glycome. We hypothesized that heat stress would hinder the colonization capacity of *B. minutum*, even when controlling for light stress, algal motility, and cell proliferation. Furthermore, we hypothesized that heat stress would alter the algal glycome in such a way that native algae recognition was hindered.

2.3 Methods

Algal and anemone maintenance:

Cultures of *Breviolum minutum* (culture ID: Mf1.05b) were grown in silicate-free F/2 media at 25°C. ViparSpectra Timer 165W LED lights (Richmond, CA, USA) were set on a 12h:12h light:dark photoperiod with a light intensity of 55 µmol photons/m^2/sec. A second incubator for heat-stress treatments was set at 32°C with identical light conditions. Aposymbiotic Aiptasia (strain ID: H2) were initially generated by menthol bleaching and maintained in the dark at 25°C. Animals were fed three times a week *ad libitum* with freshly hatched *Artemia* nauplii. Before inoculation experiments, individual anemones were moved to 6-well plates in 7 mL of artificial filtered seawater (FSW) and starved for five days in the light. Prior to inoculation with symbionts, each anemone was viewed under fluorescence microscopy (Zeiss Axio Observer A1) to confirm the absence of symbiont chlorophyll auto-fluorescence.

Heat-stress treatments

For treatments, cultures of *B. minutum* were prepared in 100 mm diameter plastic Petri dishes (VWR; Radnor, PA, USA) at a density of 1 x 10^6 cells/mL in 25 mL of silicon-free F/2 media and sealed with parafilm. Each Petri dish was placed into respective incubators set at either 25°C or 32°C for different durations depending on their treatment: "Ambient" treatments were incubated at 25°C for seven days, "3-day heat" treatments were incubated at 25°C for four days then transferred to the 32°C incubator for three days, and "7-day heat" treatments were incubated at 32°C for seven days. Algae generated for glycan and lectin analyses were cultured in 3 mL volumes in 35 mm diameter Petri dishes (VWR) for three days, in identical conditions as previously described.

Assessing algal health

The dark-adapted maximum quantum yield of photosystem II (Fv/Fm) was measured using a custom-built Fast Repetition Rate fluorometer (FRRf) (Kolber et al. 1998). Briefly, algae were adapted to the dark for 30 min in either room temperature for ambient treatments or a 32°C water bath for heat treatments. Excitation was delivered at a wavelength of 475 nm in four distinct phases. During the first phase, a saturating sequence of flashlets, each lasting 0.7 μs with a gap of 1.5 μs for a total of 100 flashlets, were delivered. Then a relaxation phase of 80 flashlets beginning with a gap of 20 μs, increasing exponentially until the end of the sequence. The third phase was a sequence of 1 600 flashlets lasting 2 μs each and with a 40 μs gap. The final relaxation phase was identical to the second phase.

Cell viability was tested using Evans Blue dye (Morera and Villanueva 2009). A stock solution of 0.05 % w/v Evans Blue (Sigma-Aldrich; Burlington, MA, USA) dissolved in FSW was diluted in a 1:5 ratio of dye to algal cells. Cells were incubated in the dye for 5 min before quantifying cell viability with a hemocytometer. Cells that took up the blue dye were counted as dead.

Colonization assays

Aposymbiotic Aiptasia were randomly assigned to each algal heat treatment (Ambient, 3-day heat, 7-day heat). Algae from Petri dishes were centrifuged for 5 minutes at 800 x g, and the media was replaced with FSW to dilute the algae to a density of 5 x 10^5 cells/mL. To inoculate anemones, seawater was removed from anemone wells and replaced with the respective algal treatment. Animals were immediately fed 40 µL of brine shrimp extract after adding algae to induce a feeding response and facilitate the inoculation of algae. The algae were allowed to colonize the anemones for 24 hours at 25°C under 12h:12h light:dark conditions.

Twenty-four hours after initial inoculation, the algal suspension was removed, and the anemones were rinsed with 7 mL of FSW to remove any remaining algae. The animals were then transferred to a new 6-well plate with 7 mL FSW to further minimize the number of algal cells outside of the host, which could interfere with subsequent analysis of symbiont density within the host. The inoculated anemones remained in this alga-free seawater for an additional 24 hours before imaging.

Heat stress can have multiple effects on the physiology of *B. minutum* which could, in turn, affect its ability to colonize Aiptasia. These might include a heat-induced decrease in algal motility and increase in the generation of reactive oxygen species. To control for the potential effect of heat stress on algal motility, the colonization experiment was repeated with hourly resuspension of the algae by repeated mixing using a 1 mL micropipette during the light period of initial inoculation. To minimize both the generation of reactive oxygen species and algal motility, the colonization experiment was repeated with the initial inoculation taking place in the dark period of the light cycle, when algae are not motile (Fitt and Trench 1983, Yacobovitch et al. 2004, Yamashita and Koike 2016).

Quantification of symbiont density

Forty-eight hours after initial inoculation, the Aiptasia were imaged with fluorescence microscopy. Aiptasia were relaxed for at least 10 min with 0.18 M $MgCl_2$ dissolved in FSW prior to imaging. Images of three tentacles per anemone in several focal depths were taken in brightfield and under the red Filter Set 15 (Carl Zeiss) to visualize algal cell auto-fluorescence and form a z-stack image. Tentacles to be imaged

were selected based on their orientation to the horizontal plane. Each manually constructed z-stack was automatically merged into a single image using the *Auto-Blend Layers* function in Adobe Photoshop.

Symbiont density was quantified from the merged photographs using ImageJ. An area of interest within a tentacle was manually selected using the brightfield image, and its 2-dimensional area was quantified in mm^2. Then the same area of interest was superimposed onto the corresponding auto-fluorescence image, and the number of algal cells within the area was automatically counted based on contrast using the functions *Watershed* and *Analyze Particles*. The algal cell counts were normalized to the area of interest, and the symbiont densities of three replicate tentacles were averaged for each anemone. The protocol is publicly available with macros for Photoshop and ImageJ at https://www.protocols.io/view/symbiont-density-quantification-in-live-aiptasia-bx43pqyn.

In the first colonization experiment, each Aiptasia was imaged 2, 5, 8, 11, 14, and 21 days after inoculation. In the subsequent colonization experiments, with hourly resuspension of algae or inoculation in the dark, the Aiptasia were only imaged 2 days post-inoculation.

The average growth rate of symbiont density was calculated by plotting the natural log of symbiont density over time and determining the linear regression slope for each anemone over 21 days.

Flow cytometry and lectin staining

Lectins Cyanovirin-N (CVN, highly specific to α1-2-mannosides present in high-mannoside oligosaccharides) and Sambucus Nigra lectin (SNA-I, highly specific for α-2,6 sialic acid oligosaccharides attached to a terminal galactose, but also to α-2,3 linkages to a lesser degree) were coupled to phycoerythrin (PE) using the Lightning-Link R-PE Antibody Labeling Kit (Novus Biologicals #703-0010) following the manufacturer's protocol. Independent samples of ambient and 3-day heat-treated algae were washed with 3.3X PBS, and 2.5×10^5 cells were stained with 5 ug/mL of respective lectins in 200 µL total volume for two hours in the dark. Two staining replicates were prepared per biological replicate. After staining, algae were washed twice with 3.3X PBS and then

resuspended in 1 mL of 3.3X PBS. Samples were then run on a CytoFLEX flow cytometer and data analyzed using FlowJo software. Unstained ambient and heat treated algal cells were used to determine gating parameters for corresponding lectin-labeled samples (Supplementary Fig. A1). First, singlet algal cell populations were identified with forward scatter width and forward scatter area. Then, live algal cells were confirmed by positive chlorophyll autofluorescence signals using 488 nm excitation and detection in the PerCP channel (690/50 band pass). Median fluorescence intensities (MFI) of the PE signal were obtained from the live algal cell population by excitation at 561 nm and capture in channel PE (585/42 band pass). Unstained cells were used as blank controls, and the MFI of stained cells were subtracted by the MFI of unstained cells.

Glycan cleavage and mass spectrometry

Triplicate samples of *B. minutum* (4.8-6.3 million cells per sample) from independent ambient and 3-day heat temperature treatments were spun down at 3 100 x g, decanted, and pellets were frozen at -80°C until further prep. Samples were thawed, washed twice with 1 mL of 2 X PBS at 14 000 x g for 1 minute, washed twice with 1 mL of 1 X PBS at 14 000 x g for 1 minute, washed with 1 mL MiliQ water at 14 000 x g for 1 minute, and finally with 1 mL of 50 mM ammonium bicarbonate at 14 000 x g for 1 minute.

Cells were then treated with glycerol free PNGase F enzyme (New England Biolabs; Rowley, Massachusetts, USA) following manufacturer's protocols for non-denaturing reaction conditions to remove N-glycans from cell surfaces. The cells were incubated in 100 μL of Glycobuffer 2, 900 μL ultrapure water, and 3 μL PNGase F (glycerol free) at 37°C for 72 hours, inverting tubes occasionally. 10K MW cut-off SnakeSkin dialysis tubing (ThermoFisher; Waltham, MA, USA) was prepared by soaking in MiliQ water with constant stirring for 72 hours with water changes every 24 hours. After PNGase F incubation, each sample was placed into a pre-prepared dialysis tube and dialyzed in 100 mL ultrapure water at 4°C with constant stirring for 72 hours. Every 24 hours, the water was replaced with clean ultrapure water, and the removed water (containing glycans) was combined and lyophilized under high vacuum. The lyophilized dialysates were then dissolved in 5 mL ultrapure water and loaded onto a C18 SPE

cartridge to capture glycans. The column was then eluted with 5 mL 5% acetic acid in water to release glycans, and the sample was lyophilized again.

One milligram from each sample (starting material of N-glycomic analysis) was taken out and desalted by an activated charcoal spin column (Harvard Apparatus). Briefly, dried sample was dissolved in 85% acetonitrile (MeCN)/water with 0.1% trifluoroacetic acid (TFA). The spin column was washed with 200 µL 85% MeCN/water (with 0.1% TFA) three times, then conditioned with 200 µL 95% MeCN/water (with 0.1% TFA) three times. Sample was loaded on the column, centrifuged, and the pass through was reloaded twice. Then, the column was washed with 200 µL 95% MeCN/water (with 0.1% TFA) twice, followed by the elution with 200 µL 50% MeCN/water (with 0.1% TFA) twice. Desalted glycans were dried and subjected for reduction and permethylation as described previously (Dong et al. 2016, Peng et al. 2019, Gautam et al. 2020). Briefly, sample was dissolved in 10 µL borane-ammonia complex solution (10 mg/mL) and incubated in a 60^{o}C water bath for 1 hour. After incubation, 1 mL of methanol was added to the sample and dried out. The addition-drying of methanol was repeated three times to remove borates. Then, sodium hydroxyl beads (stored in DMSO) were packed to an empty spin column (Harvard Apparatus) and washed by 200 µL of DMSO twice by centrifuging at 1,800 rpm for 2 min. Reduced sample was dissolved in 30 µL DMSO, 1.2 µL water, 20 µL iodomethane, and loaded to the column. Then, the column was incubated at room temperature for 25 min. Next, an additional 15 µL iodomethane was added to the column and incubated for another 15 min. After incubation, permethylated glycan solution was collected by centrifuging at 1,800 rpm for 2 min. Then, the column was washed by 30 µL of MeCN, and the wash solution was combined with previous permethylated glycan solution. The combined solution was dried and ready for LC-MS/MS analysis.

The LC-MS/MS was performed using an Ultimate 3000 nano LC system (ThermoFisher Scientific) coupled to an LTQ Orbitrap Velos mass spectrometer (ThermoFisher Scientific). N-glycans derived from 200 µg starting material was injected and separated on a 50 cm C18 micro pillar array column (µPAC) with a µPAC trap at 55^{o}C (Cho et al. 2021). The flow rate was 0.3 µL/min. A gradient was used with mobile phase A (98% water, 2% MeCN, 0.1% formic acid) and mobile phase B (80% MeCN,

20% water, 0.1% formic acid) as follows: 0-4 min, 40%B; 4-64 min, 40% - 70%B; 64-69 min, 70% - 97.5%B; 69-89, 97.5%B; 89-94 min, 97.5% - 40%B; 94 - 114 min, 40%B. A positive mode was used for MS with a full MS of 60 000 resolution. The data dependent acquisition was used to select the top 8 most intense ions for CID MS^2. The normalized collision energy of CID was 35, the activation Q was 0.25, the activation time was 10 ms. The LC-MS/MS data was first processed by MultiGlycan software, then manually checked using Xcalibur software through full MS and MS^2 to remove any false positives. Supplementary Figure A2 shows two examples of annotation of high-mannose (Supplementary Figure A2A) and complex glycan structures (Supplementary Figure A2B), respectively. N-glycan compositions were determined by their masses detected in high-resolution full MS (insets). Then, their structures were further confirmed by matching MS2 fragments to the compositions. According to the general N-glycan biosynthesis pathway (Varki et al. 2016), N-glycans have a consistent core structure and are synthesized following strict rules in an interative manner. Therefore, their putative structures could be assigned via full MS and MS2.

The algal heat treatment experiment and glycan mass spectrometric analysis was repeated in 2020. After enzymatic cleavage with PNGase F, the dialysis steps and C18 chromatography were removed from the workflow, and the samples were directly processed for LCMS analysis with similar results (Supplementary Fig. A3).

Absolute abundance was normalized by Probabilistic Quotient Normalization (PQN) without prior total area normalization, as described by Benedetti et al. (2020). PQN is a robust method for normalizing mass spectrometric data and has explicitly proven useful for glycomics (Dieterle et al. 2006, Li et al. 2016, Benedetti et al. 2020). First, a reference spectrum is generated by calculating the median value of each glycan's absolute abundance from every sample. A vector of quotients is generated for each sample by dividing the absolute abundance of each glycan to the corresponding value in the reference spectrum. A dilution factor is then calculated for each sample by calculating the median of quotients of a given sample. The final PQN value is obtained by dividing the original abundance value by the dilution factor for each sample. P-values obtained from Student's t-test on individual glycan abundances were adjusted by False Discovery Rate (FDR) analysis.

Statistical analysis

All data were tested for normality and homoscedasticity to determine the use of parametric or non-parametric statistical tests.

2.4 Results

Heat-stress hinders colonization capacity of Breviolum minutum

Increasing the duration of heat stress reduced the colonization ability of *B. minutum* (Fig. 2.1A, 2.1B). The same pattern was observed with hourly resuspension of algae and when initial inoculations occurred in darkness (Supplementary Fig. A4). The maximum quantum yield of photosystem II concomitantly decreased with the increasing duration of heat stress (Fig. 2.1C). However, as measured by positive staining with Evans Blue dye, algal viability was not significantly affected by heat stress (Supplementary Fig. A5; Kruskal-Wallis test, $p = 0.10$).

Proliferation rates were not significantly different between ambient and 3-day heat-stressed algae (ANOVA, post-hoc Tukey HSD, $p = 0.574$). In comparison, proliferation rates in 7-day heat-stressed algae remained significantly lower than in algae from the 3-day heat treatment throughout the experiment (ANOVA, post-hoc Tukey HSD, $p = 0.02$), likely due to near-zero initial colonization densities (Fig. 2.1D).

The symbiont glycome changes with heat-stress as measured by mass spectrometric analyses and lectin staining

A total of 32 individual algal N-glycans were characterized from surface glycoproteins by mass spectrometry (Fig. 2.2A). Three glycans varied significantly in their PQN abundance between treatments (Fig. 2.2A). Two galactosylated glycan abundances, IDs 34100 and 35100 were significantly reduced in ambient treatments (Fig. 2.2B; Student's t-test FDR adjusted, $p = 0.039$, $p = 0.039$, respectively). Glycan IDs 34100, 35100 are both fucosylated, biantennary hybrid glycans, with a mannose terminal residue on one branch and a galactose terminal residue on the other. Two sialylated glycans, IDs 64101 and 65101, were only identified in heat treatments and were absent from ambient conditions, but only 64101 was significantly enriched (Fig. 2.2C; Student's

t-test FDR adjusted, $p = 0.015$, $p = 0.12$, respectively). Glycan IDs 64101 and 65101 are tetraantennary glycans with one terminal N-glycolylneuraminic acid (Neu5Gc) and 65101 with an additional terminal galactose residue.

The N-glycan composition of *B. minutum* was largely high-mannose type, contributing an average of 81.3 % and 77.8% of all glycans in ambient and heat treatments, respectively (Fig. 2.3A). The second largest group were galactosylated glycans, with an average of 15.7% and 18.0% in ambient and heat treatments, respectively (Fig. 2.2A). A small percentage of glycans were sialylated, with an average of 2.3% and 3.0% in ambient and heat stress treatments, respectively (Fig. 2.3A). A single oligosaccharide featuring a N-acetylglucosamine terminus with an average of 0.7% and 0.8% was identified in ambient and heat treatments, respectively (Fig. 2.3A). The smallest group were fucosylated glycans (either sialylated or galactosylated), with 0.03% and 0.3% present in ambient and heat treatments, respectively (Fig. 2.3A).

Lectin staining as measured by flow cytometry revealed that both CVN lectin (high-mannoside specific) and SNA-I lectin (sialic acid specific) had higher binding in heat-stressed compared to control algae (Fig. 2.3B, Supplementary Fig. A6; Student's t-test, $p = 0.0014$ and $p = 0.002$, respectively), suggesting that both high-mannose and sialic acid glycans were enriched with heat-stress. However, mass spectrometry analysis found that high-mannoside and sialylated N-glycan abundances were lower in heat stressed algae compared to control algae, although differences were not statistically significant (Fig. 2.3C; Student's t-test, $p = 0.18$ and $p = 0.63$, respectively).

2.5 Discussion

Heat-induced changes in algal physiology affect the colonization capacity of algae

We found that heat stress hindered the ability of *Breviolum minutum* to colonize adult Aiptasia (Fig. 2.1). This corroborates a similar recent study by Kishimoto et al. (2020). However, it remains to be determined how heat stress reduces colonization ability (Kishimoto et al. 2020). Heat stress has been shown to have multiple physiological effects on symbiont physiology, such as decreasing cell viability, division rates, motility, and increasing light-induced generation of reactive oxygen species, all of which influence colonization ability (Lesser 1996, Tchernov et al. 2004, Nitschke et al. 2015, Fujise et al.

2018). The several experiments in this study that were conducted to address each of these confounding variables found that none of these factors alone could explain the observed decline in the colonization of Aiptasia by algae with heat stress.

Overall symbiont density was an order of magnitude higher in each resuspension treatment when compared to those without resuspensions (Fig. 2.1B, Supplementary Fig. A4A). These data suggest that motility and symbiont availability in the water column significantly affects colonization dynamics. This information can inform the design of future colonization experiments. This is particularly important for experiments when algal glycans are masked by exogenous lectins, as the addition of certain lectins can halt algal motility (Koike et al. 2004, Jimbo et al. 2010). In our study, neither equalizing symbiont availability with resuspensions, or conducting inoculations during the dark period of the light cycle when algae are not motile (Fitt and Trench 1983, Yacobovitch et al. 2004, Yamashita and Koike 2016), were successful in recovering colonization ability in heat-stressed algae. Therefore, other factors are likely to be contributing to the observed decrease in the colonization of hosts by algae exposed to elevated temperatures.

Detection method has a significant effect on glycan abundances

While lectin staining revealed increased high-mannoside and sialylated glycan abundance with heat-stress, the mass spectrometric analysis showed an opposing pattern, although differences were not statistically significant (Fig. 2.3C). The different scopes of detection could explain this discrepancy. The mass spectrometric analysis focused on N-linked glycoproteins, which can be released by PNGase F treatment. The lectin staining approach of intact algal cells is potentially able to detect other glycosylated surface moieties, such as O-linked glycans and glycolipids, in addition to N-glycans (Varki 2017). Furthermore, PNGase F activity has been shown in plants to be inhibited by α1-3 fucose residues, leading to the incomplete release of N-glycans (Wang et al. 2014). Even with this potential drawback, PNGase F is a reliable endoglycosidase that cleanly cleaves N-linked glycans from glycoproteins, leaving the deaminated protein and frees carbohydrates for mass spectrometric analysis (Morelle et al. 2009).

The heating experiment was repeated a second time with a smaller sample size, and we cleaved and purified the surface glycans in a simplified PNGase F-based protocol.

Using this approach, high-mannoside and sialylated N-glycan abundance increased with heat-stress, although not significantly (Supplementary Fig. A3). In this second analysis, we removed the dialysis and C18 column chromatography purification steps after PNGase F digestion and used the glycan solution directly for permethylation, prior to mass spectrometric analysis. The fewer cleaning steps increased the amount of glycans per sample by an order of magnitude. Molecular analysis of algal surface glycans is still in its infancy. Further refinement of protocols will enable the assessment of the entire surface glycome of symbiotic Symbiodiniaceae.

Below, we compare overall glycan abundance between control and heat-stress algae as measured by lectin staining, and for specific glycan moieties, we discuss differences found in the mass spectrometric data between the two treatment types.

High-mannoside glycan overabundance may hinder symbiosis

Previous work has suggested that high-mannoside glycans are important for host-symbiont recognition. Work by Tivey et al. (2020) found that colonization capacity of *B. minutum* declined with increased high-mannoside N-glycan abundance in the Aiptasia symbiosis as measured by CVN lectin staining. In addition, work by Tortotelli et al. (2021) found that high-mannoside glycans were consistently more abundant in non-native algal species, *Cladocopium goreaui* and *Fugacium kawagutii*, compared to *B. minutum* as measured by lectin array. This study reveals that heat-induced decrease in colonization capacity of *B. minutum* correlates with an increase in high-mannoside glycans, as measured by CVN lectin staining. The combined evidence suggests that the overabundance of high-mannoside glycans hinders colonization in the *B. minutum* – Aiptasia symbiosis. One possible explanation is that the host is mistaking the symbiont for a bacterial pathogen, as two coral lectins, Millectin from *Acropora millepora* and PdC lectin from *Pocillopora damicornis* are both mannose-specific lectins and have been found to recognize both pathogens and symbionts.

Recently, Tortorelli et al. (2021) found that masking host lectins with D-mannose reduced colonization rates of hosts by *B. minutum*. This could highlight the importance of a certain abundance of high-mannose residues, too high or too low, and colonization rates may decrease. An alternative hypothesis is that adding mannose to host lectins increased

the high-mannose lectin signal in hosts, which in turn induces an immune response, leading to the rejection of symbionts. Whatever the cause, their study and ours highlight the importance of mannose in glycan-lectin signaling in the *B. minutum* – Aiptasia symbiosis.

Galactosylated glycans may be markers for appropriate symbionts

The second-most abundant group of glycans in *B. minutum* were galactosylated glycans (Fig. 2.3A). We found two (ID 34100 and 35100) that were reduced with heat stress (Fig. 2.2A). Other studies have suggested that galactosylated glycans have a role in symbiosis. Two galactose-binding lectins SLL-2 and CeCL, from the octocoral *Sinularia lochmodes* and the coral *Ctenactis echinata,* respectively, are hypothesized to play a role in symbiosis by inducing motile symbionts to enter a sessile form (Jimbo et al. 2000, 2010, 2013). In the Aiptasia symbiosis, *B. minutum* has higher galactose abundances compared to non-native or incompatible species, *Symbiodinium pilosum*, *Cladocopium goreaui,* and *Fugacium kawagutii* (Parkinson et al. 2018, Tortorelli et al. 2021). Furthermore, the addition of β-D-galactose during inoculation increased the colonization rates of both *B. minutum* and *C. goreaui* in Aiptasia (Tortorelli et al. 2021). Altogether, these data suggest that galactosylated glycans are important for the recognition of suitable partners, and a heat-induced decline in galactosylated glycan causes the host to no longer recognize the symbiont as an appropriate partner.

Heat-specific sialic acid glycans suggest a complex role for sialylation in symbiosis

The discovery of sialic acids in the Symbiodiniacaeae has been of interest because of their role in host-pathogen interactions in deuterostomes (Varki 2017, Parkinson et al. 2018, Tivey et al. 2020, Tortorelli et al. 2021). Our study provides further evidence that sialic acids are present in Symbiodiniaceae and play a role in symbiosis.

Certain sialic acid moiety abundances increased in response to heat-stress. Two sialylated glycans, 64101 and 65101, were only identified in heat treatments and were missing from ambient treatments (Fig. 2.2C). These glycans are fucosylated, tetraantennary glycans, with a single Neu5Gc sialic acid residue. We hypothesize that they may be produced by a heat-induced error in N-glycosylation pathways, resulting in

aberrant sialylation of a tetraantennary glycan such as galactosylated glycan ID 64000 and 65000, lacking the Neu5Gc sialic acid residue. Aberrant sialylation is a hallmark of cancer in humans and can promote tumor metastasis by increasing cell adhesion and migration (Pietrobono and Stecca 2021). These aberrantly sialylated glycans are specific to heat-stressed symbionts and may act as a glycan marker for a stressed or inappropriate symbiont for the host.

We found that binding of sialic-acid-specific lectin SNA-I to algae increased with heat stress (Fig. 2.3B), and Parkinson et al. (2018) found lower SNA-I binding in their lectin array in *B. minutum* compared to free-living species *S. pilosum*, suggesting that sialic acids are a marker for inappropriate symbionts. In contrast, lectin array data by Tortorelli et al. (2021) found that SNA-I binding was highest in *B. minutum* and lower in the non-native species *C. goreaui* and *F. kawagutii*. This conflicting evidence suggests a complex role of sialic acids in symbiosis, and specific forms of sialic acids may be more important than others.

Recently discovered glycoRNAs in mammalian cells were found to be heavily sialylated and/or fucosylated, and PNGase F removed the N-glycans off glycoRNAs (Flynn et al. 2021). GlycoRNAs were localized to the cell surface, highlighting their probable role as signaling molecules (Flynn et al. 2021). Sialylated and/or fucosylated glycans were well represented in our data, and glycoRNAs could be present in the Aiptasia-Symbiodiniceae system. Future work on the role of glycoRNAs in coral-algae symbiosis would add to this discussion.

Fucosylated glycans and xylosylated glycans are poorly represented

Despite their hypothesized role in cnidarian-algal symbiosis, fucosylated glycans were not well-represented in this study (Tortorelli et al. 2021). Similarly, xylose was not detected in the data, despite the presence of xylosyltransferases in the *B. minutum* genome and their prominent role in plant and algal glycomics (Mathieu-Rivet et al. 2013, Strasser 2016, Oltmanns et al. 2019, Tivey et al. 2020). These glycans may be poorly represented in this study due to the limitations of PNGase F, as it is inhibited by N-glycans containing core α1-3 fucose, a common plant-specific glycosylation that often co-occurs with xylose (van Ree et al. 2000). Future N-glycan analysis would benefit from

using additional glycosidases to fully access the surface glycome, including N-/O-linked glycoproteins, glycolipids, and other glycan conjugates.

Outstanding questions in Symbiodiniaceae glycobiology

This study describes the effect of heat-stress on symbiont glycan diversity, structure, and abundance and is another step in discovering how glycobiology will play a role in coral survival and symbiosis dynamics in a warming planet. Several outstanding questions remain in the study of glycan-lectin interactions in cnidarian-algal symbiosis:

1) **Does the algal glycome change with heat stress *in hospite,* and does it play a role in coral bleaching?** Glycome dynamics of cultured algae are likely not the same as those occurring in algae *in hospite*, and it is unclear if changes in the algal glycome will negatively impact already established symbioses.

2) **Do other environmental factors affect the algal glycome?** Other environmental factors such as nutrition and light play a role in symbiont physiology and may also influence the glycome.

3) **Do thermally tolerant symbionts have a stable glycome?** Thermally tolerant symbionts, such as *B. psygmophilum*, do not lose colonization ability with heat stress (Kishimoto et al. 2020). Does the glycome of thermally tolerant symbionts remain correspondingly stable with heat stress? In preliminary experiments, we found that while colonization rates of *Durusdinium trenchii* in *Acropora tenuis* larvae were not affected by heat stress, a heat-induced decline in CVN labeling of *D. trenchii* was observed (Supplementary Fig. A7, Supplementary Methods A1). This suggests that high-mannose glycan abundances are not important for colonization of *A. tenuis* larvae. Unfortunately, due to pandemic-related travel restrictions, we were unable to explore glycan interactions in coral symbioses further.

Conclusions

The chemical analyses of surface glycoproteins and their carbohydrate composition has emerged as a powerful tool to study cellular interactions on the molecular level. In the field of cnidarian-algal symbiosis, we are beginning to understand what specific glycans are important to symbiosis by chemical manipulation of glycans

and by studying species-specific differences in the glycome. Our study found that heat stress can alter the glycome to become more like that of non-compatible symbiont species. We do not provide direct evidence, however, that an altered glycome caused the heat-induced decrease in colonization capacity of *B. minutum*. This and other glycan studies that have been performed in the Aiptasia – *B. minutum* symbiosis suggest that certain glycans moieties play a role in symbiosis, and lays a foundation for our understanding of glycan-lectin interactions in coral-algal symbioses. However, corals and their symbionts very likely have different glycans that promote and hinder symbiosis. Therefore, it is vital that future work begins to study these interactions in corals and their algal symbionts and test hypotheses that have arisen from the foundational work conducted with Aiptasia. Finally, with the development of CRISPR-cas9 knockdown techniques in corals (Cleves et al. 2018, 2020), it is critical to begin testing the function of host lectins to understand their role in colonization dynamics.

2.6 Acknowledgements

We thank Trevor Tivey, John Parkinson, and Donovon Adpressa for their mentorship in this work. We thank Saki Harii for her mentorship and collaboration in the brief work done in Okinawa. We thank Bobby Lust for providing algal cultures used in Okinawa. This research was funded by the National Science Foundation (NSF IOS-1557804 to VMW and SL; EF-2025476 to SL) and the National Institutes of Health (NIH 1R01GM112490-08 to YM).

2.7 References

Bay, L.K., Cumbo, V.R., Abrego, D., Kool, J.T., Ainsworth, T.D. & Willis, B.L. 2011. Infection dynamics vary between *Symbiodinium* types and cell surface treatments during establishment of endosymbiosis with coral larvae. *Diversity*. 3:356–74.

Bellantuono, A.J., Granados-Cifuentes, C., Miller, D.J., Hoegh-Guldberg, O. & Rodriguez-Lanetty, M. 2012. Coral thermal tolerance: tuning gene expression to resist thermal stress. *PLoS One*. 7:e50685.

Benedetti, E., Gerstner, N., Pučić-Baković, M., Keser, T., Reiding, K.R., Ruhaak, L.R., Štambuk, T. et al. 2020. Systematic evaluation of normalization methods for glycomics data based on performance of network inference. *Metabolites*. 10.

Cho, B.G., Jiang, P., Goli, M., Gautam, S. & Mechref, Y. 2021. Using micro pillar array columns (μPAC) for the analysis of permethylated glycans. *Analyst*. 146:4374–83.

Cleves, P.A., Strader, M.E., Bay, L.K., Pringle, J.R. & Matz, M.V. 2018. CRISPR/Cas9-mediated genome editing in a reef-building coral. *Proc. Natl. Acad. Sci. U. S. A.* 115:5235–40.

Cleves, P.A., Tinoco, A.I., Bradford, J., Perrin, D., Bay, L.K. & Pringle, J.R. 2020. Reduced thermal tolerance in a coral carrying CRISPR-induced mutations in the gene for a heat-shock transcription factor. *Proc. Natl. Acad. Sci. U. S. A.* 117:28899–905.

Dieterle, F., Ross, A., Schlotterbeck, G. & Senn, H. 2006. Probabilistic quotient normalization as robust method to account for dilution of complex biological mixtures. Application in 1H NMR metabonomics. *Anal. Chem.* 78:4281–90.

Dong, X., Zhou, S. & Mechref, Y. 2016. LC-MS/MS analysis of permethylated free oligosaccharides and N-glycans derived from human, bovine, and goat milk samples. *Electrophoresis*. 37:1532–48.

Fitt, W.K. & Trench, R.K. 1983. The relation of diel patterns of cell division to diel patterns of motility in the symbiotic dinoflagellate *Symbiodinium microadriaticum* Freudenthal in culture. *New Phytol.* 94:421–32.

Flynn, R.A., Pedram, K., Malaker, S.A., Batista, P.J., Smith, B.A.H., Johnson, A.G., George, B.M. et al. 2021. Small RNAs are modified with N-glycans and displayed on the surface of living cells. *Cell*. 184:3109-3124.e22.

Fujise, L., Nitschke, M.R., Frommlet, J.C., Serôdio, J., Woodcock, S., Ralph, P.J. & Suggett, D.J. 2018. Cell cycle dynamics of cultured coral endosymbiotic microalgae (*Symbiodinium*) across different types (species) under alternate light and temperature conditions. *J. Eukaryot. Microbiol.* 65:505–17.

Gautam, S., Peng, W., Cho, B.G., Huang, Y., Banazadeh, A., Yu, A., Dong, X. et al. 2020. Glucose unit index (GUI) of permethylated glycans for effective identification of glycans and glycan isomers. *Analyst*. 145:6656–67.

Ghosh, S. 2020. Sialic acid and biology of life: An introduction. *In Sialic Acids and Sialoglycoconjugates in the Biology of Life, Health and Disease*. pp. 1–61.

Herrera, M., Klein, S.G., Campana, S., Chen, J.E., Prasanna, A., Duarte, C.M. & Aranda, M. 2021. Temperature transcends partner specificity in the symbiosis establishment of a cnidarian. *ISME J.* 15:141–53.

Jimbo, M., Suda, Y., Koike, K., Nakamura-Tsuruta, S., Kominami, J., Kamei, M., Hirabayashi, J. et al. 2013. Possible involvement of glycolipids in lectin-mediated cellular transformation of symbiotic microalgae in corals. *J. Exp. Mar. Bio. Ecol.* 439:129–35.

Jimbo, M., Yamashita, H., Koike, K., Sakai, R. & Kamiya, H. 2010. Effects of lectin in the scleractinian coral *Ctenactis echinata* on symbiotic zooxanthellae. *Fish. Sci.* 76:355–63.

Jimbo, M., Yanohara, T., Koike, Kazuhiko, Koike, Kanae, Sakai, R., Muramoto, K. & Kamiya, H. 2000. The d-galactose-binding lectin of the octocoral *Sinularia lochmodes*: characterization and possible relationship to the symbiotic dinoflagellates.

Kishimoto, M., Baird, A.H., Maruyama, S., Minagawa, J. & Takahashi, S. 2020. Loss of symbiont infectivity following thermal stress can be a factor limiting recovery from bleaching in cnidarians. *ISME J.* 14:3149–52.

Koike, K., Jimbo, M., Sakai, R., Kaeriyama, M., Muramoto, K., Ogata, T., Maruyama, T. et al. 2004. Octocoral chemical signaling selects and controls dinoflagellate symbionts. *Biol. Bull.* 207:80–6.

Kolber, Z.S., Prasil, O. & Falkowski, P.G. 1998. Measurements of variable chlorophyll fluorescence using fast repetition rate techniques: defining methodology and experimental protocols. *Biochim. Biophys. Acta*. 1367:88–106.

Lesser, M.P. 1996. Elevated temperatures and ultraviolet radiation cause oxidative stress and inhibit photosynthesis in symbiotic dinoflagellates. *Limnol. Oceanogr.* 41:271–83.

Li, B., Tang, J., Yang, Q., Cui, X., Li, S., Chen, S., Cao, Q. et al. 2016. Performance evaluation and online realization of data-driven normalization methods used in LC/MS based untargeted metabolomics analysis. *Sci. Rep.* 6:38881.

Lin, K.-L., Wang, J.-T. & Fang, L.-S. 2000. Participation of glycoproteins on zooxanthellal cell walls in the establishment of a symbiotic relationship with the sea anemone, *Aiptasia pulchella*. *Zoological Studies*. 39:172–8.

Logan, D.D.K., LaFlamme, A.C., Weis, V.M. & Davy, S.K. 2010. Flow-cytometric characterization of the cell-surface glycans of symbiotic dinoflagellates (*Symbiodinium* spp.). *J. Phycol.* 46:525–33.

Maor-Landaw, K., Karako-Lampert, S., Waldman Ben-Asher, H., Goffredo, S., Falini, G., Dubinsky, Z. & Levy, O. 2014. Gene expression profiles during short-term heat stress in the red sea coral *Stylophora pistillata*. *Glob. Chang. Biol.* 20:3026–35.

Markell, D.A. & Wood-Charlson, E.M. 2010. Immunocytochemical evidence that symbiotic algae secrete potential recognition signal molecules in hospite. *Mar. Biol.* 157:1105–11.

Mathieu-Rivet, E., Scholz, M., Arias, C., Dardelle, F., Schulze, S., Le Mauff, F., Teo, G. et al. 2013. Exploring the N-glycosylation Pathway in Chlamydomonas reinhardtii Unravels Novel Complex Structures*. *Mol. Cell. Proteomics*. 12:3160–83.

Morelle, W., Faid, V., Chirat, F. & Michalski, J.-C. 2009. Analysis of N- and O-Linked Glycans from Glycoproteins Using MALDI-TOF Mass Spectrometry. *In* Packer,

N. H. & Karlsson, N. G. [Eds.] *Glycomics: Methods and Protocols*. Humana Press, Totowa, NJ, pp. 3–21.

Morera, C. & Villanueva, M.A. 2009. Heat treatment and viability assessment by Evans blue in cultured *Symbiodinium kawagutii* cells. *World J. Microbiol. Biotechnol.* 25:1125–8.

Nitschke, M.R., Davy, S.K., Cribb, T.H. & Ward, S. 2015. The effect of elevated temperature and substrate on free-living *Symbiodinium* cultures. *Coral Reefs*. 34:161–71.

Oakley, C.A. & Davy, S.K. 2018. Cell Biology of Coral Bleaching. *In* van Oppen, M. J. H. & Lough, J. M. [Eds.] *Coral Bleaching: Patterns, Processes, Causes and Consequences*. Springer International Publishing, Cham, pp. 189–211.

Oltmanns, A., Hoepfner, L., Scholz, M., Zinzius, K., Schulze, S. & Hippler, M. 2019. Novel Insights Into N-Glycan Fucosylation and Core Xylosylation in C. reinhardtii. *Front. Plant Sci.* 10:1686.

Parkinson, J.E., Tivey, T.R., Mandelare, P.E., Adpressa, D.A., Loesgen, S. & Weis, V.M. 2018. Subtle differences in symbiont cell surface glycan profiles do not explain species-specific colonization rates in a model cnidarian-algal symbiosis. *Front. Microbiol.* 9:842.

Peng, W., Goli, M., Mirzaei, P. & Mechref, Y. 2019. Revealing the biological attributes of N-glycan isomers in breast cancer brain metastasis using porous graphitic carbon (PGC) liquid chromatography-tandem mass spectrometry (LC-MS/MS). *J. Proteome Res.* 18:3731–40.

Petit, D., Teppa, E., Cenci, U., Ball, S. & Harduin-Lepers, A. 2018. Reconstruction of the sialylation pathway in the ancestor of eukaryotes. *Sci. Rep.* 8:2946.

Pietrobono, S. & Stecca, B. 2021. Aberrant sialylation in cancer: Biomarker and potential target for therapeutic intervention? *Cancers*. 13.

Ricci, C.A., Kamal, A.H., Chakrabarty, J.K., Ledbetter, B.E., Chowdhury, S.M. & Mydlarz, L.D. 2020. The cell-surface protein composition of a coral symbiont, *Breviolum psygmophilum*, reveals a mechanism for host specificity and displays dynamic regulation during temperature stress. *Mar. Biol.* 167:66.

Rodriguez-Lanetty, M., Harii, S. & Hoegh-Guldberg, O. 2009. Early molecular responses of coral larvae to hyperthermal stress. *Mol. Ecol.* 18:5101–14.

Seneca, F.O., Forêt, S., Ball, E.E., Smith-Keune, C., Miller, D.J. & van Oppen, M.J.H. 2010. Patterns of gene expression in a scleractinian coral undergoing natural bleaching. *Mar. Biotechnol.* . 12:594–604.

Séveno, M., Bardor, M., Paccalet, T., Gomord, V., Lerouge, P. & Faye, L. 2004. Glycoprotein sialylation in plants?

Strasser, R. 2016. Plant protein glycosylation. *Glycobiology*. 26:926–39.

Tchernov, D., Gorbunov, M.Y., de Vargas, C., Narayan Yadav, S., Milligan, A.J., Häggblom, M. & Falkowski, P.G. 2004. Membrane lipids of symbiotic algae are diagnostic of sensitivity to thermal bleaching in corals. *Proc. Natl. Acad. Sci. U. S. A.* 101:13531–5.

Tivey, T.R., Parkinson, J.E., Mandelare, P.E., Adpressa, D.A., Peng, W., Dong, X., Mechref, Y. et al. 2020. N-linked surface glycan biosynthesis, composition, inhibition, and function in cnidarian-dinoflagellate symbiosis. *Microb. Ecol.* 80:223–36.

Tortorelli, G., Rautengarten, C., Bacic, A., Segal, G., Ebert, B., Davy, S.K., van Oppen, M.J.H. et al. 2021. Cell surface carbohydrates of symbiotic dinoflagellates and their role in the establishment of cnidarian-dinoflagellate symbiosis. *ISME J.* 16:190–9.

van Oppen, M.J.H. & Lough, J.M. (Eds.) 2018. Coral Bleaching: Patterns, Processes, Causes and Consequences. Springer, Cham.

van Ree, R., Cabanes-Macheteau, M., Akkerdaas, J., Milazzo, J.P., Loutelier-Bourhis, C., Rayon, C., Villalba, M. et al. 2000. Beta(1,2)-xylose and alpha(1,3)-fucose residues have a strong contribution in IgE binding to plant glycoallergens. *J. Biol. Chem.* 275:11451–8.

Varki, A. 2017. Biological roles of glycans. *Glycobiology*. 27:3–49.

Varki, A., Cummings, R.D., Esko, J.D., Stanley, P., Hart, G.W., Aebi, M., Darvill, A.G. et al. (Eds.) 2016. Essentials of Glycobiology. Cold Spring Harbor Laboratory Press, Cold Spring Harbor (NY).

Vidal-Dupiol, J., Adjeroud, M., Roger, E., Foure, L., Duval, D., Mone, Y., Ferrier-Pages, C. et al. 2009. Coral bleaching under thermal stress: putative involvement of host/symbiont recognition mechanisms. *BMC Physiol.* 9:14.

Wang, T., Cai, Z.P., Gu, X.Q., Ma, H.Y., Du, Y.M., Huang, K., Voglmeir, J. et al. 2014. Discovery and characterization of a novel extremely acidic bacterial N-glycanase with combined advantages of PNGase F and A. *Biosci. Rep.* 34:e00149.

Weis, V.M. 2019. Cell biology of coral symbiosis: Foundational study can inform solutions to the coral reef crisis. *Integr. Comp. Biol.* 59:845–55.

Wood-Charlson, E.M., Hollingsworth, L.L., Krupp, D.A. & Weis, V.M. 2006. Lectin/glycan interactions play a role in recognition in a coral/dinoflagellate symbiosis. *Cell. Microbiol.* 8:1985–93.

Yacobovitch, T., Benayahu, Y. & Weis, V.M. 2004. Motility of zooxanthellae isolated from the Red Sea soft coral *Heteroxenia fuscescens* (Cnidaria). *J. Exp. Mar. Bio. Ecol.* 298:35–48.

Yamashita, H. & Koike, K. 2016. Motility and cell division patterns among several strains of *Symbiodinium*. *Galaxea, Journal of Coral Reef Studies*. 18:13–9.

Zeleny, R., Kolarich, D., Strasser, R. & Altmann, F. 2006. Sialic acid concentrations in plants are in the range of inadvertent contamination. *Planta*. 224:222–7.

Zhou, Z., Yu, X., Tang, J., Zhu, Y., Chen, G., Guo, L. & Huang, B. 2017. Dual recognition activity of a rhamnose-binding lectin to pathogenic bacteria and zooxanthellae in stony coral Pocillopora damicornis. *Dev. Comp. Immunol.* 70:88–93.

Zhou, Z., Zhao, S., Ni, J., Su, Y., Wang, L. & Xu, Y. 2018. Effects of environmental factors on C-type lectin recognition to zooxanthellae in the stony coral *Pocillopora damicornis*. *Fish Shellfish Immunol.* 79:228–33.

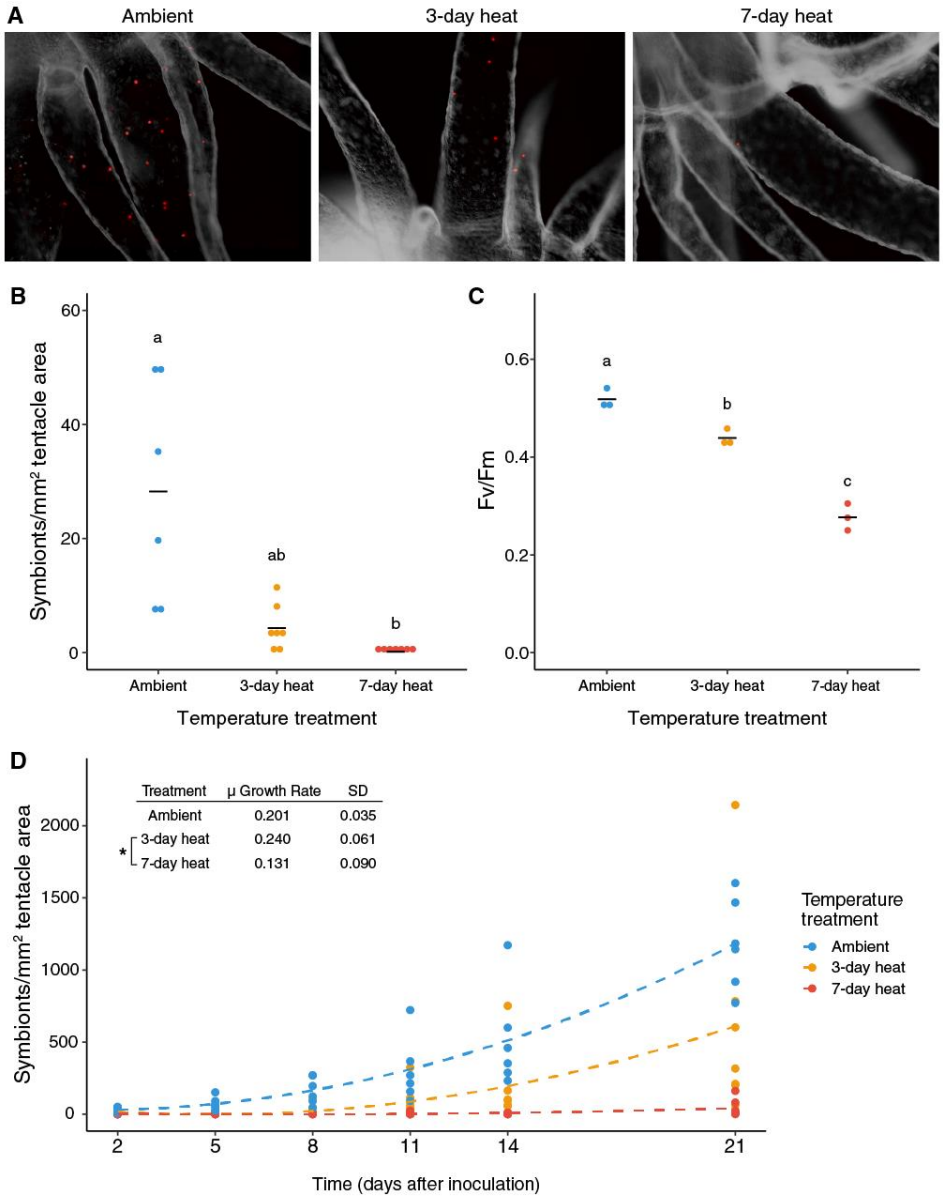

Figure 2.1 – **Heat stressed symbionts have decreased ability to colonize aposymbiotic hosts. (A)** Representative images of symbiont densities from each inoculation. **(B)** Symbiont densities in Aiptasia 2 days after initial inoculation by respective heat-treated algae. **(C)** Photosynthetic efficiency was measured in heat-stressed algae. **(D)** Symbiont density was tracked over time over a period of 21 days to determine algal proliferation rates. µ is a unitless slope of the linear regression of the log transformed data. Letters indicate significant differences ($p \leq 0.05$) as determined by Kruskal-Wallis and post-hoc Dunn Tests. Stars indicate significant differences ($p \leq 0.05$) as determined by ANOVA and post-hoc Tukey test.

Figure 2.2 – The effect of heat stress on the glycome of *Breviolum minutum*. (A) Mass spectrometric analysis of PQN normalized glycan abundances of ambient and heat stressed algae. Glycan structures are represented with illustrations following standards set by the Symbol Nomenclature of Glycans. Glycans are separated into four structural groups by their terminal residues: High-mannose, Galactosylated, Sialylated, and GlcNAc. Boxed sections **(B)-(D)** are zoomed in graphs of corresponding boxes in **(A)**. Statistical differences were determined with FDR adjusted Student's t-tests. * indicate a $p < 0.05$ and $n = 3$.

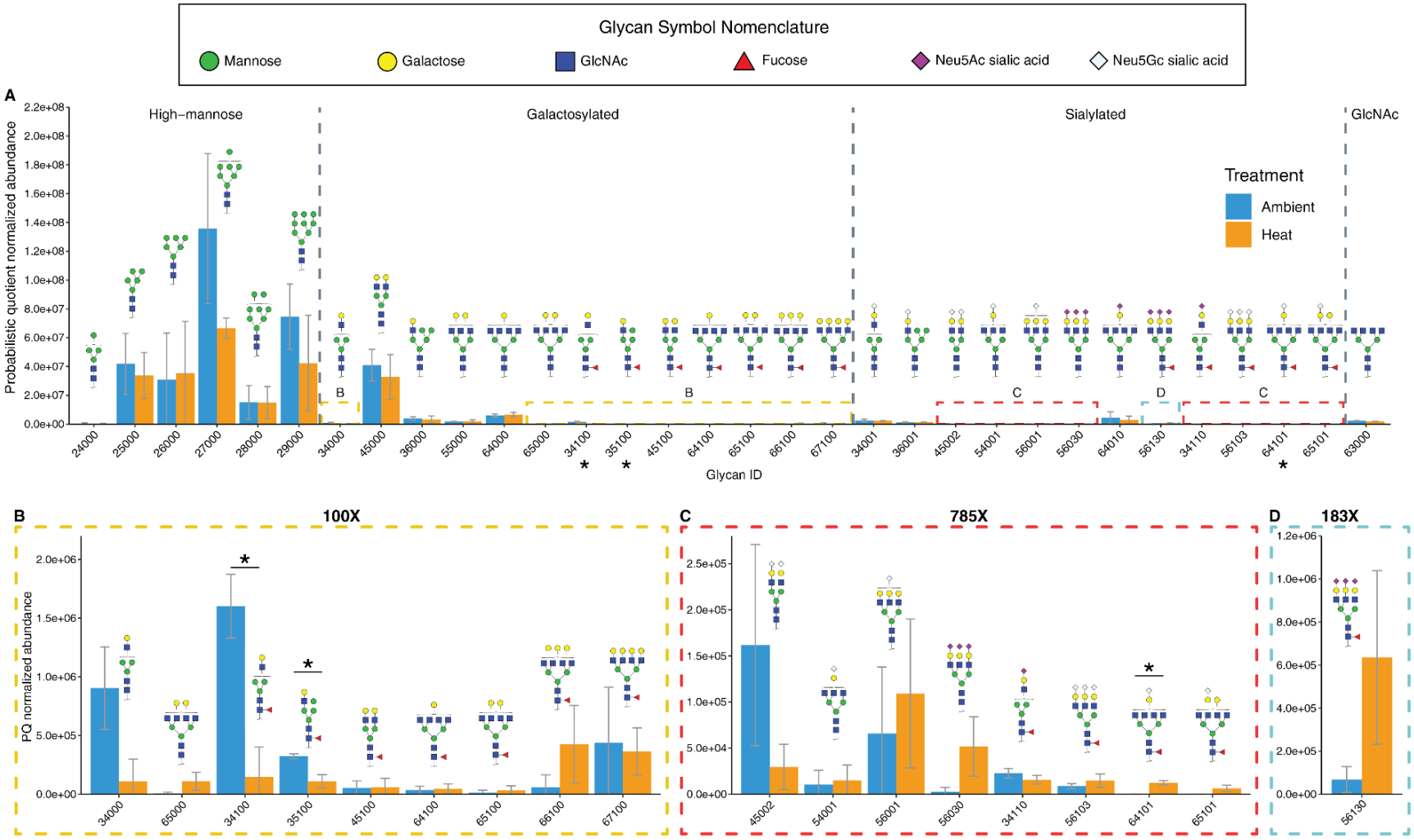
Glycan Symbol Nomenclature
Mannose
Galactose
GlcNAc
Fucose
Neu5Ac sialic acid
Neu5Gc sialic acid
A
High−mannose
Galactosylated
Sialylated
GlcNAc
Probabilistic quotient normalized abundance
Treatment
Ambient
Heat
Glycan ID
B
100X
C
785X
D
183X
PQ normalized abundance

Figure 2.2

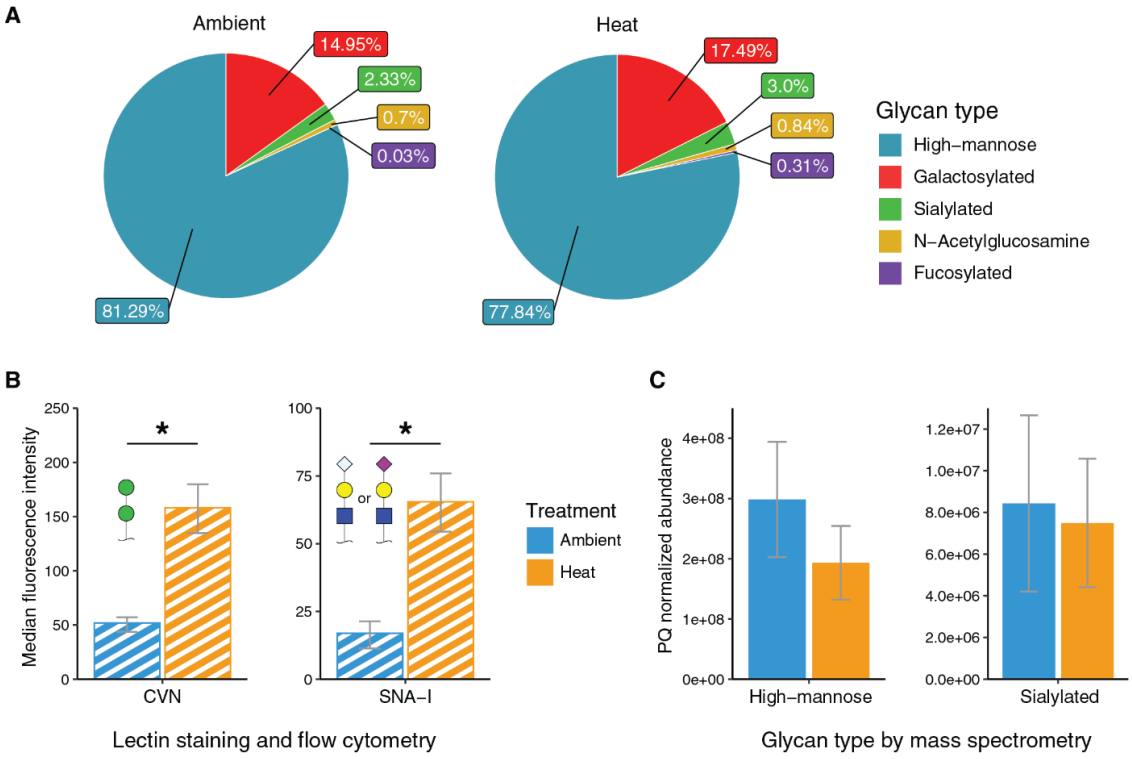

Figure 2.3 – Heat stress affects abundance of certain glycan types. (A) Relative abundance of glycans by type. The "Galactosylated" and "Sialylated" categories do not include their fucosylated counterparts. Any fucosylated glycans were included in the "Fucosylated" category. **(B)** Median fluorescence intensity of algae stained with phycoerythrin conjugated lectin. CVN is a high-mannose specific lectin and SNA-I is a sialic acid specific lectin. **(C)** Abundance of glycans separated by terminal residues as measured by mass spectrometry. The glycan types correspond to their lectin targets in **(B)**.

3. Limitations of using cultured algae to study cnidarian-algal symbioses and suggestions for future studies

Shumpei Maruyama
Virginia M. Weis

Published in *Journal of Phycology*
John Wiley and Sons, on behalf of the Phycological Society of America
8272 Moss Landing Road
Moss Landing, CA 95039 USA
https://doi.org/10.1111/jpy.13102

3.1 Abstract

Much of our understanding of the cellular mechanisms underlying cnidarian-algal symbiosis comes from comparing the biology of the partners when they are engaged in symbiosis with when they are isolated from one another. When comparing the *in hospite* and *ex hospite* state in Symbiodiniaceae, the *in hospite* state is represented by algae sampled from hosts, and the *ex hospite* state is commonly represented by cultured algae. The use of cultured algae in this comparison may introduce nutrition as a confounding variable because, while hosts are kept in nutrient depleted conditions, culture media is nutrient rich and designed to facilitate algal growth. In this perspective, we reexamine how nutrition may be a confounding variable in studies that compare the biology of Symbiodiniaceae *in hospite* and in culture. We also suggest several innovations in experimental design to strengthen the comparison of the two lifestyles, including the adoption of nutritional controls, alternatives to culture for the representation of Symbiodiniaceae *ex hospite*, and the adoption of several proteomic approaches to find novel Symbiodiniaceae genes important for symbiosis.

3.2 Introduction

Coral reefs are among the most diverse and economically valuable ecosystems in our oceans and are currently under threat from anthropogenic climate change (Hughes et al. 2018). Corals owe their ecological success to their symbiotic relationship with dinoflagellates from the family Symbiodiniaceae (Davy et al. 2012). In this mutualism, the host provides inorganic carbon and nutrients to the symbiont, in return for photosynthetic products from the symbiont. To maintain symbiosis, the symbiont must also evade destruction and/or rejection by host innate immunity pathways (Weis 2019). However, with heat stress, the delicate balance of symbiosis is disrupted by metabolic dysregulation and the breakdown of photosynthetic machinery (Blackstone and Golladay 2018). This results in dysbiosis and the removal of algal symbionts by the host, leading to coral bleaching and ultimately coral reef decline (Blackstone and Golladay 2018). Despite the threat of climate change to corals, we have only a partial understanding of the cellular mechanisms involved in the maintenance and breakdown of cnidarian-algal symbiosis.

To better understand coral-algal symbiosis and dysbiosis, it is useful to compare the biology of each partner when they are engaged in symbiosis and when they are isolated from one another. Experiments with corals and other cnidarians that serve as model systems for coral symbiosis that compare hosts with and without their algal symbionts have described many host mechanisms that participate in symbiosis regulation (for review, see Mansfield and Gilmore 2019). Likewise, it is useful to compare the biology of Symbiodiniaceae inside (*in hospite*) and outside (*ex hospite*) the host. Researchers have discovered many key aspects of symbiosis by using cultured algae to represent the *ex hospite* state, such as the importance of nutrient and metabolite exchange between the partners (Hambleton et al. 2019, Xiang et al. 2020).

These comparisons, however, cannot provide a full picture of Symbiodiniaceae in symbiosis because algae in culture are not a perfect proxy for the *ex hospite* state as it occurs in nature (herein referred to as environmental *ex hospite*) (Fig. 3.1). Cultured algae are typically grown in nutrient rich media (Table 1) that are designed to optimize algal growth and do not mimic the oligotrophic conditions in which corals typically occur (Hallock and Schlager 1986). In contrast, *in hospite* algae are commonly represented by

freshly isolating symbionts from hosts that are maintained in oligotrophic seawater – from natural or artificial sources. This discrepancy in nutrient conditions may be a confounding variable in studies that compare Symbiodiniaceae *in hospite* to those in culture. There are other variables that may differ between cultures and environmental *ex hospite* Symbiodiniaceae such as the microbiome, light, and inorganic carbon availability, however this perspective will focus on nutrition.

What then, would more accurately represent the environmental *ex hospite* state for Symbiodiniaceae? Ideally, the biology of symbionts *in hospite* would be compared to that of *ex hospite* conspecific algae found in nature. Important factors to consider, reviewed by Thornhill et al. (2017), are that: 1) the environmental *ex hospite* community of Symbiodiniaceae are often genetically distinct from symbionts found in host communities, 2) it is likely that symbiotic species of Symbiodiniaceae in the wild do not persist in the environment, and 3) instead are transient and continuously expelled by hosts as part of a host homeostatic mechanism to maintain symbiont density. Perhaps symbiotic species of Symbiodiniaceae that are found *ex hospite* are quiescent propagules that are continuously seeking hosts, a phenotype that requires further study. However, the direct collection of environmental samples for comparative studies is difficult, especially with the inability to easily identify and sort out symbionts that are genetically identical to those found *in hospite*. For future studies is would be useful to explore other representations of the *ex hospite* state, such as the use of isolated or recently expelled algae. This idea will be developed further below.

In this perspective, we first reexamine studies that have compared *in hospite* algae to cultures, keeping in mind that cultures do not perfectly represent the environmental *ex hospite* state. We then suggest innovations to experimental design that could strengthen the comparison between the *in hospite* and *ex hospite* states in future studies. Finally, we advocate for the adoption of proteomics and a selection of other under-utilized techniques to further examine the two lifestyles in Symbiodiniaceae.

3.3 Differences in symbiont growth and cell division are heavily influenced by nutrition

The regulation of symbiont populations in hosts is essential for the maintenance of cnidarian-algal symbiosis (Davy et al. 2012). Studies that explore algal population growth find that cultured algae divide faster than symbionts *in hospite* (Smith and Muscatine 1999, Tivey et al. 2020). It is hypothesized that the host actively inhibits the proliferation of symbionts by limiting nutrient transfer (Falkowski et al. 1993, Smith and Muscatine 1999, Tivey et al. 2020, Xiang et al. 2020). However, the lower symbiont growth rate *in hospite* compared to in culture could be explained by lower ambient nutrient availability and may not be caused by host inhibitory mechanisms. Indeed, there is substantial evidence that when hosts are supplemented with nutrients by feeding or addition of inorganic nutrients, there is an increase in symbiont proliferation and/or density (Hoegh-Guldberg and Smith 1989, Muscatine et al. 1989, Stambler and Stimson 1991, Falkowski et al. 1993, Hoegh-Guldberg 1994, Muller-Parker et al. 1994, Marubini and Davies 1996, Smith and Muscatine 1999, Ferrier-Pagès et al. 2001, Houlbrèque et al. 2004, Tivey et al. 2020). These studies support an alternative hypothesis that hosts will allocate nutrients to their symbionts when they are available, instead of actively inhibiting symbiont proliferation. To further test the hypothesis that symbiont growth rate is controlled by the host, growth rates between symbionts *in hospite* to those in cultures could be directly compared in experiments where nutrient availability is controlled. These experiments may reveal a more accurate picture of the extent to which hosts inhibit symbiont proliferation, since the data will not be confounded by differing nutrient availability.

3.4 Differences in symbiont morphology and ultrastructure highlight the interactive effects of nutrition and symbiosis

There are several morphological differences between algae *in hospite* and those in culture. For example, Pasaribu et al. (2015) found more lipid droplets (see also Wang et al. 2015) and smaller chloroplasts in cells *in hospite* compared to those in culture. There is strong evidence that this phenotype is the result of differences in nutrient availability. In nutrient-starved algal cultures, there is an increase in lipid droplet formation and a decrease in chloroplast size (Jiang et al. 2014, Rosset et al. 2015, 2017, Pasaribu et al. 2016). Similarly, algae in hosts that have either been starved or nutrient deprived show

the same phenotype (Cook et al. 1988, Muller-Parker et al. 1996, Weng et al. 2014, Rosset et al. 2015). Interestingly, simply changing seawater nutrient concentrations affected symbionts *in hospite*, possibly indicating that the host has a limited capacity to control nutrient availability to the symbiont (Rosset et al. 2015). The generation of lipid bodies is thought to be caused by an accumulation of excess fixed carbon that would otherwise be used for cellular growth if nutrients were available (Rosset et al. 2017). The reduction in chloroplast size is hypothesized to be due to a lack of nutrients needed to maintain function (Cook et al. 1988, Muller-Parker et al. 1996). These phenotypic differences between algae *in hospite* and in culture may therefore be due to differences in nutrient availability rather than symbiotic state.

Another morphological difference between Symbiodinaceae *in hospite* and in culture is cell-wall thickness, however this phenotypic trait appears to be affected by both symbiosis and nutrition. Decreasing nutrient availability causes an increase in cell-wall thickness, both *in hospite* and in culture (Jiang et al. 2014, Weng et al. 2014). It is hypothesized that the thicker cell-walls are a consequence of a build-up of carbon-rich cellulose from the decreased rate of cell division, similar to how lipid bodies accumulate as described above (Jiang et al. 2014). However, despite having lower nutrient availability compared to algae in culture, symbionts *in hospite* nonetheless have thinner cell walls than those in culture (Palincsar et al. 1988, Pasaribu et al. 2015). The thinner cell wall *in hospite* may be an adaptation to the symbiotic lifestyle, as a thinner barrier may facilitate the exchange of material with the host. These studies highlight the benefit of nutritional controls and how they might tease apart the interactive effects of nutrition and symbiosis.

3.5 Nutrient transporter gene expression is affected by nutrition and symbiont density

Several studies have compared the transcriptomes of algae *in hospite* to those in culture (Bellantuono et al. 2019, Maor-Landaw et al. 2020, Xiang et al. 2020). In *Breviolum minutum*, a naturally-occurring symbiont in the sea anemone *Exaiptasia pallida* (called Aiptasia), there is an upregulation of nitrate and/or ammonia transporters (*NRT* and *AMT*, respectively) *in hospite* compared to in culture (Maor-Landaw et al.

2020, Xiang et al. 2020). The holobionts in these experiments were maintained in relatively nutrient-depleted conditions, while the algal cultures were grown in nutrient-rich media. As seen by studies in other algal taxa, the upregulation of nutrient transporters in the algae *in hospite* may have been caused by the oligotrophic seawater conditions (Hildebrand 2005, Miller et al. 2010). Indeed, Xiang et al. (2020) examined the expression of *AMT* and *NRT* genes in cultured *B. minutum* under different nutrient conditions and in algae from fed *versus* starved hosts and confirmed that expression of these genes was negatively correlated with nutrient availability or feeding. Importantly, Xiang et al. (2020) found that feeding the host every two days had a smaller effect on nutrient transporter gene expression in the symbiont than did the addition of nutrients to algal culture media. This suggests that feeding alone is not sufficient to reach nutrient levels present in algal media. Further experimentation is needed to determine how much nutrition the algal symbionts obtain from host feeding.

In contrast, a different pattern was observed in the unnatural colonization of Aiptasia by *Durusdinium trenchii*. *D. trenchii in hospite* in Aiptasia downregulates *AMT* and other nitrogen transport genes compared to when it is in culture (Bellantuono et al. 2019). This suggests that *D. trenchii* is not nitrogen-limited *in hospite*. A recent study verified that in Aiptasia, *D. trenchii* assimilates significantly higher amounts of nitrogen than *B. minutum*; however, *D. trenchii* was present at a much lower density than was *B. minutum* (Sproles et al. 2020). The observation that *D. trenchii* is not nutrient limited *in hospite* could result from differential symbiont densities and therefore, nutrient availability. Compared to *B. minutum*, *D. trenchii* does not colonize Aiptasia at high densities, likely because it is an unnatural host-symbiont pairing (Gabay et al. 2018, Medrano et al. 2019, Sproles et al. 2020). Additional evidence that symbiont density affects nutrient availability comes from studies in *B. minutum* that found that when algal density in Aiptasia was low, *B. minutum* was not nitrogen limited (Sproles et al. 2020) and *AMT* and *NRT* transcripts were not upregulated compared to those in culture (Xiang et al. 2020). These data together suggest that low density of *D. trenchii* in Aiptasia results in the algae not being nutrient limited *in hospite*. Other host factors could be limiting the density of *D. trenchii* within Aiptasia, such as an innate immune response to an unnatural symbiont (Matthews et al. 2017). Future experiments could control for symbiont density

in both *D. trenchii* and *B. minutum* to tease apart the relationship between nutrient uptake and nutrient transporter gene expression.

3.6 Changes in experimental design aimed at strengthening comparisons between the *in hospite* and *ex hospite* state

When studying the differences between Symbiodiniaceae *in hospite* and in culture, we suggest the inclusion of nutrient controls, such as cultures maintained in nutrient-depleted media, holobionts maintained in nutrient-enriched seawater, and both starved and fed holobionts. These additional controls will provide a more complete picture of the comparison between *in hospite* and *ex hospite* lifestyles and can help test whether previously identified phenotypes and differentially expressed genes (DEGs) are due to symbiotic state, differences in nutrition, or a combination. At a minimum, regular reporting of the nutritional state of experimental holobionts (i.e., how often and how much they are fed) would also improve interpretation of findings.

Given that cultured Symbiodiniaceae are not perfect representations of the environmental *ex hospite* state, we suggest the exploration of other proxies, such as isolated or host-expelled algae. To represent the *in hospite* state, isolated symbionts are typically separated from hosts, through homogenization of host tissue, and sampled immediately (Stochaj and Grossman 1997, Perez et al. 2001, Goulet et al. 2005, Karako-Lampert et al. 2005, Godinot et al. 2009, Hoogenboom et al. 2010, Pasaribu et al. 2015, Bellantuono et al. 2019, Maor-Landaw et al. 2020, Xiang et al. 2020). However, isolated symbionts can also be maintained briefly in seawater to represent the *ex hospite* state (Colley and Trench 1983, Palincsar et al. 1988, Goiran et al. 1996, Tansik et al. 2017). There are many considerations for the use of isolated symbionts to represent the *ex hospite* state – how long should they be kept out of the host before sampling? What media should they be kept in? What kind of stress do isolated symbionts experience during the extraction process? For example, the *in hospite* environment has dramatically different ion concentrations than does seawater (Seibt and Schlichter 2001), and it takes at least 3 hours for isolated symbionts to regulate sodium ion concentrations back to equilibrium (Goiran et al. 1997). Studies must also consider the presence of host tissue contamination, such as symbiosome membranes that can be difficult to remove from the

algae without harsh chemical or mechanical disruption (Kazandjian et al. 2008, Peng et al. 2010). These questions are ripe for experimentation and testing that could result in new proxies for the environmental *ex hospite* state.

Another advantage to the use of isolated symbionts is that their genetic makeup is more representative of the symbionts that are present in the host than are algal populations in culture, provided that they are sampled soon after isolation (Santos et al. 2001). With model systems such as Aiptasia, it is possible to inoculate hosts with cultured algae to control for symbiont genotype, but in corals, algal cultures are often different than the community of symbionts that is present within a host, even when the culture is originally started as an isolate from the same host species (Santos et al. 2001, Parkinson et al. 2015). This problem can arise because, given time, the most common symbiont species from a host may fail to thrive and is replaced by one or more that grow readily in culture (Santos et al. 2001, Parkinson et al. 2015). However, the length of time required for the community shift to take place is not known and requires further examination. In addition, many symbiotic Symbiodiniaceae, e.g., the vast majority of the hyperdiverse *Cladocopium* genus, have not been successfully brought into culture, likely because they are highly obligate symbionts that require specific host-provided and as yet undescribed factors to survive in culture (Krueger and Gates 2012).

The most accurate representation of the environmental *ex hospite* state may be recently-expelled algae (Fig. 3.1). As reviewed by Thornhill et al. (2017), the absence of evidence that symbiotic Symbiodiniaceae persist in the environment *ex hospite* suggests that symbionts are transient in the environment and shed continuously by hosts. Thornhill et al. (2017) hypothesize that expelled Symbiodiniaceae are largely transitory propagules that are continuously seeking new hosts. Perhaps in nature, the temporary expelled state is the only state that symbiotic Symbiodiniaceae species persist *ex hospite* and the term "free-living" should be reserved for species that do not form symbioses with any hosts. The use of expelled algae in the laboratory setting shares some of the advantages of using isolated symbionts rather than cultures: expelled algae are likely to be representative of the *in hospite* community of symbionts and species that are not available in culture can be sampled in an *ex hospite* state. Importantly, there is evidence that expelled algae can still be photosynthetically viable and can colonize new hosts (Steele 1975, Ralph et al. 2001,

Schwarz et al. 2002, Hill and Ralph 2007, Fujise et al. 2013, 2014). Future studies could investigate more deeply the biology of expelled algae and their role in Symbiodiniaceae life histories.

Important factors to consider when sampling expelled algae is the exclusion of contaminating algae from the environment and minimizing stress to the host resulting from the collecting process. Expelled algae can be sampled directly from the seawater containing corals by isolating colonies in a chamber and collecting the seawater at certain intervals. This method was employed by Hoegh-Guldberg et al. (1987), but the sediment was not excluded in this method, and so contamination of environmental Symbiodiniaceae from the sediment was likely. A more commonly employed method is to temporarily place hosts into closed-system aquaria with filtered seawater and to filter out the symbionts from the seawater after a certain period (Hoegh-Guldberg et al. 1987, Baghdasarian and Muscatine 2000, Bhagooli and Hidaka 2004, LaJeunesse et al. 2004, Hill and Ralph 2007, Fujise et al. 2013, 2014). While this method excludes nearly all potential external sources of Symbiodiniaceae, the transfer of hosts from the environment to aquaria may cause stress. Even moderate amounts of heat stress can dramatically increase expulsion of algae in corals (Fujise et al. 2014), and the context in which algae are expelled in can affect their health (Bhagooli and Hidaka 2004, Hill and Ralph 2007). In a preliminary test, we found that various *Acropora* spp., collected from the wild, released measurable amounts of algae (about 1×10^5 to 1×10^6 cells from fist-sized nubbins a day) only for the first week in captivity, but quickly declined to undetectable amounts thereafter (data not shown). This suggests the initial algal release may have been caused by the stress of collection and that release was reduced once corals acclimated to their new conditions. Further testing could be performed on other host taxa to assess best practices for the collection of expelled algae in the field and in the laboratory environment.

3.7 Expression of H^+-ATPase, a putative symbiosis-specific algal gene, is not connected to nutrition

To date, just one putative symbiosis-specific Symbiodiniaceae gene has been characterized: H^+-ATPase (Al-Moghrabi et al. 1996, Bertucci et al. 2010). H^+-ATPase is

upregulated in *Symbiodinium microadriaticum* when in symbiosis with the coral *Stylophora pistillata*, but not in culture (Bertucci et al. 2010). H^+-ATPase is hypothesized to be a plasma membrane protein that in symbiotic algae plays a role in carbon concentrating mechanisms by increasing the acidity of the symbiosome membrane compartment. The decreased pH tips the balance of inorganic carbon from HCO_3^- to CO_2 with the help of carbonic anhydrase (Al-Moghrabi et al. 1996). CO_2 then diffuses into the algal symbiont, destined for fixation by photosynthesis (Al-Moghrabi et al. 1996). In contrast, algae in culture express a Na^+-based HCO_3^- transporter as a carbon concentrating mechanism (Al-Moghrabi et al. 1996). The functioning of H^+-ATPase is dependent on the host symbiosome environment and would not function *ex hospite*, lending further support for the idea of H^+-ATPase as a symbiosis-specific protein.

While H^+-ATPase is a strong candidate for a symbiosis-specific gene in symbionts, it has only been characterized in *S. microadriaticum* and appears to be poorly conserved among other Symbiodiniaceae (Mies et al. 2017). No transcriptomic studies of *B. minutum* or *D. trenchii* have identified a H^+-ATPase as a DEG when comparing algae *in hospite* and in culture (Bellantuono et al. 2019, Maor-Landaw et al. 2020, Xiang et al. 2020). Apparent absence of H^+-ATPase as a DEG may come from the low sensitivity or specificity of RNA-seq, could be an example of how different taxa employ different strategies to maintain symbiosis, or could result from differential post-transcriptional and post-translational modifications depending on species (Roy et al. 2018). Our limited understanding of symbiosis-specific Symbiodiniaceae genes highlights the need for the adoption of other techniques beyond transcriptomics to enable more discovery.

3.8 Unraveling the *in hospite* and *ex hospite* states with proteomics

Studies of Symbiodiniaceae RNA editing (Liew et al. 2017), proteomics (Stochaj and Grossman 1997), and dinoflagellate transcriptomics (for review, see Roy et al. 2018) suggest that Symbiodiniaceae employ post-transcriptional and post-translational modification for gene regulation. An early study found dramatic differences in the two-dimensional gel protein profiles between unidentified Symbiodiniaceae from Aiptasia, *in hospite* and in culture (Stochaj and Grossman 1997). Only four polypeptides had similar isoelectric and mass characteristics when comparing the two lifestyles (Stochaj and

Grossman 1997). However, the study pre-dates efforts to genetically type the algae, so the interpretation of these data is limited. Nevertheless, a similar transcriptomic study comparing *B. minutum* from Aiptasia, *in hospite* and in culture, found that 71% of the transcriptome showed no significant changes in expression between the two lifestyles (Maor-Landaw et al. 2020). The nature of dinoflagellate gene regulation suggests that proteomic studies may be key in identifying additional differences between the *in hospite* and *ex hospite* states. Characterization of whole Symbiodiniaceae proteomes is becoming more accessible through mass spectrometry, and current research efforts are focusing on Symbiodiniaceae proteomics using this high-throughput method (Amir Mashini and Simon Davy, Victoria University of Wellington, NZ, pers comm).

There are other targeted proteomic approaches that have the advantage of high sensitivity and confidence in characterizing proteins (Chandramouli and Qian 2009). For example, a recent study isolated proteins from the algal cell-surface of heat-treated *B. psygmophilum* in culture and found many differentially expressed proteins that were hypothesized to be functionally relevant to symbiosis (Ricci et al. 2020). The isolation of cell-surface proteins is an attractive method because it simplifies the sample complexity, thereby improving the characterization of low abundance proteins (Chandramouli and Qian 2009). In addition, the cell-surface is a critical interface for host-symbiont interactions (Ricci et al. 2020). Therefore, many symbiosis-related changes in the cell-surface proteome would be expected to occur when comparing algae *in hospite* to those in culture.

Other promising techniques for identifying functionally relevant cell-surface proteins include antibody phage display and aptamer Cell-SELEX (Selective Evolution of Ligands by EXponential enrichment). Neither technique has been used in the field of symbiosis, but their application in the identification of novel proteins is well established in studies of human disease, pathogens and parasites (Azzazy and Highsmith 2002, Tonelli et al. 2012, Dunn et al. 2017). Briefly, antibodies and aptamers are ligands that bind to proteins with high specificity and affinity. Through several rounds of selection (Fig. 3.2) antibodies or aptamers can be identified that bind to target specific cell types (e.g. cancer cells, virulent parasite strains, or freshly isolated symbionts) but not to off-target cells (e.g. healthy cells, nonvirulent parasite strains, or cultured algae). Selected

antibodies and aptamers can be used in pull-down assays to purify their target proteins and identify them using mass spectrometry. Antibodies and aptamers can also be used in other downstream applications, such as *in situ* visualization, protein expression studies, and in functional studies by blocking target function *in vivo*. Of the two techniques, aptamer Cell-SELEX has several advantages over phage display for the study of Symbiodiniaceae proteins because it has a lower production cost, it can be performed in a typical molecular laboratory, and has been successfully used in related taxa, such as diatoms and apicomplexans (Tonelli et al. 2012, Santamaria et al. 2015, Dunn et al. 2017). Current efforts in the Weis lab are exploring the use of Cell-SELEX in identifying symbiosis-specific proteins from *B. minutum* isolated from Aiptasia and have successfully performed three rounds of SELEX to develop fluorescent DNA aptamers that bind specifically to freshly isolated *B. minutum* (data not shown).

3.9 Conclusion

The study of Symbiodiniaceae will continue to rely on the use of cultures as proxies for the *ex hospite* state. Cultures are readily available, allow for sampling of high biomass, and are amenable to experimental manipulation. However, it is valuable to be mindful that cultured Symbiodiniaceae are typically grown in nutrient-replete, artificial media that are designed to maximize growth and health of the symbiont. In contrast, environmental symbionts *ex hospite* may not persist in nature and are typically found in oligotrophic environments. To reinforce the comparison between symbionts *in hospite* and *ex hospite*, we recommend: 1) the addition of nutritional controls, such as nutrient-depleted cultures or starved hosts into comparative experiments, 2) the adoption of isolated or expelled symbionts as alternative representations of the *ex hospite* state, and 3) the use of proteomic techniques to better characterize the molecular changes between the two lifestyles. Uncovering the *in hospite* state of Symbiodiniaceae will inextricably rely on a better understanding of the environmental *ex hospite* state and updating our perspective on experiments using cultured symbionts.

3.10 Acknowledgements

We thank members of the Weis and Parkinson Labs, Valeri Sawiccy, Jack Koch, Jason Presnell, Erick White, Raúl González-Pech, Matthew Gamache, and John Parkinson for encouragement and feedback on drafts. We also thank the pandemic lockdown for giving us the time to write this manuscript instead of doing lab work. This work was supported by NSF grant IOS:1645164 to V.M.W.

3.11 References

Al-Moghrabi, S., Goiran, C., Allemand, D., Speziale, N. & Jaubert, J. 1996. Inorganic carbon uptake for photosynthesis by the symbiotic coral-dinoflagellate association II. Mechanisms for bicarbonate uptake. *J. Exp. Mar. Bio. Ecol.* 199:227–48.

Azzazy, H.M.E. & Highsmith, W.E., Jr 2002. Phage display technology: clinical applications and recent innovations. *Clin. Biochem.* 35:425–45.

Baghdasarian, G. & Muscatine, L. 2000. Preferential expulsion of dividing algal cells as a mechanism for regulating algal-cnidarian symbiosis. *Biol. Bull.* 199:278–86.

Bellantuono, A.J., Dougan, K.E., Granados-Cifuentes, C. & Rodriguez-Lanetty, M. 2019. Free-living and symbiotic lifestyles of a thermotolerant coral endosymbiont display profoundly distinct transcriptomes under both stable and heat stress conditions. *Mol. Ecol.* 28:5265–81.

Bertucci, A., Tambutte, E., Tambutte, S., Allemand, D. & Zoccola, D. 2010. Symbiosis-dependent gene expression in coral-dinoflagellate association: cloning and characterization of a P-type H+-ATPase gene. *Proc. R. Soc. Lond. B Biol. Sci.* 277:87–95.

Bhagooli, R. & Hidaka, M. 2004. Release of zooxanthellae with intact photosynthetic activity by the coral *Galaxea fascicularis* in response to high temperature stress. *Mar. Biol.* 145:329–37.

Blackstone, N.W. & Golladay, J.M. 2018. Why do corals bleach? Conflict and conflict mediation in a host/symbiont community. *Bioessays*. 40:e1800021.

Chandramouli, K. & Qian, P.-Y. 2009. Proteomics: challenges, techniques and possibilities to overcome biological sample complexity. *Hum. Genomics Proteomics*. 2009.

Colley, N. & Trench, R. 1983. Selectivity in phagocytosis and persistence of symbiotic algae by the scyphistoma stage of the jellyfish. *Proceedings of the Royal Society B: Biological Sciences*. 219:61–82.

Cook, C.B., D'Elia, C.F. & Muller-Parker, G. 1988. Host feeding and nutrient sufficiency for zooxanthellae in the sea anemone *Aiptasia pallida*. *Marine Biology*. 262:253–62.

Davy, S.K., Allemand, D. & Weis, V.M. 2012. Cell biology of cnidarian-dinoflagellate symbiosis. *Microbiol. Mol. Biol. Rev.* 76:229–61.

den Haan, J., Huisman, J., Brocke, H.J., Goehlich, H., Latijnhouwers, K.R.W., van Heeringen, S., Honcoop, S.A.S. et al. 2016. Nitrogen and phosphorus uptake rates of different species from a coral reef community after a nutrient pulse. *Sci. Rep.* 6:28821.

Dunn, M.R., Jimenez, R.M. & Chaput, J.C. 2017. Analysis of aptamer discovery and technology. *Nature Reviews Chemistry*. 1:Article number: 0076.

Falkowski, P.G., Dubinsky, Z. & Muscatine, L. 1993. Population Control in Symbiotic Corals Ammonium ions and organic materials maintain the dens of zooxanthellae. 43:606–11.

Ferrier-Pagès, C., Schoelzke, V., Jaubert, J., Muscatine, L. & Hoegh-Guldberg, O. 2001. Response of a scleractinian coral, *Stylophora pistillata*, to iron and nitrate enrichment. *J. Exp. Mar. Bio. Ecol.* 259:249–61.

Fujise, L., Yamashita, H., Suzuki, G. & Koike, K. 2013. Expulsion of zooxanthellae (*Symbiodinium*) from several species of scleractinian corals: comparison under non-stress conditions and thermal stress conditions. *Galaxea (Tokyo)*. 15:29–36.

Fujise, L., Yamashita, H., Suzuki, G., Sasaki, K., Liao, L.M. & Koike, K. 2014. Moderate thermal stress causes active and immediate expulsion of photosynthetically damaged zooxanthellae (*Symbiodinium*) from corals. *PLoS One*. 9:1–18.

Gabay, Y., Weis, V.M. & Davy, S.K. 2018. Symbiont identity influences patterns of symbiosis establishment, host growth, and asexual reproduction in a model cnidarian-dinoflagellate symbiosis. *Biol. Bull.* 234:1–10.

Godinot, C., Ferrier-Pagès, C. & Grover, R. 2009. Control of phosphate uptake by zooxanthellae and host cells in the scleractinian coral *Stylophora pistillata*. *Limnology and Oceanography*. 54:1627–33.

Goiran, C., Allemand, D. & Galgani, I. 1997. Transient Na^+ stress in symbiotic dinoflagellates after isolation from coral-host cells and subsequent immersion in seawater. *Marine Biology*. 129:581–9.

Goiran, C., Al-moghrabi, S. & Allemand, D. 1996. Inorganic carbon uptake for photosynthesis by the symbiotic coral/dinoflagellate association I. Photosynthetic performances of symbionts and dependence on sea water bicarbonate. *Journal of Experimental Marine Biology and Ecology*. 199:207–25.

Goulet, T.L., Cook, C.B. & Goulet, D. 2005. Effect of short-term exposure to elevated temperatures and light levels on photosynthesis of different host-symbiont combinations in the *Aiptasia pallida-Symbiodinium* symbiosis. *Limnology and Oceanography*. 50:1490–8.

Hallock, P. & Schlager, W. 1986. Nutrient excess and the demise of coral reefs and carbonate platforms. *Palaios*. 1:389–98.

Hambleton, E.A., Jones, V.A.S., Maegele, I., Kvaskoff, D., Sachsenheimer, T. & Guse, A. 2019. Sterol transfer by atypical cholesterol-binding NPC2 proteins in coral-algal symbiosis. *Elife*. 8.

Hildebrand, M. 2005. Cloning and functional characterization of ammonium transporters from the marine diatom *Cylindrotheca fusiformis* (Bacillariophyceae). *J. Phycol.* 41:105–13.

Hill, R. & Ralph, P.J. 2007. Post-bleaching viability of expelled zooxanthellae from the scleractinian coral *Pocillopora damicornis*. *Mar. Ecol. Prog. Ser.* 352:137–44.

Hoegh-Guldberg, O. 1994. Population Dynamics of Symbiotic Zooxanthellae in the Coral *Pocillopora damicornis* Exposed to Elevated Ammonium [$(NH_4)_2SO_4$] Concentrations. *Pacific Science*. 48:263–72.

Hoegh-Guldberg, O., McCloskey, L.R. & Muscatine, L. 1987. Expulsion of zooxanthellae by symbiotic cnidarians from the Red Sea. *Coral Reefs*. 5:201–4.

Hoegh-Guldberg, O. & Smith, G.J. 1989. Influence of population density of zooxanthellae and supply of ammonium on the biomass and metabolic characterisitics of the reef corals *Seriatopora hystrix* and *Stylophora pistillata*. *Marine Ecology Progress Series*. 57:173–86.

Hoogenboom, M., Beraud, E. & Ferrier-Pagès, C. 2010. Relationship between symbiont density and photosynthetic carbon acquisition in the temperate coral *Cladocora caespitosa*. *Coral Reefs*. 29:21–9.

Houlbrèque, F., Tambutté, E., Allemand, D. & Ferrier-Pagès, C. 2004. Interactions between zooplankton feeding, photosynthesis and skeletal growth in the scleractinian coral *Stylophora pistillata*. *J. Exp. Biol.* 207:1461–9.

Hughes, T.P., Kerry, J.T., Baird, A.H., Connolly, S.R., Dietzel, A., Eakin, C.M., Heron, S.F. et al. 2018. Global warming transforms coral reef assemblages. *Nature*. 556:492–6.

Jiang, P.-L., Pasaribu, B. & Chen, C.-S. 2014. Nitrogen-Deprivation Elevates Lipid Levels in *Symbiodinium* spp. by Lipid Droplet Accumulation: Morphological and Compositional Analyses. *PLoS ONE*. 9.

Karako-Lampert, S., Katcoff, D.J., Achituv, Y., Dubinsky, Z. & Stambler, N. 2005. Responses of *Symbiodinium microadriaticum* clade B to different environmental conditions. *J. Exp. Mar. Bio. Ecol.* 318:11–20.

Kazandjian, A., Shepherd, V.A., Rodriguez-Lanetty, M., Nordmeier, W., Larkum, A.W.D. & Quinnell, R.G. 2008. Isolation of symbiosomes and the symbiosome membrane complex from the zoanthid *Zoanthus robustus*. *Phycologia*. 47:294–306.

Krueger, T. 2020. MiCORE Manual. Available At: https://www.researchgate.net/project/The-MiCORE-manual.

Krueger, T. & Gates, R.D. 2012. Cultivating endosymbionts - Host environmental mimics support the survival of *Symbiodinium* C15 *ex hospite*. *J. Exp. Mar. Bio. Ecol.* 413:169–76.

LaJeunesse, T.C., Bhagooli, R., Hidaka, M., DeVantier, L., Done, T., Schmidt, G.W., Fitt, W.K. et al. 2004. Closely related *Symbiodinium* spp. differ in relative dominance in coral reef host communities across environmental, latitudinal and biogeographic gradients. *Mar. Ecol. Prog. Ser.* 284:147–61.

Liew, Y.J., Li, Y., Baumgarten, S., Voolstra, C.R. & Aranda, M. 2017. Condition-specific RNA editing in the coral symbiont *Symbiodinium microadriaticum*. *PLoS Genet.* 13:e1006619.

Mansfield, K.M. & Gilmore, T.D. 2019. Innate immunity and cnidarian-Symbiodiniaceae mutualism. *Dev. Comp. Immunol.* 90:199–209.

Maor-Landaw, K., van Oppen, M.J.H. & McFadden, G.I. 2020. Symbiotic lifestyle triggers drastic changes in the gene expression of the algal endosymbiont *Breviolum minutum* (Symbiodiniaceae). *Ecol. Evol.* 10:451–66.

Marubini, F. & Davies, P.S. 1996. Nitrate increases zooxanthellae population density and reduces skeletogenesis in corals. *Mar. Biol.* 127:319–28.

Matthews, J.L., Crowder, C.M., Oakley, C.A., Lutz, A., Roessner, U., Meyer, E., Grossman, A.R. et al. 2017. Optimal nutrient exchange and immune responses operate in partner specificity in the cnidarian-dinoflagellate symbiosis. *Proc. Natl. Acad. Sci. U. S. A.* 114:13194–9.

Medrano, E., Merselis, D.G., Bellantuono, A.J. & Rodriguez-Lanetty, M. 2019. Proteomic basis of symbiosis: A heterologous partner fails to duplicate homologous colonization in a novel cnidarian – Symbiodiniaceae mutualism. *Front. Microbiol.* 10:1153.

Mies, M., Voolstra, C.R., Castro, C.B., Pires, D.O., Calderon, E.N. & Sumida, P.Y.G. 2017. Expression of a symbiosis-specific gene in *Symbiodinium* type A1

associated with coral, nudibranch and giant clam larvae. *Royal Society Open Science*. 4:179253.

Miller, R., Wu, G., Deshpande, R.R., Vieler, A., Gärtner, K., Li, X., Moellering, E.R. et al. 2010. Changes in transcript abundance in *Chlamydomonas reinhardtii* following nitrogen deprivation predict diversion of metabolism. *Plant Physiology*. 154:1737–52.

Muller-Parker, G., Lee, K.W. & Cook, C.B. 1996. Changes in the ultrastructure of symbiotic zooxanthellae (*Symbiodinium* sp. Dinophyceae) in fed and starved sea anemones maintained under high and low light. *J. Phycol.* 32:987–94.

Muller-Parker, G., McCloskey, L.R., Hoegh-Guldberg, O. & McAuley, P.J. 1994. Effect of ammonium enrichment on animal and algal biomass of the coral *Pocillopora damicornis*. *Pac. Sci.* 48:273–83.

Muscatine, L., Falkowski, P.G., Dubinskey, Z., Cook, P.A. & McCloskey, L.R. 1989. The effect of external nutrient resources on the population dynamics of zooxanthellae in a reef coral. *Proceedings of the Royal Society London B.* 236:311–24.

Palincsar, J.S., Jones, W.R. & Palincsar, E.E. 1988. Effects of isolation of the endosymbiont *Symbiodinium microadriaticum* (Dinophyceae) from Its host *Aiptasia pallida* (Anthozoa) on cell wall ultrastructure and mitotic rate. *Trans. Am. Microsc. Soc.* 107:53–66.

Parkinson, J.E., Coffroth, M.A. & LaJeunesse, T.C. 2015. New species of Clade B *Symbiodinium* (Dinophyceae) from the greater Caribbean belong to different functional guilds: *S. aenigmaticum* sp. nov., *S. antillogorgium* sp. nov., *S. endomadracis* sp. nov., and *S. pseudominutum* sp. nov. *J. Phycol.* 51:850–8.

Pasaribu, B., Li, Y.-S., Kuo, P.-C., Lin, I.-P., Tew, K.S., Tzen, J.T.C., Liao, Y.K. et al. 2016. The effect of temperature and nitrogen deprivation on cell morphology and physiology of *Symbiodinium*. *Oceanologia*. 58:272–8.

Pasaribu, B., Weng, L.-C., Lin, I.-P., Camargo, E., Tzen, J.T.C., Tsai, H., Ho, S.-L. et al. 2015. Morphological variability and distinct protein profiles of cultured and endosymbiotic *Symbiodinium* cells isolated from *Exaiptasia pulchella*. *Sci. Rep.* 5:15353.

Peng, S.E., Wang, Y.B., Wang, L.H., Chen, W.N.U., Lu, C.Y., Fang, L.S. & Chen, C.S. 2010. Proteomic analysis of symbiosome membranes in cnidaria-dinoflagellate endosymbiosis. *Proteomics*. 10:1002–16.

Perez, S.F., Cook, C.B. & Brooks, W.R. 2001. The role of symbiotic dinoflagellates in the temperature-induced bleaching response of the subtropical sea anemone *Aiptasia pallida*. *J. Exp. Mar. Bio. Ecol.* 256:1–14.

Ralph, P.J., Gademann, R. & Larkum, A.W.D. 2001. Zooxanthellae expelled from bleached corals at 33°C are photosynthetically competent. *Mar. Ecol. Prog. Ser.* 220:163–8.

Ricci, C.A., Kamal, A.H., Chakrabarty, J.K., Ledbetter, B.E., Chowdhury, S.M. & Mydlarz, L.D. 2020. The cell-surface protein composition of a coral symbiont , *Breviolum psygmophilum*, reveals a mechanism for host specificity and displays dynamic regulation during temperature stress. *Marine Biology*. 167:66.

Rosset, S., Angelo, C.D. & Wiedenmann, J. 2015. Ultrastructural biomarkers in symbiotic algae reflect the availability of dissolved inorganic nutrients and particulate food to the reef coral holobiont. *Front. Mar. Sci.* 2:103.

Rosset, S., Wiedenmann, J., Reed, A.J. & D'Angelo, C. 2017. Phosphate deficiency promotes coral bleaching and is reflected by the ultrastructure of symbiotic dinoflagellates. *Mar. Pollut. Bull.* 118:180–7.

Roy, S., Jagus, R. & Morse, D. 2018. Translation and translational control in dinoflagellates. *Microorganisms*. 6.

Santamaria, G., Esposito, C.L., Cerchia, L., Benvenuto, G., Nanjappa, D., Sarno, D., Zingone, A. et al. 2015. Aptamers are an innovative and promising tool for phytoplankton taxonomy and biodiversity research. *Chemistry and Ecology*. 31:92–103.

Santos, S.R., Taylor, D.J. & Coffroth, M.A. 2001. Genetic comparisons of freshly isolated versus cultured symbiotic dinoflagellates: Implications for extrapolating to the intact symbiosis. *J. Phycol.* 37:900–12.

Schwarz, J.A., Weis, V.M. & Potts, D.C. 2002. Feeding behavior and acquisition of zooxanthellae by planula larvae of the sea anemone *Anthopleura elegantissima*. *Mar. biol*. 140:471–8.

Seibt, C. & Schlichter, D. 2001. Compatible intracellular ion composition of the host improves carbon assimilation by zooxanthellae in mutualistic symbioses. *Naturwissenschaften*. 88:382–6.

Smith, G.J. & Muscatine, L. 1999. Cell cycle of symbiotic dinoagellates : variation in G_1 phase-duration with anemone nutritional status and macronutrient supply in the *Aiptasia pulchella-Symbiodinium pulchrorum* symbiosis. *Marine Biology*. 134:405–18.

Sproles, A.E., Oakley, C.A., Krueger, T., Grossman, A.R., Weis, V.M., Meibom, A. & Davy, S.K. 2020. Sub-cellular imaging shows reduced photosynthetic carbon and increased nitrogen assimilation by the non-native endosymbiont *Durusdinium trenchii* in the model cnidarian Aiptasia. *Environ. Microbiol.* 22:3741–53.

Stambler, N. & Stimson, J. 1991. Effects of nutrient enrichment and water motion on the coral *Pocillopora damicornis*. *Pacific Science*. 45:299–307.

Steele, R.D. 1975. Stages in the life history of a symbiotic zooxanthella in pellets extruded by its host *Aiptasia tagetes* (Duch and Mich.) (Coelenterata, Anthozoa). *Biol. Bull.* 149:590–600.

Stochaj, W.R. & Grossman, A.R. 1997. Differences in the protein profiles of cultured and endosymbiotic *Symbiodinium* sp. (Pyrrophyta) from the anemone *Aiptasia pallida* (Anthozoa). *J. Phycol.* 33:44–53.

Tansik, A.L., Fitt, W.K. & Hopkinson, B.M. 2017. Inorganic carbon is scarce for symbionts in scleractinian corals. *Limnol. Oceanogr.*

Thornhill, D.J., Howells, E.J., Wham, D.C., Steury, T.D. & Santos, S.R. 2017. Population genetics of reef coral endosymbionts (*Symbiodinium*, Dinophyceae). *Mol. Ecol.* 26:2640–59.

Tivey, T.R., Parkinson, J.E. & Weis, V.M. 2020. Host and symbiont cell cycle coordination is mediated by symbiotic state, nutrition, and partner identity in a model cnidarian-dinoflagellate symbiosis. *MBio*. 11:e02626-19.

Tonelli, R.R., Colli, W. & Alves, M.J.M. 2012. Selection of binding targets in parasites using phage-display and aptamer libraries in vivo and in vitro. *Front. Immunol.* 3:1–16.

Wang, L.-H., Chen, H.-K., Jhu, C.-S., Cheng, J.-O. & Chen, C.-S. 2015. Different strategies of energy storage in cultured and freshly isolated *Symbiodinium* sp. *Journal of Phycol.* 1136:1127–36.

Weis, V.M. 2019. Cell biology of coral symbiosis: Foundational study can inform solutions to the coral reef crisis. *Integr. Comp. Biol.* 59:845–55.

Weng, L.-C., Pasaribu, B., Tsai, C.-H., Chen, C.-S. & Jiang, P.-L. 2014. Droplet Accumulation and Alters Fatty Acid Metabolism in Symbiotic Dinoflagellates Isolated from *Aiptasia pulchella*. *Scientific Reports*. 4:5777.

Xiang, T., Lehnert, E., Jinkerson, R.E., Clowez, S., Kim, R.G., DeNofrio, J.C., Pringle, J.R. et al. 2020. Symbiont population control by host-symbiont metabolic interaction in Symbiodiniaceae-cnidarian associations. *Nat. Commun.* 11:108.

Nutrient	Natural seawater in Curaçao (den Haan et al. 2016)	f/2	K	L1	Prov50	ASP-8A	Daigo's IMK
NO_3	0.15 ± 0.02	882	882	882	882	605	2353
NH_4	1.45 ± 0.14	0	50	0	50	15	50
PO_4	0.032 ± 0.003	36.2	0	36.2	36.2	74	38.6

Table 3.1 – **Nutrient concentrations from a representative coral reef seawater sample and culture media commonly used for growing Symbiodiniaceae.**
All values are in μM. Table adapted from Krueger (2020).

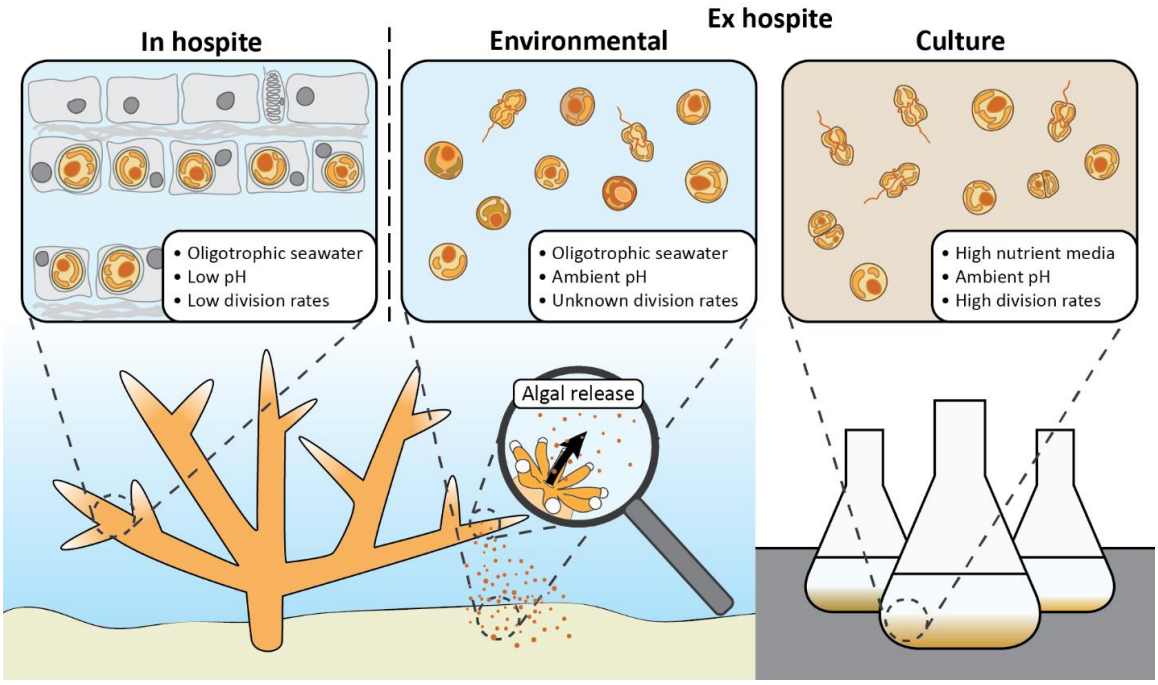

Fig. 3.1 – **Differences between Symbiodiniaceae *in hospite*, *ex hospite* in the environment, and *ex hospite* in culture.**
Symbionts *in hospite* are engaged in an intracellular, endosymbiotic relationship and are contained inside host cells within host symbiosome membranes. Symbiodiniaceae *in hospite* generally have low division rates and the symbiosome compartment is acidic. Typically, a single species dominates the population *in hospite*, but background strains are also present. Environmental Symbiodiniaceae are found in the sediment and seawater and include both transient symbionts that are released by hosts and non-symbiotic species that have entirely free-living life histories. Cultured symbionts have high division rates due to their nutrient rich media and are generally monoclonal populations. Some cultures have been maintained *ex hospite* for decades, and strains may now be significantly different from their original isolates.

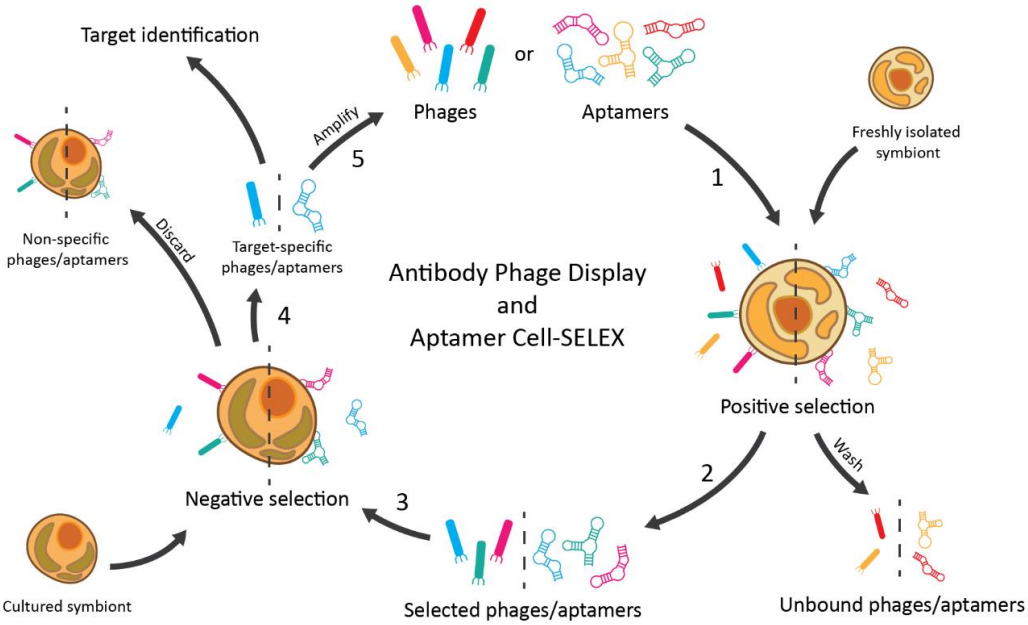

Fig. 3.2. – **A schematic illustration of both antibody phage display and aptamer Cell-SELEX.**
In antibody phage display, phages express antibodies on their surface and contain the genetic code for the respective antibody. Aptamers are self-folding RNA or DNA oligonucleotides that bind specifically to targets. 1) The ligands (phages or aptamers) are incubated together with target cells in a positive selection step. 2) Unbound ligands are washed away and selected ligands are eluted from target cells. 3) Selected ligands are incubated with off-target cells in a negative selection step, important for removing non-specific ligands. For example, in the case of Symbiodiniaceae, this would remove ligands that bind to cellulose and other constitutively present targets. 4) Target-specific ligands that did not bind to off-target cells are recovered. 5) Target-specific ligands are amplified – the phages are amplified in *E. coli* and aptamers are amplified by PCR. Both methods undergo several cycles of selection to obtain ligands that are highly specific to their targets. After several rounds of selection, antibodies and aptamers can be used in affinity-based purification methods to purify their target proteins that can then be identified through tandem mass spectrometry.

4. Algae from Aiptasia egesta are robust representations of Symbiodiniaceae in the free-living state

Shumpei Maruyama
Julia R. Unsworth
Valeri Sawiccy
Students of Oregon State University's Z362 Spring 2021
Virginia M. Weis

Formatted for *PeerJ*
PeerJ, Inc.
PO Box 910224
San Diego, CA 92191 USA

4.1 Abstract

Many cnidarians rely on their dinoflagellate partners from the family Symbiodiniaceae for their ecological success. Symbiotic species of Symbiodiniaceae have two distinct life stages: inside the host, *in hospite,* and outside the host, *ex hospite*. Several aspects of coral-algal symbiosis can be understood by comparing these two life stages. Most commonly, algae in culture are used in comparative studies to represent the *ex hospite* life stage, however, nutrition becomes a confounding variable for this comparison because algal culture media is nutrient rich, while algae *in hospite* are sampled from hosts maintained in oligotrophic seawater. In contrast to cultured algae, expelled algae may be a more robust representation of the *ex hospite* state, as the host and expelled algae are in the same seawater environment, removing differences in culture media as a confounding variable. Here, we studied the physiology of algae released from the sea anemone *Exaiptasia diaphana* (commonly called Aiptasia), a model system for the study of coral-algal symbiosis. In Aiptasia, algae are released in distinct pellets, referred to as egesta, and we explored its potential as an experimental system to represent Symbiodiniaceae in the *ex hospite* state. Observation under confocal and differential interference contrast microscopy revealed that egesta contained discharged nematocysts, host tissue, and were populated by a diversity of microbes, including protists and cyanobacteria. Further experiments revealed that egesta were released at night. In addition, algae in egesta had a higher mitotic index than algae *in hospite,* were photosynthetically viable for at least 48 hrs after expulsion, and could competently establish symbiosis with aposymbiotic Aiptasia. We then studied the gene expression of nutrient-related genes and studied their expression using qPCR. From the genes tested, we found that algae from egesta closely mirrored gene expression profiles of algae *in hospite* and were dissimilar to those of cultured algae, suggesting that algae from egesta are in a nutritional environment that is similar to their *in hospite* counterparts. Altogether, evidence is provided that algae from Aiptasia egesta are a robust representation of Symbiodiniaceae in the *ex hospite* state and their use in experiments can improve our understanding of cnidarian-algal symbiosis.

4.2 Introduction

The family Symbiodiniaceae is a diverse group of dinoflagellates, many of which form symbioses with a variety of cnidarian hosts, including corals and sea anemones. In this symbiosis, the algal symbiont is housed within host gastrodermal cells where they provide photosynthate to the host and in return, the host provides inorganic nutrients, protection and a high light environment (Davy et al. 2012, Marcelino et al. 2013). The two partners must work cooperatively to maintain and regulate symbiosis. For example, the host utilizes carbonic anhydrase and bicarbonate transporters to supply inorganic carbon to the symbiont to maximize photosynthesis (Tansik et al. 2017, Koch et al. 2020). Reciprocally, the symbiont may be modulating the host's immune system to prevent immune destruction or expulsion by the host (Detournay et al. 2012, Mansfield et al. 2017, Jacobovitz et al. 2021, Jinkerson et al. 2022). However, our understanding of the cellular mechanisms involved in maintaining symbiosis remains limited.

Studies often compare the biology of Symbiodiniaceae between its two life stages: inside the host, *in hospite* and outside the host, *ex hospite*. In this comparison, algae that are freshly isolated from the host are used to represent algae *in hospite*, while cultured algae are often used to represent algae *ex hospite*. Studies have found that compared to algae in culture, algae *in hospite* have lower cell division rates (Smith & Muscatine, 1999; Tivey, Parkinson & Weis, 2020) and differential expression of genes that are tightly linked to nutrient limitation (Maor-Landaw et al. 2020, Xiang et al. 2020, Cui et al. 2022). Based on these data, it is commonly hypothesized that the host limits nutrient transfer to the symbiont as a mechanism to maintain a stable population of symbionts (Falkowski et al. 1993, Smith and Muscatine 1999, Tivey et al. 2020, Xiang et al. 2020, Cui et al. 2022). This comparison, however, introduces nutrition as a confounding variable because while algae *in hospite* are sampled from hosts maintained in oligotrophic seawater, algae *ex hospite* are sampled from cultures grown in nutrient-rich media. The nutrient-depleted phenotype found in algae *in hospite* could therefore not be caused by host-inhibitory mechanisms and instead simply reflect the low nutrient availability in the water column compared to the nutrient-replete state of culture (for in-depth discussion, see Maruyama & Weis, 2021). In fact, studies have found that supplementing nutrients to the host, by feeding or by the addition of inorganic nutrients

to the water column, will return the algae to a nutrient-enriched phenotype as measured by cell division rates or gene expression profiles, suggesting that the host readily supplies nutrients to their symbionts when available (Hoegh-Guldberg and Smith 1989, Stambler et al. 1991, Falkowski et al. 1993, Hoegh-Guldberg 1994, Muller-Parker et al. 1994, Smith and Muscatine 1999, Ferrier-Pagès et al. 2001, Houlbrèque et al. 2004, Rosset et al. 2015, Tivey et al. 2020, Xiang et al. 2020, Cui et al. 2022). Further work is necessary to tease apart the effects of symbiosis and nutrient availability on algal phenotypes to determine whether the host is limiting nutrient transfer to its symbionts.

Multiple transcriptomic studies have found that nutrient-related genes are differentially expressed between algae *in hospite* and those in culture (Maor-Landaw et al. 2020, Xiang et al. 2020, Cui et al. 2022). Examples include ammonium transporter *AMT*, nitrate transporter *NRT*, purine nucleoside permease *NUP*, and nitrate reductase *NR* that are upregulated and glutamine synthetase *GS* that is downregulated in algae *in hospite* compared to those in culture. This gene expression pattern is indicative of nutrient limitation in Symbiodiniaceae and other marine algae (Hildebrand, 2005; Kang et al., 2007; Xiang et al., 2020). Some differentially expressed genes, however, are probably not linked to nutrition, such as the sugar transporter *SWEET1*, that is hypothesized to play a role in transferring photosynthate to the host. Sampling a more robust representation of Symbiodiniaceae in the *ex hospite* state that controls for nutrient availability could confirm whether these differentially regulated genes are reflective of nutrition, the symbiotic state, or both.

In cnidarian-algal symbiosis, the host regularly expels viable algae as a homeostatic mechanism to maintain a stable population of symbionts (Steele, 1975; Hoegh-Guldberg, McCloskey & Muscatine, 1987; Hill & Ralph, 2007; Thornhill et al., 2017). In this study, we hypothesized that sampling expelled algae as a representation of the *ex hospite* state in Symbiodiniaceae for comparison with their *in hospite* counterparts could remove nutrition as a confounding variable, as both the host and the expelled algae are in the same oligotrophic seawater environment. Therefore, physiological and/or gene expression differences found between algae *in hospite* and expelled algae in this comparison would be modulated by the host, and not be masked by the high-nutrient state of cultured algae as in the traditional comparison. In the sea anemone *Exaiptasia*

diaphana (commonly called Aiptasia), a model system for the study of coral-algal symbiosis, algae are released in distinct, brown pellets, herein referred to as egesta. The brown egesta primarily consist of algae, and are released separately from pellets containing digested food (Steele, 1975). The discrete nature of egesta, with their high abundance of algae, made them a promising experimental system for sampling purposes.

To begin the practice of sampling expelled algae in symbiosis studies, we first explored the basic biology of algae from Aiptasia egesta and characterized egesta appearance, timing of egesta expulsion, and characteristics of the algae including mitotic index, photosynthetic health, and ability to initiate symbiosis with new hosts. Then, we studied the gene expression of several nutrient-related genes to determine the nutrient status of algae from egesta. Finally, we discuss several practical considerations of the use of algae from Aiptasia egesta as an experimental model system to represent Symbiodiniaceae in the *ex hospite* state.

4.3 Materials & Methods

Animal and algal culture maintenance

Aiptasia (clone ID: H2) symbiotic with *Breviolum minutum* (culture ID: SSB01) and SSB01 cultures were used in this study. Animals were maintained in Coralife Instant Ocean (Tempe, AZ, USA) artificial seawater (ASW), and algae were maintained in F/2 media made in filtered artificial seawater (FSW). Animals and algae were housed at 25 °C in a Percival AL-41L4 incubator (Perry, IA, USA) with Zoo Med Laboratories (San Luis Obispo, CA, USA) 10,000k fluorescent lamps set to 40 µmol photons/m^2/s using shadecloth on a 12h:12h light:dark cycle. Aposymbiotic anemones were originally bleached using menthol (Matthews *et al.*, 2016) and maintained symbiont-free by incubation in the dark for several months before use. Unless otherwise stated, animals were fed three times a week *ad libitum* with freshly hatched brine shrimp and the water was changed three times a week with ASW.

Confocal imagery and light microscopy

Live egesta samples were imaged on a Zeiss LSM 780 NLO confocal microscope system (Oberkochen, Germany). Images were taken on three separate channels, with

excitation from a 405 nm Diode, Argon (488), and 633 nm HeNe. Emission was detected between 410-470 nm, 491-572 nm, and 647-722 nm, respectively. Simultaneously, using laser illumination, a transmitted light detector (T-PMT) acquired transmitted light images in bright field. Confocal z-stack images were processed for pseudocoloring and merged to create a maximum intensity projection using ZEN Black (Carl Zeiss AG) and ImageJ software. Separately, differential interference contrast (DIC) images were obtained using an Olympus Vanox-T AH2 microscope to image nematocysts.

Time-lapse of egesta release

Sixteen to twenty Aiptasia were transferred to twenty cm diameter glass Carolina Biological (Burlington, NC, USA) culture dishes with one L of ASW. Animals were allowed to settle for at least 24 hrs prior to time-lapse photography. Immediately before imaging began, the culture dish was cleaned with a cotton swab and the water was changed. For time-lapse imaging, a Canon 5D Mark II DSLR with external flash was set to photograph the entire dish hourly for 24 hrs. To control for any effect of cleaning on timing of egesta release, two time-lapses (Experiment 1 & 2) began at 16:30 and two other time-lapses (Experiment 3 & 4) began at 22:30. Following their original light schedule, lights were set to come on at 7:00 and off at 19:00. Animals were not fed during the experiment. Each image was analyzed with ImageJ using the Cell Counter plugin, and each dark particle in an image were counted as egesta. The number of egesta in each time point was subtracted from the total number of egesta in the previous time point to calculate the quantity of egesta released in the hour. The quantity of egesta was then normalized to anemone number per container to obtain the number of egesta per anemone at each time point.

Mitotic Index

Thirty-two Aiptasia were housed individually in two mL FSW in 24-well plates and allowed to settle for 24 hrs. After settlement, each well was cleaned with a cotton swab and the water was changed. Egesta were collected after an additional 24 hrs. Of the 32 original anemones, eight released egesta large enough to be imaged. The eight anemones that released usable egesta were homogenized with a microcentrifuge pestle in

300 µL FSW, spun down at 800 x g for five min, and resuspended in twenty µL FSW. Resuspended algae and egesta were then imaged under DIC light microscopy.

Images were analyzed using ImageJ with the Cell Counter plugin by students enrolled in Oregon State University's Spring 2021 Z362 Invertebrate Biology laboratory. Following the method of Baghdasarian and Muscatine (2000), individual cells in each image were scored based on presence of a cell wall division plate, and at least 700 cells were counted per sample. Students were tasked to save their cell counter files, and their counts were manually verified by loading the counter files onto the images. The mitotic index was calculated as the percent of cells in the entire population that were undergoing division and paired t-tests were performed for statistical analysis.

Photosynthetic health and cell viability

Egesta were collected from Aiptasia less than 24 hrs after last cleaning, to ensure collection of freshly expelled egesta. All collected egesta were pooled together and pelleted at 800 x g for five min, the supernatant was removed and the cells resuspended in one mL FSW. The pooled sample was divided into two 500 µL aliquots. One was kept intact, while the other was homogenized using a motorized microcentrifuge pestle. From the homogenized sample, twenty µL was used to quantify cell number using a Thermo Fisher Scientific (Waltham, MA, USA) Countess II automated cell counter. Homogenized and intact egesta samples were then dispensed into twelve well plates in 95 µL (20,000 cells per sample, $n = 5$) and FSW was added up to two mL. Cultured algae (SSB01) was also collected, pelleted at 800 x g for five min and resuspended in FSW. Five culture samples of 20,000 cells were then dispensed in twelve well plates and FSW added up to two mL. All plates were then returned to their original incubator.

Maximum quantum yield of photosystem II (Fv/Fm) was obtained using a Light Induced Fluorescence Transient Fast Repetition Rate fluorometer (LIFT-FRRf; Soliense Inc, Santa Cruz, CA). Fv/Fm was measured once a day at 13:00 following dark acclimation for 30 min to ensure measurement of maximum quantum yield. To measure Fv/Fm, excitation was delivered at 475 nm wavelength in four phases and fluorescence detected at 685 nm. The first phase was a saturating sequence of 100 flashlets, each lasting 0.7 µs with a 1.5 µs gap. The second phase was a relaxation phase of 80 flashlets

beginning with a gap of twenty μs, increasing exponentially until the end of the sequence. The third phase was a sequence of 1600 flashlets lasting two μs each with a 40 μs gap. The final relaxation phase was identical to the second phase. Data were fitted using LIFT software with the three-component exponential model (SEQ_3).

To test the ratio of live and dead cells, we used an Evans Blue cell viability dye (Morera & Villanueva, 2009). Approximately ten pellets of egesta less than 24 hrs old were collected and homogenized together using a motorized microcentrifuge pestle in 500 μL of ASW. Cells were then pelleted at 800 x g for five min and the pellet resuspended in 100 μL of FSW. Cells were then stained with 20 μL of Evans Blue dye and incubated for ten min. The sample was imaged under light microscopy and algal cells that internalized the blue dye were counted as dead while cells that were not stained were counted as alive.

Inoculation of Aiptasia with algae

Aposymbiotic anemones (n = 9) were plated into 24 well plates in two mL FSW. Plates were placed in their original incubators set on a 12h:12h light:dark cycle for 72 hrs. After incubation in the light, animals were manually checked under fluorescence microscopy to verify aposymbiotic status.

Egesta were collected from Aiptasia less than 24 hrs after last cleaning. Samples of both egesta and algae in culture were pelleted at 800 x g for five min and resuspended in 300 μL FSW. To obtain freshly isolated symbionts, one symbiotic anemone was homogenized using a motorized microcentrifuge pestle in 300 μL of FSW. Egesta and cultured algae were also homogenized using a motorized microcentrifuge pestle. All samples were then washed twice by centrifugation at 800 x g for five min and resuspension in two mL FSW. Algal samples were counted using a Countess II automated cell counter, and samples were diluted to 1×10^6 algal cells/mL in FSW.

To inoculate aposymbiotic Aiptasia, 1×10^5 algal cells in a 100 μL volume were gently pipetted over anemone mouths. Immediately after the addition of algae, twenty μL of brine shrimp extract was pipetted to anemones to induce a feeding response. Negative controls were fed the brine shrimp extract with no algae added. Anemones were allowed to take up algae for 24 hrs. The water was then changed, and anemones were moved to

clean wells of a 24 well plate in two mL FSW. After an additional 24 hrs, the anemones were imaged under fluorescence microscopy. Briefly, anemones were relaxed in 0.18 M $MgCl_2$ dissolved in FSW, and images of three tentacles per anemone were taken in several focal depths under brightfield and under the red Filter Set 15 (Carl Zeiss) to visualize algal cell auto-fluorescence using a Zeiss Axio Observer inverted microscope. Each manually contructed z-stack was merged into a single image using Adobe Photoshop. Symbiont density was determined from each image using ImageJ as the number of fluorescent algal cells normalized to two-dimensional tentacle area.

Primer design

Target genes were selected based on their function and differential expression between algae in culture and *in hospite* from Xiang et al. (2020). Primer and transcript sequences were obtained from Xiang et al. (2015, 2020) for an ammonium transporter (*AMT*, transcript ID: s6_38207), a nitrate transporter (*NRT*, s6_422), purine nucleoside permease (*NUP*, s6_27864), and nitrate reductase (*NR*, s6_34). New primers were designed for glutamine synthetase (*GS*, s6_5551), photosystem II protein D1 (*psbA*, s6_1009), and a sugar transporter (*SWEET1*, s6_35311). We chose to study the expression of *psbA* because its expression was consistent between algae in culture and *in hospite* (Xiang et al., 2020). Cyclophilin was chosen as an algal housekeeping gene (Rosic et al. 2011) and primers were designed to be specific for *B. minutum* and not amplify Aiptasia cyclophilin. Primer pairs were verified for amplification efficiency of at least 90% by assessing the slope of standard curves generated from quantitative PCR reactions of serial dilutions of template cDNA. Primers sequences are available in Supplementary Table B1.

Quantitative PCR

To quantify gene expression, 54 anemones were placed in three separate containers with 500 mL ASW (eighteen anemones per container). The average oral disk diameter of the anemones was 5.4 mm (data not shown). Anemones were fed every other day *ad libitum*. Egesta containing algae were collected 24 hrs after feeding, and the container cleaned after egesta were collected. We did not sample egesta containing

digested food and they are easy to distinguish due to the pink color of the cartenoids from digested *Artemia* sp. nauplii. To obtain enough material for gene expression studies (approximately 1 x 10^6 cells), egesta were collected a total of six times from each container. Immediately after collection, egesta were processed for RNA extraction as follows. First, egesta were homogenized in cold FSW with a motorized microcentrifuge pestle. To completely isolate algae from host cells, the sample was then further homogenized by passing the sample seven times through a three mL syringe fitted with a 23 gauge needle. Following protocols from Xiang et al. (2020), the homogenate was then loaded on a 50% isotonic Percoll solution made in FSW and spun for twenty min at 9000 x g. The supernatant containing host material was carefully removed, and the algae were resuspended in one mL cold FSW. The sample was then pelleted at 3,000 x g for five min and the supernatant removed. The pellet was then frozen at -80 °C until further processing.

To obtain algae *in hospite*, four random anemones from each container were sampled immediately after the last collection of egesta and processed for RNA extraction following the same procedure as those for egesta, and the algal pellets frozen for at least ten min. Three independent, but identical cultures of SSB01 grown in F/2 culture media were made simultaneously and allowed to grow for three weeks. These cultures were also sampled and followed the same procedure for RNA processing and the algal pellets were frozen for at least ten min.

After the final sample of egesta was collected, the frozen samples from each repeated collection were pooled together corresponding to their respective Aiptasia containers. Each frozen freshly isolated, culture, and egesta sample was then resuspended in 300 µL Trizol. Sterilized glass beads were added to the sample, and the sample was homogenized with a bead beater for two min set at 4,000 RPM. The beads were then removed, the samples were centrifuged at 16,000 x g for one min, and the supernatant containing RNA was extracted. The RNA was purified using a Zymo Direct-zol kit following the manufacturer's instructions. RNA samples were further processed using a Turbo DNA-free kit to remove genomic DNA contaminants. Samples were then purified again using a New England Biolabs (Ipswich, MA, USA) Monarch RNA purification kit,

followed by a One-Step PCR inhibitor removal kit to remove carbohydrate contaminants. The RNA samples were analyzed for purity and concentration using a Nanodrop.

All samples were then diluted to ten ng/µL and cDNA was synthesized from nine µL (90 ng total) of RNA in 30 µL reactions using the New England Biolabs Protoscript II cDNA synthesis kit with oligo $d(T)_{23}$ VN primers following the manufacturer's instructions. Quantitave PCR reactions were performed in twenty µL volumes using 1X Power SYBR Green PCR Mastermix, 0.5 µM of each primer pair, and one µL of template cDNA. A BioRad CFX96 Real-Time System was used to carry out reactions using a two-step amplification phase (95 °C/ten min, followed by 40 cycles of 95 °C/ten s and 58 °C/30 s) and then a melting-curve analysis performed to confirm the presence of single amplicons. No-reverse transcription, no-primer, and no-template controls were included as negative controls.

For each sample and target gene, Δ*Ct* values were calculated by subtracting the *Ct* value of the target gene from the *Ct* value of the housekeeping gene (cyclophilin). Then, the Δ*Ct* value was subtracted from the mean Δ*Ct* value of corresponding genes from cultured algae samples to calculate relative expression ΔΔ*Ct*. Fold gene expression was then calculated as $2^{-\Delta\Delta Ct}$ for each gene from each sample. Statistical analyses were conducted on ΔΔ*Ct* values for each gene by ANOVA and post-hoc Tukey's HSD.

4.4 Results

Physical characteristics of egesta

Egesta observed under confocal microscopy revealed several autofluorescent features (Figure 1). Chlorophyll autofluorescence was readily apparent from *B. minutum* under 633 nm excitation. Under 488 nm excitation, autofluorescence of putative pyrenoids from *B. minutum*, phycobillins from cyanobacteria, and host tissue were detected (Figure 1A). A signal was also detected under 405 nm excitation within egesta (Figure 1A), and we hypothesize that its origin comes from dead remains of an unidentified ciliate protist that autofluoresced under the same excitation wavelength (Figure 1C). Differential interference contrast microscopy revealed that the surface of egesta contained discharged nematocysts (Figure 1D) and the remains of nematocyst capsules (Figure 1E). Egesta were also colonized by several kinds of unidentified protists

and microbes (data not shown). None of the protists were observed to phagocytose *B. minutum*.

Algal physiology

Egesta were released at night, beginning five to six hrs after lights off and peaking at seven to eight hrs after lights off (Figure 2A). The rate of release slowly decreased until lights were turned on, and release decreased to background levels at the onset of light. The timing of dish cleaning prior to time-lapse imaging had a minor effect on timing of egesta release by delaying the time of peak egesta release by one hr (Figure 2A). We noticed that the size of egesta was not uniform (data not shown) – presumably containing different amounts of algae, but we were unable to quantify the size of egesta and the number of symbionts per egestum in our experiments. Therefore, the time series data reflects only the number of discrete pellets that were released by anemones and is a proxy for the true number of expelled algae.

The released algae were alive and biologically active. The mitotic index of algae from egesta was higher than that of algae *in hospite* (Figure 2B; $p = 0.01$, paired t-test), and the photosynthetic health of algae in egesta, disrupted and intact, at time zero was the same as those in symbiotic anemones (Figure 2C). Algae from egesta then declined in photosynthetic health over time, with Fv/Fm remaining relatively high for two days before declining rapidly, with photosynthetic health becoming unmeasurable by day five. Mechanically disrupting the egesta did not have a significant impact on photosynthetic health. Algae from culture started at a lower Fv/Fm than those from egesta or anemones, but photosynthetic health did not decline over time. Cell staining with Evans Blue dye found that 1.5% (17 out of 1132 total cells) of algae from egesta were dead. Algae from egesta were capable of initiating symbiosis with aposymbiotic Aiptasia, reaching symbiont densities just as high as Aiptasia inoculated with cultured and freshly isolated algae (Figure 2D). Negative controls remained aposymbiotic for the duration of the experiment (data not shown). While freshly isolated symbionts reached the highest density of symbionts, the difference was not significant ($p = 0.06$, Kruskal-Wallis test).

Gene expression

Nitrogen transporter and nitrogen metabolism genes, *AMT*, *NRT*, *NUP*, and *NR*, were significantly upregulated in algae from egesta and algae *in hospite* compared to culture (Figure 3). Expression levels of these genes were not significantly different between algae from egesta and algae *in hospite*. Glutamine synthetase, *GT*, gene expression showed no significant difference between algal sources. Expression levels of *psbA* and sugar transporter, *SWEET1*, were highest in cultured algae compared to algae from egesta and algae *in hospite*. Overall, with the exception of glutamine synthetase, expression levels of the tested genes were similar between algae from egesta and algae *in hospite* compared to algae in culture.

4.5 Discussion

Egesta are sticky communities of microbes

Egesta primarily consisted of *B. minutum* as previously reported (Steele, 1975) and these egesta were released separately from digested food. In addition, egesta contained host material and a variety of microbes (Figure 1). In sample handling, we noted that egesta were sticky and tended to adhere to plastic surfaces. The stickiness is possibly caused by the presence of fired nematocysts that were present on the egesta surface (Figure 1D, 1E). The presence of nematocysts, both fired and unfired, were previously described in algae-containing egesta from the sebae anemone, *Heteractis crispa* (Alan Verde, Cleveland & Lee, 2015). The authors noted that egesta released by *H. crispa* were consumed by symbiotic anemonefish (Alan Verde, Cleveland & Lee, 2015). It is not known if other animals consume Aiptasia egesta in nature, but if so, they may aid in algal dispersal, as algae often survive digestion (Parker 1984, Grupstra et al. 2021, 2022).

Evidence for the preferential expulsion of dividing algae

The mitotic index of algae was higher in egesta than *in hospite*, a result that agrees with previous findings in Aiptasia and several corals (Baghdasarian & Muscatine, 2000). It was hypothesized by Bhagdasarian and Muscatine (2000) that the host preferentially expels dividing algae. This hypothesis is well-supported from a temporal perspective because the egesta were released at night, and several studies have shown that

peak cell division occurs at night in cultured Symbiodiniaceae (Fitt & Trench, 1983; Smith & Muscatine, 1999; Yamashita & Koike, 2016; Fujise et al., 2018). In contrast, algal cell division was not elevated at night *in hospite* in Aiptasia (Smith & Muscatine, 1999). In that study, however, the dividing algae may have been expelled by the host prior to sampling, leading to the detection of unchanged cell division at night (Smith & Muscatine, 1999). Measuring the mitotic index of algae from egesta that are released over a diurnal cycle may help complete the picture of algal population dynamics *in hospite*.

Nutrition may also explain the higher division rates in algae from egesta compared to those *in hospite*. As nutrient availability has been shown to strongly predict cell division rates in Symbiodiniaceae (Smith and Muscatine 1999, Karako-Lampert et al. 2005, Tivey et al. 2020), the host may be preferentially expelling algae that sequester more nutrients for cell division than their more cooperative counterparts that remain undivided *in hospite*. Indeed, in competitive inoculation experiments, the symbiont *Durusdinium trenchii*, known to sequester more nitrogen than *B. minutum* in Aiptasia (Sproles *et al.*, 2020), failed to proliferate in Aiptasia in the presence of the homologous *B. minutum* (Gabay *et al.*, 2019). The preferential expulsion of dividing algae could be a mechanism for the removal of uncooperative symbionts. Future experiments using methods such as stable isotope analysis and NanoSIMS could investigate whether expelled algae sequester more nutrients than their counterparts *in hospite* and whether they continue to sequester more nutrients when establishing symbiosis with new hosts.

Timing of algal release varies depending on host taxa

The night-time release of algae in egesta by Aiptasia is not shared by other hosts. In several corals, including *Pocillopora damicornis* and *Acropora digitifera*, expulsion rates increased with the onset of light and peaked in the middle of the day (Stimson and Kinzie 1991, Koike et al. 2007). Other studies in the coral *Stylophora pistillata*, the soft coral *Xenia macrospiculata*, and the giant clam *Tridacna crocea* found no clear diel pattern for algal release (Hoegh-Guldberg, McCloskey & Muscatine, 1987; Umeki et al., 2020). Some corals released algae at night, with peak expulsion rates occuring at night for the corals *Millepora dichotoma* and *Heteroxenis fuscescens* (Hoegh-Guldberg, McCloskey & Muscatine, 1987). These contrasting patterns may reflect the actual

differences in patterns of algal release between species, or it could reflect differences in sampling methodology. As peak algal motility occurs at midday for Symbiodiniaceae (Fitt & Trench, 1983; Yamashita & Koike, 2016), some sampling approaches could miss subpopulations of algae in the vessel depending on time of sampling.

Algae from egesta are competent symbionts, but are short-lived ex hospite

Algae from egesta were short-lived *ex hospite* compared to their cultured counterparts, possibly due to nutrient limitation and/or the unknown effects of being in a microbial community (Figure 2C). This supports the hypothesis that expelled algae do not form stable populations *ex hospite* (Thornhill et al., 2017). However, freshly expelled algae from egesta had high viability and were fully capable of initiating symbiosis with aposymbiotic hosts (Figure 2D). In nature, larval and juvenile recruits probably rely on the continuous release of algae from adult hosts for a source of symbionts (Thornhill et al., 2017). This is supported by studies that found that the presence of adult coral colonies, presumably releasing algae, aided in symbiont acquisition by juvenile corals in aquarium experiments (Nitschke, Davy & Ward, 2016; Ali et al., 2019). In addition, a study found that a giant clam harboring Symbiodiniaceae released viable symbionts that were able to establish symbiosis with *Acropora tenuis* larvae (Umeki et al., 2020). Egesta are also potential vectors for the transmission of the microbiome between adults and recruits. In corals, there is evidence that *Acropora tenuis* and *Pocillopora damicornis* expel beneficial microbes into the seawater after spawning (Ceh, van Keulen & Bourne, 2013). Additional experiments are required to test these hypotheses, particularly in coral recruits.

Evidence that algae from egesta have a similar nutritional status to algae in hospite

In general, in our study, gene expression profiles of algae from egesta were more like those of algae *in hospite* than those of algae in culture. Several of the tested genes were nitrogen transporters or metabolizers. Transcriptional regulation of these genes is rapid (less than a day) in *B. minutum* and other marine algae in response to nutrient levels (Hildebrand, 2005; Kang *et al.*, 2007; Xiang *et al.*, 2020). As the algae from sampled egesta were 1-2 days old, changes in transcript levels for these genes should have

occurred in this experiment if nutrient levels had significantly changed once algae were expelled by their hosts. Our data suggest that algae from egesta have a similar nutritional status to algae *in hospite*, challenging the hypothesis that the host is actively limiting nutrient transport to the symbiont (Maor-Landaw, van Oppen & McFadden, 2020; Xiang et al., 2020; Cui et al., 2022). The identification of nutrient-related genes as differentially expressed in symbiosis studies that used cultured algae to represent the *ex hospite* state may instead reflect the nutrient-rich state of algae in culture (Maor-Landaw et al. 2020, Xiang et al. 2020, Cui et al. 2022). In addition, we found that the sugar transporter *SWEET1* (s6_35311), was not differentially regulated with symbiosis, challenging the hypothesis that this gene copy of *SWEET1* functions to transfer photosynthate from the symbiont to the host (Xiang et al., 2020). These results warrant further testing of gene expression in algae from egesta using high throughput methods to develop a better understanding of symbiosis.

Practical considerations for the use of Aiptasia *egesta in experiments*

Based on findings in this study, we argue that it is critical to further explore the biology of expelled algae as a representation of the *ex hospite* state of Symbiodiniaceae to better understand cnidarian-algal symbiosis. To facilitate their use by researchers, we discuss below practical considerations for the use of Aiptasia egesta in experiments.

We found that while egesta are primarily composed of Symbiodiniacean algae, they are also populated with microbes, including several protists and cyanobacteria. In our experience, processing of egesta by homogenization and separation by density centrifugation yielded samples of high purity. Collecting ample biological material for use in qPCR and inoculation experiments was difficult. To obtain 1×10^6 algal cells from egesta, pellets had to be collected six times every other day from approximately twenty anemones with an average oral disk size of 5.4 mm. We also found that collection was variable between days and yield was not consistent (data not shown). For collection of egesta, if Aiptasia are housed without water flow, we recommend using a glass pasteur pipet, as the egesta tended to stick to plastic pipets. Egesta can also be mistaken for pedal lacerates, so it is recommended that a dissection microscope be used to aid in identification. It is possible that various factors, such as anemone size, light levels, and

feeding, all influence the rate of egesta release, but these variables were not empirically tested. Another consideration is the induction of algal release by mild stress to increase sample biomass, however, the health of the algae may be affected, so this method will require further experimentation.

4.6 Conclusions

Overall, this study establishes the foundation for using Aiptasia egesta in experiments as a representation of algae in the *ex hospite* state. We found that egesta were released at night, and that algae from egesta had a higher mitotic index than algae *in hospite*, were photosynthetically active but short lived, and could establish symbiosis with new hosts. Finally, we found that algae from egesta had a similar gene expression profile to that of algae *in hospite* compared to algae in culture, warranting future high-throughput studies to determine symbiosis-specific genes in this comparison. Although there are limitations to the use of algae from egesta, their use in experiments alongside algae in culture and algae *in hospite* can provide valuable insight into cnidarian-algal symbiosis.

4.7 Acknowledgements

We would like to thank animal care staff, Isabella Hansen, Alex Bridge, Lily Miksell, Julia Johnston, Kyra Lenderman, and Noah Tjandra for maintaining Aiptasia used in experiments. We also thank Weis lab members, Erick White, Jun Cai, Keyla Plichon, Dr. Samuel Bedgood and visiting researcher Dr. Lucia Pita for feedback on drafts. We thank Dr. Tingting Xiang at University of North Carolina, Charlotte, for providing Aiptasia animals and algal culture used in experiments. Finally, we would like to thank the three reviewers for their critical feedback that allowed us to improve the manuscript.

4.8 Students of Oregon State University's Z362 Spring 2021

Dawson Loehner, Joseph Stewart, Bree Feliciano George, Emily Denise Miller, Sinaiah Sorcha Harrington, Julia Amber Kennedy, Lucas Parvin, Violet Carrillo, Alex Michael Bridge, Kaitlyn Ashley Allison, Kennedy Judith Grant, Jess Alt, Margaret Mae Zackery,

Conor Ringwald, Ian Reed, Neosha Hubbs, Madalyn Rose Machinski, Mahala Grace Gilbert, and Bell Hansen.

4.9 References

Alan Verde, E., Cleveland, A. & Lee, R.W. 2015. Nutritional exchange in a tropical tripartite symbiosis II: direct evidence for the transfer of nutrients from host anemone and zooxanthellae to anemonefish. *Mar. Biol.* 162:2409–29.

Ali, A., Kriefall, N.G., Emery, L.E., Kenkel, C.D., Matz, M.V. & Davies, S.W. 2019. Recruit symbiosis establishment and Symbiodiniaceae composition influenced by adult corals and reef sediment. *Coral Reefs*. 38:405–15.

Baghdasarian, G. & Muscatine, L. 2000. Preferential expulsion of dividing algal cells as a mechanism for regulating algal-cnidarian symbiosis. *Biol. Bull.* 199:278–86.

Ceh, J., van Keulen, M. & Bourne, D.G. 2013. Intergenerational transfer of specific bacteria in corals and possible implications for offspring fitness. *Microb. Ecol.* 65:227–31.

Cui, G., Liew, Y.J., Konciute, M.K., Zhan, Y., Hung, S.-H., Thistle, J., Gastoldi, L. et al. 2022. Nutritional control regulates symbiont proliferation and life history in coral-dinoflagellate symbiosis. *BMC Biol.* 20:103.

Davy, S.K., Allemand, D. & Weis, V.M. 2012. Cell biology of cnidarian-dinoflagellate symbiosis. *Microbiol. Mol. Biol. Rev.* 76:229–61.

Detournay, O., Schnitzler, C.E., Poole, A. & Weis, V.M. 2012. Regulation of cnidarian-dinoflagellate mutualisms: Evidence that activation of a host TGFβ innate immune pathway promotes tolerance of the symbiont. *Dev. Comp. Immunol.* 38:525–37.

Falkowski, P.G., Dubinsky, Z., Muscatine, L. & McCloskey, L. 1993. Population control in symbiotic corals. *Bioscience*. 43:606–11.

Ferrier-Pagès, C., Schoelzke, V., Jaubert, J., Muscatine, L. & Hoegh-Guldberg, O. 2001. Response of a scleractinian coral, *Stylophora pistillata*, to iron and nitrate enrichment. *J. Exp. Mar. Bio. Ecol.* 259:249–61.

Fitt, W.K. & Trench, R.K. 1983. The relation of diel patterns of cell division to diel patterns of motility in the symbiotic dinoflagellate *Symbiodinium microadriaticum* Freudenthal in culture. *New Phytol.* 94:421–32.

Fujise, L., Nitschke, M.R., Frommlet, J.C., Serôdio, J., Woodcock, S., Ralph, P.J. & Suggett, D.J. 2018. Cell cycle dynamics of cultured coral endosymbiotic microalgae (*Symbiodinium*) across different types (species) under alternate light and temperature conditions. *J. Eukaryot. Microbiol.* 65:505–17.

Gabay, Y., Parkinson, J.E., Wilkinson, S.P., Weis, V.M. & Davy, S.K. 2019. Inter-partner specificity limits the acquisition of thermotolerant symbionts in a model cnidarian-dinoflagellate symbiosis. *ISME J.* 13:2489–99.

Grupstra, C.G.B., Lemoine, N.P., Cook, C. & Correa, A.M.S. 2022. Thank you for biting: dispersal of beneficial microbiota through "antagonistic" interactions. *Trends Microbiol.*

Grupstra, C.G.B., Rabbitt, K.M., Howe-Kerr, L.I. & Correa, A.M.S. 2021. Fish predation on corals promotes the dispersal of coral symbionts. *Anim Microbiome.* 3:25.

Hildebrand, M. 2005. Cloning and functional characterization of ammonium transporters from the marine diatom *Cylindrotheca fusiformis* (Bacillariophyceae). *J. Phycol.* 41:105–13.

Hill, R. & Ralph, P.J. 2007. Post-bleaching viability of expelled zooxanthellae from the scleractinian coral *Pocillopora damicornis*. *Mar. Ecol. Prog. Ser.* 352:137–44.

Hoegh-Guldberg, O. 1994. Population dynamics of symbiotic zooxanthellae in the coral *Pocillopora damicornis* exposed to elevated ammonium [$(NH_4)_2SO_4$] concentrations. *Pac. Sci.* 48.

Hoegh-Guldberg, O., McCloskey, L.R. & Muscatine, L. 1987. Expulsion of zooxanthellae by symbiotic cnidarians from the Red Sea. *Coral Reefs*. 5:201–4.

Hoegh-Guldberg, O. & Smith, G.J. 1989. Influence of the population density of zooxanthellae and supply of ammonium on the biomass and metabolic characteristics of the reef corals *Seriatopora hystrix* and *Stylophora pistillata*. *Mar. Ecol. Prog. Ser.*

Houlbrèque, F., Tambutté, E., Allemand, D. & Ferrier-Pagès, C. 2004. Interactions between zooplankton feeding, photosynthesis and skeletal growth in the scleractinian coral *Stylophora pistillata*. *J. Exp. Biol.* 207:1461–9.

Jacobovitz, M.R., Rupp, S., Voss, P.A., Maegele, I., Gornik, S.G. & Guse, A. 2021. Dinoflagellate symbionts escape vomocytosis by host cell immune suppression. *Nat Microbiol*. 6:769–82.

Jinkerson, R.E., Russo, J.A., Newkirk, C.R., Kirk, A.L., Chi, R.J., Martindale, M.Q., Grossman, A.R. et al. 2022. Cnidarian-Symbiodiniaceae symbiosis establishment is independent of photosynthesis. *Curr. Biol.*

Kang, L.-K., Hwang, S.-P.L., Gong, G.-C., Lin, H.-J., Chen, P.-C. & Chang, J. 2007. Influences of nitrogen deficiency on the transcript levels of ammonium transporter, nitrate transporter and glutamine synthetase genes in *Isochrysis galbana* (Isochrysidales, Haptophyta). *Phycologia*. 46:521–33.

Karako-Lampert, S., Katcoff, D.J., Achituv, Y., Dubinsky, Z. & Stambler, N. 2005. Responses of *Symbiodinium microadriaticum* clade B to different environmental conditions. *J. Exp. Mar. Bio. Ecol.* 318:11–20.

Koch, J.C., Verde, E.A. & Weis, V.M. 2020. Carbonic anhydrases are influenced by the size and symbiont identity of the aggregating sea anemone *Anthopleura elegantissima*. *J. Exp. Biol.* 223.

Koike, K., Yamashita, H., Oh-Uchi, A., Tamaki, M. & Hayashibara, T. 2007. A quantitative real-time PCR method for monitoring *Symbiodinium* in the water column. *Journal of the Japanese Coral Reef Society*. 9:1–12.

Mansfield, K.M., Carter, N.M., Nguyen, L., Cleves, P.A., Alshanbayeva, A., Williams, L.M., Crowder, C. et al. 2017. Transcription factor NF-κB is modulated by symbiotic status in a sea anemone model of cnidarian bleaching. *Sci. Rep.* 7:16025.

Maor-Landaw, K., van Oppen, M.J.H. & McFadden, G.I. 2020. Symbiotic lifestyle triggers drastic changes in the gene expression of the algal endosymbiont *Breviolum minutum* (Symbiodiniaceae). *Ecol. Evol.* 10:451–66.

Marcelino, L.A., Westneat, M.W., Stoyneva, V., Henss, J., Rogers, J.D., Radosevich, A., Turzhitsky, V. et al. 2013. Modulation of light-enhancement to symbiotic algae by light-scattering in corals and evolutionary trends in bleaching. *PLoS One*. 8:e61492.

Maruyama, S. & Weis, V.M. 2021. Limitations of using cultured algae to study cnidarian-algal symbioses and suggestions for future studies. *J. Phycol.* 57:30–8.

Matthews, J.L., Sproles, A.E., Oakley, C.A., Grossman, A.R., Weis, V.M. & Davy, S.K. 2016. Menthol-induced bleaching rapidly and effectively provides experimental aposymbiotic sea anemones (*Aiptasia* sp.) for symbiosis investigations. *J. Exp. Biol.* 219:306–10.

Morera, C. & Villanueva, M.A. 2009. Heat treatment and viability assessment by Evans blue in cultured *Symbiodinium kawagutii* cells. *World J. Microbiol. Biotechnol.* 25:1125–8.

Muller-Parker, G., McCloskey, L.R., Hoegh-Guldberg, O. & McAuley, P.J. 1994. Effect of ammonium enrichment on animal and algal biomass of the coral Pocillopora damicornis. *Pac. Sci.*

Nitschke, M.R., Davy, S.K. & Ward, S. 2016. Horizontal transmission of *Symbiodinium* cells between adult and juvenile corals is aided by benthic sediment. *Coral Reefs*. 35:335–44.

Parker, G.M. 1984. Dispersal of zooxanthellae on coral reefs by predators on cnidarians. *Biol. Bull.* 167:159–67.

Rosic, N.N., Pernice, M., Rodriguez-Lanetty, M. & Hoegh-Guldberg, O. 2011. Validation of housekeeping genes for gene expression studies in Symbiodinium exposed to thermal and light stress. *Mar. Biotechnol.* . 13:355–65.

Rosset, S., D'Angelo, C. & Wiedenmann, J. 2015. Ultrastructural biomarkers in symbiotic algae reflect the availability of dissolved inorganic nutrients and particulate food to the reef coral holobiont. *Front. Mar. Sci.* 2:103.

Smith, G.J. & Muscatine, L. 1999. Cell cycle of symbiotic dinoflagellates: variation in G1 phase-duration with anemone nutritional status and macronutrient supply in the *Aiptasia pulchella–Symbiodinium pulchrorum* symbiosis. *Mar. Biol.* 134:405–18.

Sproles, A.E., Oakley, C.A., Krueger, T., Grossman, A.R., Weis, V.M., Meibom, A. & Davy, S.K. 2020. Sub-cellular imaging shows reduced photosynthetic carbon and increased nitrogen assimilation by the non-native endosymbiont *Durusdinium trenchii* in the model cnidarian Aiptasia. *Environ. Microbiol.* 22:3741–53.

Stambler, N., Popper, N., Dubinsky, Z.V.Y. & Stimson, J. 1991. Effects of nutrient enrichment and water motion on the coral *Pocillopora damicornis*. *Pacific Science*. 45:299–307.

Steele, R.D. 1975. Stages in the life history of a symbiotic zooxanthella in pellets extruded by its host *Aiptasia tagetes* (Duch. and Mich.) (Coelenterata, Anthozoa). *Biol. Bull.* 149:590–600.

Stimson, J. & Kinzie, R.A. 1991. The temporal pattern and rate of release of zooxanthellae from the reef coral *Pocillopora damicornis* (Linnaeus) under nitrogen-enrichment and control conditions. *J. Exp. Mar. Bio. Ecol.* 153:63–74.

Tansik, A.L., Fitt, W.K. & Hopkinson, B.M. 2017. Inorganic carbon is scarce for symbionts in scleractinian corals. *Limnol. Oceanogr.* 62:2045–55.

Thornhill, D.J., Howells, E.J., Wham, D.C., Steury, T.D. & Santos, S.R. 2017. Population genetics of reef coral endosymbionts (*Symbiodinium*, Dinophyceae). *Mol. Ecol.* 26:2640–59.

Tivey, T.R., Parkinson, J.E. & Weis, V.M. 2020. Host and symbiont cell cycle coordination is mediated by symbiotic state, nutrition, and partner identity in a model cnidarian-dinoflagellate symbiosis. *MBio*. 11:e02626-19.

Umeki, M., Yamashita, H., Suzuki, G., Sato, T., Ohara, S. & Koike, K. 2020. Fecal pellets of giant clams as a route for transporting Symbiodiniaceae to corals. *PLoS One*. 15:e0243087.

Xiang, T., Lehnert, E., Jinkerson, R.E., Clowez, S., Kim, R.G., DeNofrio, J.C., Pringle, J.R. et al. 2020. Symbiont population control by host-symbiont metabolic interaction in Symbiodiniaceae-cnidarian associations. *Nat. Commun.* 11:108.

Xiang, T., Nelson, W., Rodriguez, J., Tolleter, D. & Grossman, A.R. 2015. *Symbiodinium* transcriptome and global responses of cells to immediate changes in light intensity when grown under autotrophic or mixotrophic conditions. *Plant J.* 82:67–80.

Yamashita, H. & Koike, K. 2016. Motility and cell division patterns among several strains of *Symbiodinium*. *Galaxea, Journal of Coral Reef Studies*. 18:13–9.

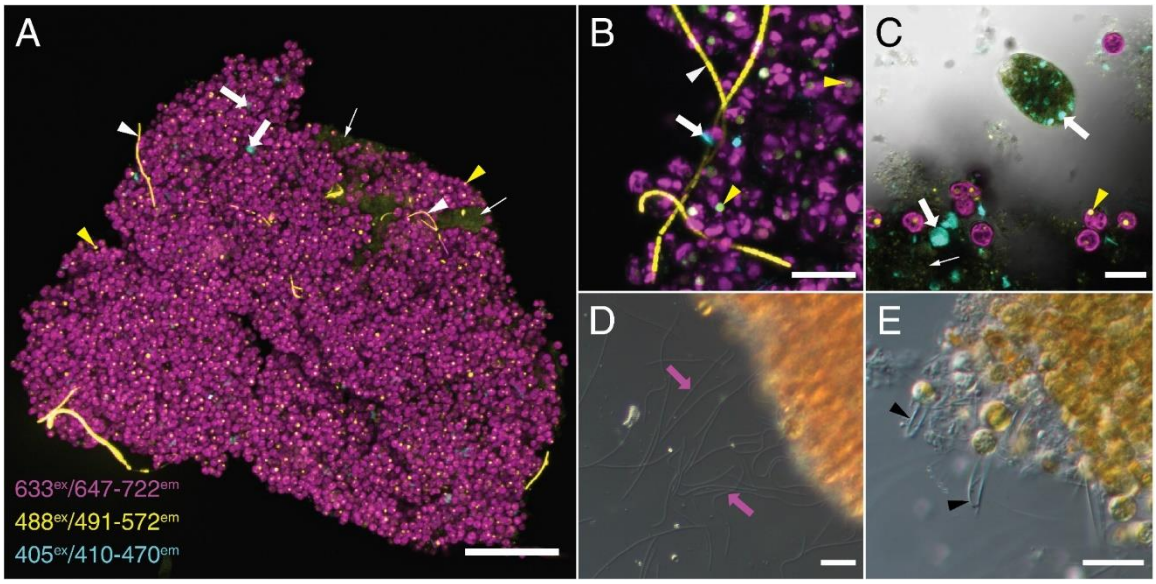

Figure 4.1 – Confocal and DIC images of whole Aiptasia egesta.
(A-C) Confocal images of whole Aiptasia egesta. Magenta: *Breviolum minutum* chlorophyll is detected with excitation at 633 nm and emission at 647-722 nm. Yellow: Cyanobacteria phycobillin (white arrowhead), host tissue (small white arrow), and *B. minutum* pyrenoids (yellow arrowhead) are detected with excitation at 488 nm and emission at 491-572 nm. Cyan: Pigment from an unknown protist (white arrow) is detected with excitation at 405 nm and emission at 410-470 nm. **(D-E)** Fired nematocysts (magenta arrows) and empty capsules (black arrowheads) are seen on the superficial surface of egesta under DIC microscopy. Scale bars: (A) 100 µm and (B-E) 20 µm.

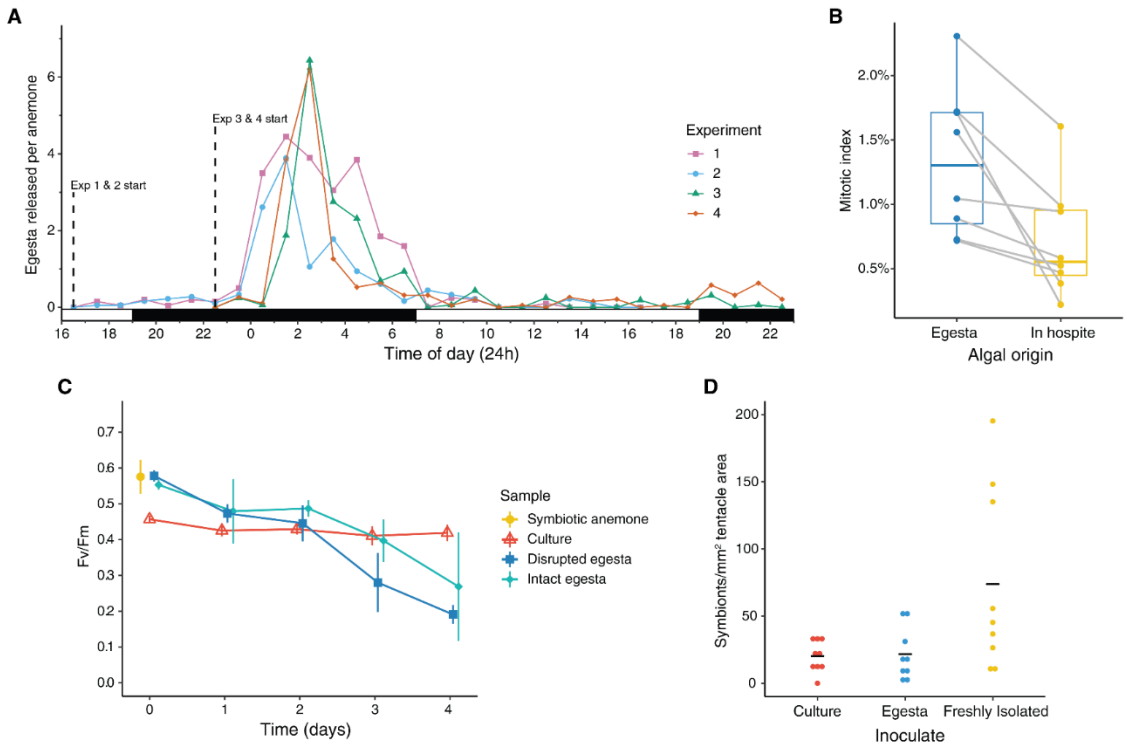

Figure 4.2 – The physiology of algae from egesta.
(A) Amount of egesta released per anemone every hour over 24 hours. Experiments 1 and 2 began at 17:00 and experiments 3 and 4 began at 23:00. Black and white bars on x-axis depict dark and light periods, respectively. **(B)** The mitotic index of algae in egesta and in the host. Dots indicate individual samples and lines connecting dots indicate paired samples. The difference was statistically significant (p = 0.01, Paired t-test). **(C)** The photosynthetic health of algae over time as measured by FRRf. Vertical lines indicate standard deviations around the mean. **(D)** Symbiont density in aposymbiotic Aiptasia inoculated with algae in culture, from egesta, or freshly isolated from hosts. Horizontal lines indicate mean symbiont density. Differences were not statistically significant (p = 0.06, Kruskal-Wallis test).

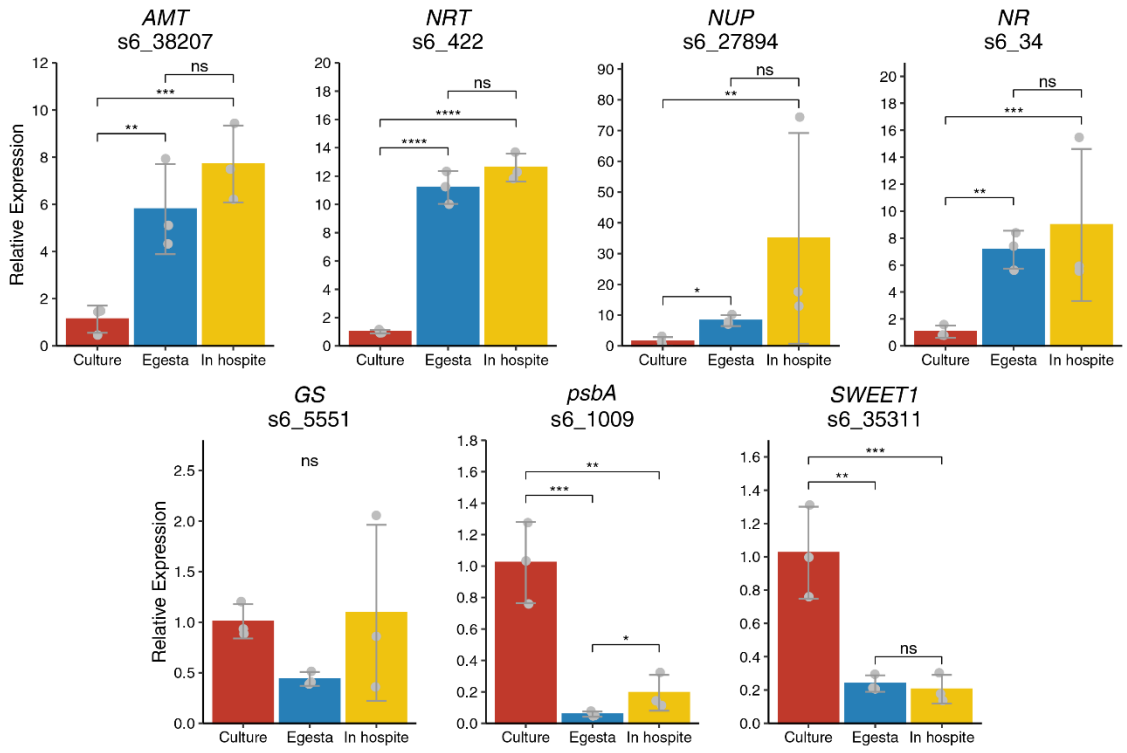

Figure 4.3 – Gene expression of nutrient-related, photosynthesis, and sugar transporting genes between cultured algae, algae from egesta, and algae *in hospite*. With the exception of *GS*, Expression of genes was similar in algae from egesta and algae *in hospite* compared to that of cultured algae. Bars indicate standard deviations around the mean. Transcript IDs are listed under gene abbreviations based on Xiang et al. (2015). Stars indicate statistically significant differences calculated on $\Delta\Delta Ct$ values as determined by ANOVA and post-hoc Tukey's tests. * $p < 0.05$, ** $p > 0.01$, *** $p < .0001$, **** $p < 0.00001$

5. Identifying symbiosis-specific proteins from *Breviolum minutum* using aptamer cell-SELEX

5.1 Introduction

Like pathogens, Symbiodiniaceae must successfully invade host cells and avoid destruction, but our understanding of the interpartner interactions involved is incomplete (Davy et al. 2012). As reviewed in Chapter 3, it is hypothesized that the algal symbiont changes its physiology in order to maintain symbiosis (Stochaj and Grossman 1997, Pasaribu et al. 2015, Bellantuono et al. 2019, Maor-Landaw et al. 2020, Xiang et al. 2020). To date, two studies have found proteomic differences between Symbiodiniaceae in culture and those *in hospite*, but each had their limitations in characterizing symbiosis-specific proteins (Stochaj and Grossman 1997, Pasaribu et al. 2015). Only one putative symbiosis-specific protein has been characterized: a plasma membrane H^+-ATP-ase (Bertucci et al. 2010). However, the gene is poorly conserved among Symbiodiniaceae and has only been found in *Symbiodinium microadriaticum* (Bertucci et al. 2010). New strategies must be employed if we are to identify additional symbiosis-specific proteins.

A biomarker is a molecule whose presence is indicative of a specific disease or phenotype. In biomedicine, biomarkers are useful for detecting subtle differences, such as in the diagnoses and treatment of cancers, as cancers are molecularly similar to healthy tissue, or in the detection of malaria, as the parasite evades detection by the immune system by hiding in red blood cells. Often, discovered biomarkers are not just indicative of the disease, but hold functional significance to disease pathology. For example, the well-studied human epidermal growth factor receptor 2 cell-surface biomarker is overexpressed in many breast cancers and promotes cell proliferation (Yarden and Sliwkowski 2001). Another example is the histidine-rich protein I cell-surface biomarker found only in malaria-infected red blood cells, and it is hypothesized to play a role in the adhesion of infected cells to blood vessels (Jain et al. 2014).

Antibodies and aptamers are often used for the discovery of novel biomarkers (Tonelli et al. 2012) . Antibodies are immunoglobulin proteins and aptamers are single-stranded oligonucleotides. Both are molecular probes that bind specifically to a wide range of molecular targets. Through a variety of selection processes, antibodies and aptamers can be identified that bind specifically to molecules or cells that indicate certain

phenotypes. In addition, these molecular markers are sensitive enough to target proteins of low abundance, alleviating the sensitivity issue of standard proteomic approaches (Huang et al. 2021). Once generated, they are powerful molecular tools. By isolating target proteins with antibodies or aptamers, follow-up characterization of biomarkers is simplified (Berezovski et al. 2008). Both antibodies and aptamers can also be used in assays for protein purification, quantification, and visualization through fluorescent conjugates (Huang et al. 2021).

Huang and coworkers (2017) attempted to generate antibodies specific to a *Cladocopium* sp. in the symbiotic-state. The authors first inoculated mice with symbiotic gastrodermal cells, including both host and symbiont material. Monoclonal antibodies were generated from the immunized mice using hybridomas, and a total of 56 antibodies were initially identified. Through Western blots against host and symbiont protein (in the symbiotic or free-living state), one antibody was selected for its specificity to algae in the symbiotic state. However, the antibody stained multiple protein bands, suggesting that the antibody was not specific to a single protein.

As discussed in Chapter 3, aptamer Cell-SELEX is an alternative, cheaper method for the development of ligands that will aid in biomarker discovery. In this chapter, I used aptamer Cell-SELEX to develop single-stranded DNA (ssDNA) aptamers that are specific to freshly isolated *Breviolum minutum* (representing the *in hospite* state) and used cultured *B. minutum* (representing the *ex hospite* state) during negative selection as an off-target cell. Ultimately, this work failed to develop aptamers that were specific to freshly isolated *B. minutum*. In this chapter, I discuss the SELEX protocol, aptamer candidates, possible reasons for why cell-SELEX failed in this project, and provide improvements that can increase the success rate of SELEX in future attempts at implementing this technology in cnidarian-algal symbiosis.

5.2 Methods

Animal and algal culture

For this study, the model sea anemone, Aiptasia populated with *B. minutum* (culture ID SSB01), and SSB01 in culture were used. SSB01 is an axenic culture and was used in this study to minimize the effect of microbial contamination in the Cell-SELEX

process. All animals and algal cultures were maintained under 55 μmol/m^2/s of light on a 12h:12h day:night cycle.

Animals were maintained in artificial seawater (ASW) made with Instant Ocean and algal cultures were maintained in autoclaved filtered artificial seawater (FSW) with F/2 marine algal media.

Aptamer library sequences

All aptamers and oligonucleotides were ordered from IDTDNA (Coralville, IA). The DNA aptamer library was designed by TriLink Biotechnologies (San Diego, CA) to contain a 40 nucleotide randomized region flanked by 23 nucleotide primer-binding regions (5'-TAGGGAAGAGAAGGACATATGAT -N40- TTGACTAGTACATGACCACTTGA-3'). Unmodified forward and reverse primers targeting the flanking regions were used routinely (AptFor: 5'-TAGGGAAGAGAAGGACATATGAT-3'; AptRev: 5'-TCAAGTGGTCATGTACTAGTCAA-3'). To generate a fluorescent aptamer, a 6-FAM modified forward primer that had the first five nucleotides phosphorothiorated to prevent nuclease digestion, was used during SELEX (FluorFor: 5'-6-FAM-TAGGGAAGAGAAGGACATATGAT-3'). Unfortunately, the fluorescently labeled aptamer was not utilized in further experiments due to lack of success in the SELEX experiment. To recover single stranded DNA (ssDNA) aptamers from double-stranded PCR amplicons, a phosphorylated reverse primer was used, allowing the use of lambda exonuclease which targets the phosphorylated strand for digestion (RevPhos: 5'-phosphate- TCAAGTGGTCATGTACTAGTCAA-3'). A reverse complement of the forward primer was used to block the flanking region during SELEX (5'Comp: 5'-ATCATATGTCCTTCTCTTCCCTA-3'). The flanking regions of aptamer sequences can interfere with proper folding of the aptamer and masking them with oligos (5'Comp and AptRev) can maximize the number of functional aptamers and decrease the number of SELEX rounds necessary for the generation of high-affinity binding aptamers (Ouellet et al. 2014).

Aptamer library preparation

Cell-SELEX conditions were modified from a Cell-SELEX protocol developed by Sefah et al. (2010) and aptamer concentrations varied depending on the round of SELEX (Table 5.1). First, ssDNA aptamers were incubated in binding buffer (Dulbecco's phosphate buffered saline with 5.5 mM $MgCl_2$, 0.9 mM $CaCl_2$, 1 mg/mL bovine serum albumin, and 0.1 mg/mL of salmon sperm DNA) containing 5'Comp and AptRev oligonucleotides at equimolar concentrations to the aptamer and heated to 95 °C for 5 minutes then slowly cooled down to 25 °C at a rate of 0.5 °C/min in a thermocycler. The melting and slow cooling of the aptamer ensured proper folding of the aptamer's secondary structure and that the flanking regions were blocked by the 5'Comp and AptRev oligonucleotides.

PCR amplification of aptamers

PCR amplification was performed using emulsion PCR (ePCR) following methods developed by Shao et al. (2011) to prevent the generation of PCR by-product that can cause the failure of SELEX (Figure 5.1). First, an aqueous PCR mix was prepared using Phusion High-Fidelity DNA Polymerase in 220 µL volumes containing 1 X Phusion HF buffer, 0.4 mM dNTPs, 0.4 µM each of FlourFor and RevPhos primer, 10 mg/mL of bovine serum albumen, 62.5 units/mL of Phusion HF Polymerase, and 20-70 µL of aptamer library (optimized between each round of SELEX). An oil phase containing 4.5% (v/v) Span 80, 0.4% (v/v) Tween 80, 0.05% (v/v) Triton X-100, and 95.05% (v/v) mineral oil was prepared and 400 µL of the oil phase was added to a two mL self-standing round-bottom cryogenic vials (VWR cat no. 89094-810) with a micro-stir bar (2 mm diameter, 5 mm length; VWR cat no. 58948-377). With the stirrer speed set to six (max speed at 7; Magnestir cat no. 1250), 200 µL of the aqueous PCR mix was added dropwise (20 µL every twelve seconds) over two min into the oil phase. The emulsion was allowed to stir for an additional five min, then the emulsion was aliquoted into 200 µL PCR tubes. To prevent evaporation and preserve the emulsion, 10 µL of mineral oil was added to the top of each reaction. Emulsions were then run on a thermocycler (98 °C for 1 min followed by 30 cycles of 98 °C for 10 sec, 60 °C for 30 sec, 72 °C for 30 sec, and a final elongation step at 72 °C for 5 min). The ePCR reaction

was scaled up as necessary by repeating this process to generate enough aptamer for use in SELEX.

To purify DNA from emulsions, aliquots were pooled together after PCR amplification (up to 1,200 μL of emulsion per 1.5 mL tube). Reactions were centrifuged at 13,000 x g for five min and the upper oil layer was removed. To break the emulsion, one mL of water saturated diethyl ether was added to each sample and vortexed for 10 sec. Samples were then centrifuged at 5,000 x g for five sec, and the upper ether layer was removed. The ether extraction was repeated once and samples were dried for ten min in a SpeedVac centrifuge to remove remaining diethyl ether. One μL of each sample was then loaded onto a 3% agarose gel to confirm amplification of a single product. DNA was purified from samples using a Monarch PCR & DNA cleanup kit (New England Biolabs, Ipswich, MA) following the manufacturer's instructions. Samples were assessed for purity and DNA concentration using a Nanodrop.

Lambda exonuclease digestion

To generate ssDNA from double-stranded PCR amplicons, PCR reaction products were digested with lambda exonuclease (New England Biolabs), which specifically digests the 5' phosphorylated DNA strand provided by the RevPhos primer. Lambda exonuclease reactions were conducted following the manufacturer's instructions in 50 μL reactions. Samples were then cleaned using a Monarch PCR & DNA cleanup kit (New England Biolabs) following the manufacturer's instructions for purifying ssDNA.

Cell-SELEX protocol

To prepare freshly isolated algae, two to four anemones of approximately 0.75 cm oral disk diameter were homogenized in two mL of FSW by twenty passes of a ground glass tissue grinder. The homogenate was washed twice with two mL of FSW and centrifugation at 800 x g. The algal pellet was resuspended in two mL of FSW and was further homogenized to remove symbiosome membranes by passing the sample seven times through a 26 gauge needle fitted on a three mL syringe. To remove host material, a Percoll density gradient (two mL each of 100%, 80%, 60%, and 40% Percoll) made with Instant Ocean was prepared in a fifteen mL conical tube. Algae were loaded immediately

onto the gradient and centrifuged at 2,000 x g for twenty min. Host material separated in the lower density layers and clean algae were harvested from the 100%-80% Percoll boundary. To pellet the algae, an equal volume of FSW was added to the algal cells suspended in Percoll, and the cells were washed twice by centrifugation at 800 x g for five min and resuspension in two mL of FSW. After the final wash, cells were resuspended in one mL of FSW and cell density quantified using a Countess II cell counter. One million freshly isolated algal cells were harvested for positive selection and pelleted in a fifteen mL conical tube by centrifugation at 800 x g for 5 min. Algal cells were then resuspended in a volume of binding buffer (Table 5.1). Cultured algae were prepared in the same manner as freshly isolated algae but were first harvested from culture by centrifugation at 800 x g for five min before homogenization, and five million cells were harvested for negative selection.

Each round of SELEX began with negative selection to remove aptamers that are non-specific to the symbiotic state (Figure 5.2). Prepared aptamer libraries suspended in binding buffer were added to five million cultured algal cells suspended in binding buffer for one hr at room temperature with constant shaking on a Brinkmann Orbimix 1010 set to 350 rotations/min. After incubation, cells were pelleted by centrifugation at 3,100 x g for 5 min and the pellet containing non-specific aptamers bound to cultured algae was discarded. The supernatant was then directly transferred to the algal pellet containing one million freshly isolated algae to begin positive selection. Aptamers were incubated with freshly isolated algae under the same conditions as negative selection. After positive selection, cells were pelleted at 3,100 x g for 5 min and the supernatant containing unbound aptamers was removed. Algal cells were then washed several times in 3 mL of wash buffer (Dulbecco's phosphate buffered saline with 5.5 mM $MgCl_2$ and 0.9 mM $CaCl_2$) and centrifuged at 3,100 x g for 5 min. Algal cells were initially washed three times during round 1 and selective pressure was gradually increased to obtain aptamers of high specificity and affinity by adding an additional wash every round (i.e. four washes at round 2, five washes at round 3, and so on). After the last wash, pellets containing algae bound to aptamers were resuspended in 200 μL of nuclease-free water. The algae were then transferred to a 1.5 mL tube and heated at 95 °C for ten min to elute aptamers.

Heated samples were centrifuged at 13,100 x g for 5 min to remove cell debris and the supernatant containing aptamers was collected.

A total of six rounds of SELEX were performed. Rounds 4-6 were repeated starting from the aptamer library generated after round 3 with 10 pmol of aptamers (Rounds 4B-6B) used in SELEX instead of the original 50 pmol used (Rounds 2, 3, 4A-6A). SELEX experiments including Rounds 4A-6A will herein be identified as SELEX-A and experiments including Rounds 4B-6B will herein be identified as SELEX-B.

Aptamer library sequencing

Aptamer libraries from each round were sequenced by Illumina MiSeq at Oregon State University's Center for Quantitative Life Sciences (CQLS). Indexed sequencing libraries were prepared by the CQLS for each aptamer library using 150 ng of DNA using a PrepX DNA library kit. Libraries were size selected for 215 bp DNA using a BluePippin (Sage Science) size selection kit due to the presence of PCR by-products in the sequencing libraries. Samples were pooled to equimolar concentrations as quantified by qPCR and 10% PhiX spike-in was added. Sequencing was run on a single MiSeq lane with 150bp paired end sequencing.

Aptamer candidate selection

Demultiplex reads from Illumina MiSeq were processed with AptaSuite, a software suite designed to analyze high-throughput SELEX data (Hoinka et al. 2018). Aptamer sequences were extracted from the reads based on the presence of flanking regions (Hoinka and Przytycka 2016). Abundance of each aptamer sequence was also tracked over each round of cell-SELEX. Aptamer sequences were analyzed using AptaTrace and AptaCluster to find aptamer sequence motifs and identify aptamer families based on sequence similarity, respectively (Hoinka et al. 2014, Dao et al. 2016). Aptamers from SELEX-A were analyzed separately from those of SELEX-B, but both included rounds 1-3 in their analyses. Predicted aptamer secondary structures were determined by mFold set to fold in binding buffer conditions at 25 °C, 137 nM NaCl and 5.5 Mg mM and the structure with the lowest ΔG value among the predicted structures was used for assessing aptamer quality (Zuker 2003).

Candidate aptamers to be tested in binding assays were identified from SELEX-A and SELEX-B based on their abundance in the sixth round of cell-SELEX, enrichment of sequence over proceeding rounds of cell-SELEX, and evidence of secondary structures. Candidate aptamers sequence were ordered from IDTDNA.

Aptamer binding assay

Binding of aptamers to freshly isolated algae, cultured algae, and empty blank tubes were tested adopting methods developed by Ouellet et al. (2014). Aptamer candidates were first prepared at 200 nM in binding buffer with 5'Comp and AptRev oligonucleotides and allowed to form secondary structures as previously described. Freshly isolated and cultured algae were prepared as previously described, and 250 μL of prepared candidate aptamers were incubated with 100,000 freshly isolated or cultured algae (n = 2-5) or with blanks (n = 2) in 15 mL conical tubes with constant shaking for one hr. Cells were then washed three times with one mL of wash buffer by repeated centrifugation at 3100 x g for five min. After the last wash, cells were pelleted at 3,100 x g for five min and resuspended in 100 μL of nuclease-free water and transferred to a 1.5 mL microcentrifuge tube. Resuspended algae were heated at 95 °C for 10 min to elute aptamers. Samples were then centrifuged at 13,100 x g for 5 min to pellet cell debris and the supernatant containing aptamers was extracted.

Bound aptamer concentration was determined by quantitative PCR (qPCR). qPCR was carried out in 20 μL reactions using Power SYBR Green containing 1 X Power SYBR Green PCR Master Mix, 0.5 μM of each AptFor and AptRev primer, and 2 μL template. A standard curve for each aptamer was generated using serial dilutions of aptamers of known concentration as template DNA (100 nM, 1 nM, 10 pM, 100 fM, and 1 fM). A BioRad CFX96 Real-Time System was used to carry out reactions using a two-step amplification phase (95 °C/ten min, followed by 40 cycles of 95 °C/ten s and 58 °C/30 s). All reactions were performed in duplicate and no-template controls were included. Aptamer concentrations were determined using the standard curve and background corrected by subtracting aptamer concentrations from blank controls.

An initial screen of aptamers following the above procedure using those bound to freshly isolated algae and blanks (n = 1) revealed that aptamers 3, 6, and 8 bound strongly

to plastic tubes and not to cells and so were not included in the data. Aptamer 10 was excluded from tests because it was later discovered that the aptamer contained primer binding regions and was a product of non-specific amplification (Figure 5.3).

5.3 Results and Discussion

Aptamer SELEX library by-product formation

A total of six cycles of cell-SELEX were conducted. Rounds 4-6 were repeated due to the increasing amount of PCR by-products found in these rounds during library preparation for sequencing. The lower library concentration was used in SELEX-B to increase the selective pressure of SELEX and decrease the amount of aptamer by-products. The presence of library by-products is a signal that SELEX has failed and is caused by non-specific amplification from product-product hybridization (Shao et al. 2011, Tolle et al. 2014, Takahashi et al. 2016). During initial development of the cell-SELEX protocol, these amplification by-products were present after amplification of the starting aptamer library (Round 0) using conventional PCR methods (Figure 5.1). It was found that ePCR could mitigate by-product formation (Figure 5.1) by separating aptamers into individual PCR reaction droplets and ePCR was, therefore, used throughout the cell-SELEX protocol. PCR amplicons were monitored at each round of SELEX with gel electrophoresis and by-product formation was not detected. However, during library preparation for sequencing, conventional PCR was employed to amplify the aptamer libraries, revealing the presence of non-specific aptamers in the SELEX libraries caused by-product formation (Figure 5.4). The reduction of library concentration for SELEX B was not successful in preventing aptamer by-product formation in the sequencing libraries. Despite the problem of by-products, sequencing of aptamer libraries was still possible by size-selection.

Aptamer sequences and binding characteristics

Aptamer libraries were successfully sequenced, generating 2,397,083 total reads with matching sequencing indices (Table 5.2). While AptaTrace and AptaCluster were used to further analyze the sequences, these analyses did not identify any binding motifs or sequence families of interest. Ten aptamer candidates were selected for further

analysis. Aptamer 2 was noteworthy for being present in both SELEX A and SELEX B, with strong enrichment in both. Aptamer 1 was the only aptamer that was present in all rounds of SELEX from 1-6 in SELEX A. While Aptamer 4 did not enrich over time, it was chosen for having a robust secondary structure that included most of the sequence (Figure 5.5). Aptamer 10 contained primer-binding regions, but still enriched over several rounds of SELEX and was one of the most abundant sequences by round 6 of SELEX A.

Candidate aptamers were tested for their binding specificity to freshly isolated algae compared to cultured algae, but none of the aptamers bound specifically to freshly isolated algae, with many aptamers binding equally to cultured and freshly isolated algae. Unexpectedly, aptamer 9 bound better to cultured algae than to freshly isolated algae (p = 0.03, Student's t-test).

Causes of SELEX failure and improvements for the future

Cell-SELEX failed to select for aptamers that were specific to freshly isolated *B. minutum* (Figure 5.6). There are several reasons for why SELEX may have failed in this experiment. The enrichment of aptamers that could cause by-product formation is a sign that SELEX has failed, suggesting that selection was not stringent enough. Other SELEX protocols employ a mild detergent such as 0.005% Tween 20 in the wash buffer to remove non-specific aptamers. The addition of detergent, however, is rarely used in whole cell-SELEX and instead more commonly used for SELEX targeting immobilized molecules, and so was not included in this work. More stringent washes, however, could decrease the number of non-specific aptamers (Kim et al. 2020), such as those that bound strongly to plastic (aptamers 3, 6, and 8) and those that bound better to cultured algae (aptamer 9).

There are multiple biological variables that could influence the success of SELEX. First, it is unknown if dinoflagellate algae readily take up DNA molecules from the environment. Cells that actively absorb DNA molecules from the environment can make SELEX difficult, as internalized, non-specific aptamers are not efficiently removed during washes. A way to mitigate this problem is to incubate the cells with the aptamers at 4 °C to minimize aptamer internalization (Sefah et al. 2010), but this method could also cause the enrichment of aptamers that only function at 4 °C, limiting its use as a

molecular tool. Second, the binding and wash buffer salinities were designed for biomedical applications and are not ideal for Symbiodiniaceae biology. The lower salinity of Dulbecco's PBS used in the binding and wash buffers could cause osmotic stress to the algae during SELEX, causing failure by negatively affecting algal physiology. Preliminary tests, however, showed that the algae did not die, as measured by Evans Blue viability stain (data not shown). In addition, there is evidence that algae within host cnidarians experience very low salinities, at around 60 mM NaCl (Goiran et al. 1997), so the use of Dulbecco's PBS may be appropriate for freshly isolated algae. Aptamer secondary structure is also heavily influenced by salt concentrations (Neves et al. 2010), and the literature is scant on whether aptamers can function at all in seawater.

The presence of by-products during amplification of the initial starting aptamer library is concerning. A recent study revealed that initial aptamer libraries can contain "biased sequences" that result in high by-product formation (Takahashi et al. 2016). This bias can result in the failure of SELEX, but can potentially be mitigated by altering aptamer flanking region sequences (Tolle et al. 2014). If this work would continue in the future, I recommend that a different template sequence be used in the initial aptamer library. In addition, while ePCR can reduce byproduct formation, reaction droplet size is highly variable (Takahashi et al. 2016). A similar technology, digital droplet PCR, creates an emulsion of uniform droplet sizes, providing a more robust method for the amplification of aptamers and is therefore recommended over ePCR (Ouellet et al. 2015).

There are several innovative modifications to cell-SELEX that could be implemented in future attempts to identify aptamers that are specific to *B. minutum* in the symbiotic state. Differential binding SELEX is a method that employs fluorescently labeled aptamers and flow cytometry to sort for cells that contain bound sequence during positive selection (Dwivedi et al. 2013, Pleiko et al. 2019). This method allows for the identification of aptamers targeting abundant cell surface moieties and can be modified to exclude dead cells that can interfere with SELEX (Sefah et al. 2010, Dwivedi et al. 2013, Pleiko et al. 2019). Other non-SELEX methods exist, including RIDA (rapid isolation of DNA aptamers), which only requires a single round of selection and could be completed in a few days. However, this method is protected under a patent and so could not be explored in this thesis (Gilman 2012, Kaur et al. 2018). Another single-round SELEX

method was recently employed to target *Escheria coli* by repeated washes of cells containing bound aptamer (up to 10 times), but this work was unfortunately published after initiation of this experiment (Kim et al. 2020).

5.4 Conclusion

Overall, using cell-SELEX to target symbiotic-state specific markers in *B. minutum* was and ambitious, high-risk project. There is no precedent for the application of cell-SELEX in cnidarian-algal symbiosis and a considerable amount of time was spent on developing the cell-SELEX protocol itself. Cell-SELEX has limited checkpoints after each round of SELEX that ensures the success of aptamer selection and can only be confirmed after completion of the entire process. In addition, the covid-19 pandemic lockdown in 2020 severely hampered the progress of cell-SELEX, with limited access to lab space and supply chain issues. This work nonetheless lays the groundwork for future attempts at the implementation of this promising and cutting-edge technique in the field of cnidarian-algal symbiosis.

5.5 References

Bellantuono, A.J., Dougan, K.E., Granados-Cifuentes, C. & Rodriguez-Lanetty, M. 2019. Free-living and symbiotic lifestyles of a thermotolerant coral endosymbiont display profoundly distinct transcriptomes under both stable and heat stress conditions. *Mol. Ecol.* 28:5265–81.

Berezovski, M.V., Lechmann, M., Musheev, M.U., Mak, T.W. & Krylov, S.N. 2008. Aptamer-facilitated biomarker discovery (AptaBiD). *J. Am. Chem. Soc.* 130:9137–43.

Bertucci, A., Tambutté, E., Tambutté, S., Allemand, D. & Zoccola, D. 2010. Symbiosis-dependent gene expression in coral-dinoflagellate association: cloning and characterization of a P-type H+-ATPase gene. *Proc. Biol. Sci.* 277:87–95.

Dao, P., Hoinka, J., Takahashi, M., Zhou, J., Ho, M., Wang, Y., Costa, F. et al. 2016. AptaTRACE elucidates RNA sequence-structure motifs from selection trends in HT-SELEX experiments. *Cell Syst.* 3:62–70.

Davy, S.K., Allemand, D. & Weis, V.M. 2012. Cell biology of cnidarian-dinoflagellate symbiosis. *Microbiol. Mol. Biol. Rev.* 76:229–61.

Dwivedi, H.P., Smiley, R.D. & Jaykus, L.-A. 2013. Selection of DNA aptamers for capture and detection of *Salmonella typhimurium* using a whole-cell SELEX approach in conjunction with cell sorting. *Appl. Microbiol. Biotechnol.* 97:3677–86.

Gilman, V.L. 2012. Methods for identifying nucleic acid ligands.

Goiran, C., Allemand, D. & Galgani, I. 1997. Transient Na+ stress in symbiotic dinoflagellates after isolation from coral-host cells and subsequent immersion in seawater. *Mar. Biol.* 129:581–9.

Hoinka, J., Backofen, R. & Przytycka, T.M. 2018. AptaSUITE: A full-featured bioinformatics framework for the comprehensive analysis of aptamers from HT-SELEX experiments. *Mol. Ther. Nucleic Acids*. 11:515–7.

Hoinka, J., Berezhnoy, A., Sauna, Z.E., Gilboa, E. & Przytycka, T.M. 2014. AptaCluster - A method to cluster HT-SELEX aptamer pools and lessons from its application. *Res. Comput. Mol. Biol.* 8394:115–28.

Hoinka, J. & Przytycka, T. 2016. AptaPLEX - A dedicated, multithreaded demultiplexer for HT-SELEX data. *Methods*. 106:82–5.

Huang, J., Chen, X., Fu, X., Li, Z., Huang, Y. & Liang, C. 2021. Advances in aptamer-based biomarker discovery. *Front Cell Dev Biol*. 9:659760.

Huang, K.-J., Huang, Z.-Y., Lin, C.-Y., Wang, L.-H., Chou, P.-H., Chen, C.-S. & Li, H.-H. 2017. Generation of clade- and symbiont-specific antibodies to characterize marker molecules during cnidaria-*Symbiodinium* endosymbiosis. *Sci. Rep.* 7:5488.

Jain, P., Chakma, B., Patra, S. & Goswami, P. 2014. Potential biomarkers and their applications for rapid and reliable detection of malaria. *Biomed Res. Int.* 2014:852645.

Kaur, S.J., Gilman, V., Duong, M., Asher, D.M. & Gregori, L. 2018. Rapid selection of single-stranded DNA aptamers binding Staphylococcus epidermidis in platelet concentrates. *Biotechniques*. 65:331–8.

Kim, H.R., Song, M.Y. & Chan Kim, B. 2020. Rapid isolation of bacteria-specific aptamers with a non-SELEX-based method. *Anal. Biochem.* 591:113542.

Maor-Landaw, K., van Oppen, M.J.H. & McFadden, G.I. 2020. Symbiotic lifestyle triggers drastic changes in the gene expression of the algal endosymbiont *Breviolum minutum* (Symbiodiniaceae). *Ecol. Evol.* 10:451–66.

Neves, M.A.D., Reinstein, O., Saad, M. & Johnson, P.E. 2010. Defining the secondary structural requirements of a cocaine-binding aptamer by a thermodynamic and mutation study. *Biophys. Chem.* 153:9–16.

Ouellet, E., Foley, J.H., Conway, E.M. & Haynes, C. 2015. Hi-Fi SELEX: A high-fidelity digital-PCR based therapeutic aptamer discovery platform. *Biotechnol. Bioeng.* 112:1506–22.

Ouellet, E., Lagally, E.T., Cheung, K.C. & Haynes, C.A. 2014. A simple method for eliminating fixed-region interference of aptamer binding during SELEX. *Biotechnol. Bioeng.* 111:2265–79.

Pasaribu, B., Weng, L.-C., Lin, I.-P., Camargo, E., Tzen, J.T.C., Tsai, H., Ho, S.-L. et al. 2015. Morphological variability and distinct protein profiles of cultured and endosymbiotic *Symbiodinium* cells isolated from *Exaiptasia pulchella*. *Sci. Rep.* 5:15353.

Pleiko, K., Saulite, L., Parfejevs, V., Miculis, K., Vjaters, E. & Riekstina, U. 2019. Differential binding cell-SELEX method to identify cell-specific aptamers using high-throughput sequencing. *Sci. Rep.* 9:8142.

Sefah, K., Shangguan, D., Xiong, X., O'Donoghue, M.B. & Tan, W. 2010. Development of DNA aptamers using cell-SELEX. *Nat. Protoc.* 5:1169–85.

Shao, K., Ding, W., Wang, F., Li, H., Ma, D. & Wang, H. 2011. Emulsion PCR: a high efficient way of PCR amplification of random DNA libraries in aptamer selection. *PLoS One*. 6:e24910.

Stochaj, W.R. & Grossman, A.R. 1997. Differences in the protein profiles of cultured and endosymbiotic *Symbiodinium* sp. (Pyrrophyta) from the anemone *Aiptasia pallida* (Anthozoa). *J. Phycol.* 33:44–53.

Takahashi, M., Wu, X., Ho, M., Chomchan, P., Rossi, J.J., Burnett, J.C. & Zhou, J. 2016. High throughput sequencing analysis of RNA libraries reveals the influences of initial library and PCR methods on SELEX efficiency. *Sci. Rep.* 6:33697.

Tolle, F., Wilke, J., Wengel, J. & Mayer, G. 2014. By-product formation in repetitive PCR amplification of DNA libraries during SELEX. *PLoS One*. 9:e114693.

Tonelli, R.R., Colli, W. & Alves, M.J.M. 2012. Selection of binding targets in parasites using phage-display and aptamer libraries in vivo and in vitro. *Front. Immunol.* 3:1–16.

Xiang, T., Lehnert, E., Jinkerson, R.E., Clowez, S., Kim, R.G., DeNofrio, J.C., Pringle, J.R. et al. 2020. Symbiont population control by host-symbiont metabolic interaction in Symbiodiniaceae-cnidarian associations. *Nat. Commun.* 11:108.

Yarden, Y. & Sliwkowski, M.X. 2001. Untangling the ErbB signalling network. *Nat. Rev. Mol. Cell Biol.* 2:127–37.

Zuker, M. 2003. Mfold web server for nucleic acid folding and hybridization prediction. *Nucleic Acids Res.* 31:3406–15.

SELEX Round	Total amount of aptamer	Volume of binding buffer used in aptamer prep	Volume of binding buffer used to resuspend algae	Total volume
1	750 pmol	370 µL	340 µL	700 µL
2, 3, 4A-6A	50 pmol	300 µL	400 µL	700 µL
4B-6B	10 pmol	300 µL	400 µL	700 µL

Table 5.1 – Cell-SELEX conditions used in each round.
Different aptamer rounds followed slight variations in amount of aptamer used and amount of buffer used in aptamer preparation. A high numbers of aptamers were used in the first round to maximize aptamer diversity to begin SELEX. Lower amounts were used in later rounds (2-6) to minimize non-specific binding.

SampleID	# Reads	# Reads containing aptamers	# of >= Q30 Bases (PF)	Mean Quality Score (PF)
Round 1	291645	253679	71259580	36.29
Round 2	348363	320893	85380427	36.4
Round 3	362221	326958	88818684	36.43
Round 4	265479	213290	64375571	36.11
Round 5	278657	197394	67913621	36.26
Round 6	342494	258521	83015603	36.11
Round 4B	269918	242390	65965838	36.31
Round 5B	279715	244585	68208451	36.25
Round 6B	296841	232931	72599965	36.33

Table 5.2 – Number of reads and quality score data from Illumina MiSeq of aptamer sequences.
The number of reads reflects the number of reads that were able to be matched to an index, and the number of reads containing aptamers were the total number of reads that contained both forward and reverse primer-binding regions.

ID	SELEX ID	nt length	Sequence (without flanking regions)	R6 CPM	R5 CPM	R4 CPM	R3 CPM	R2 CPM	R1 CPM
1	A	40	TCACGCAGCATGTTAACCTGAGCGCCATTGTTGAATCTCA	42.6	55.7	37.5	3.1	3.1	3.9
2	A	40	TCATCACCAACTACACGTTACGTCATTTCCGTTCTGTCCT	92.8	35.5	32.8	9.2	0	0
3	A	40	CAGTGCTATAATCCGAATTCAGGTCCAATGGAAACAGTTG	61.9	25.3	28.1	0	0	0
4	B	40	GTAGGACAGTTGGAACGGTGCCTCTTCGTCGGCTGTTAGG	4.3	0	16.5	0	0	0
5	A	40	CACCATGCTTTAGAGAGTCCGCTTACTCTTCTCTGTTTGA	31	15.2	9.4	0	0	0
6	B	40	GGCACCCAATCCATGTCTGATCGTTTCCAACCTGGTGTTC	17.2	16.4	0	0	0	0
7	B	40	CTATGTCGTTACTTCCATACATACTCCTAGATCAGTAGAA	17.2	20.4	0	0	0	0
8	B	40	GGCGCTACGTTTCTCCTAACCTCCTTTCGCTAATTTTACT	21.5	4.1	0	0	0	0
9	B	40	CCATTTTACTTCGCATTCTATATCCTGGTTCTTGCTCATA	77.3	0	0	0	0	0
2	B	40	TCATCACCAACTACACGTTACGTCATTTCCGTTCTGTCCT	30.1	32.7	0	9.2	0	0
10	A	44	TGACTAGTACATGACCACTTGATAGGGAAGAGAAGGACATATGA	42.6	15.2	4.7	0	0	0

Table 5.3 – List of candidate aptamer sequences.
Ten candidates were selected based on quality of their secondary structure, enrichment over SELEX rounds, and aptamer abundance in the sixth round of SELEX. Aptamer counts were normalized to number of reads (counter per million; CPM).

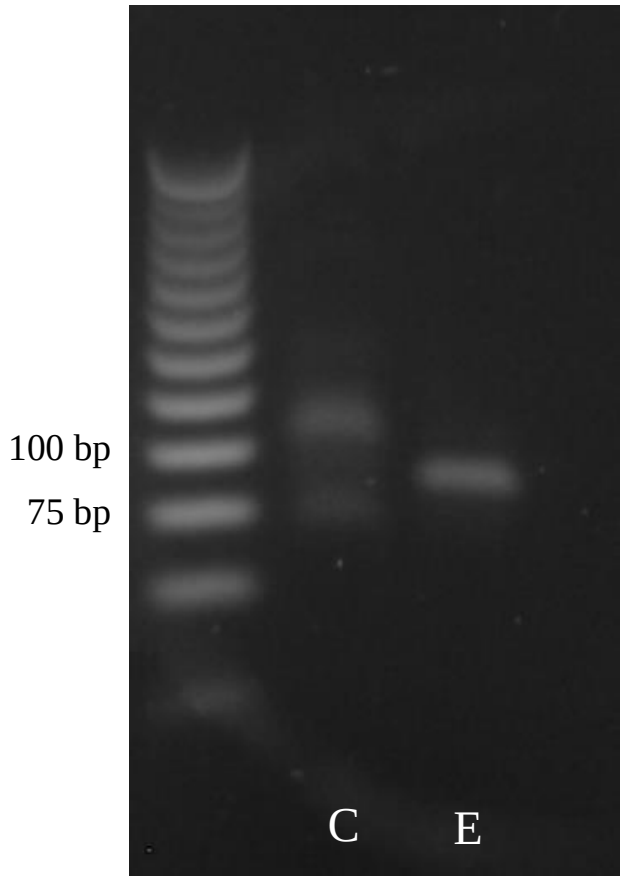

Figure 5.1 – Gel electrophoresis of aptamer products using conventional and emulsion PCR.
Amplification of the initial aptamer pool using conventional PCR (lane C) resulted in the formation by-product amplification. Amplification using emulsion PCR (lane E) prevented by-product formation and successfully amplified aptamers in the expected size (86 bp library).

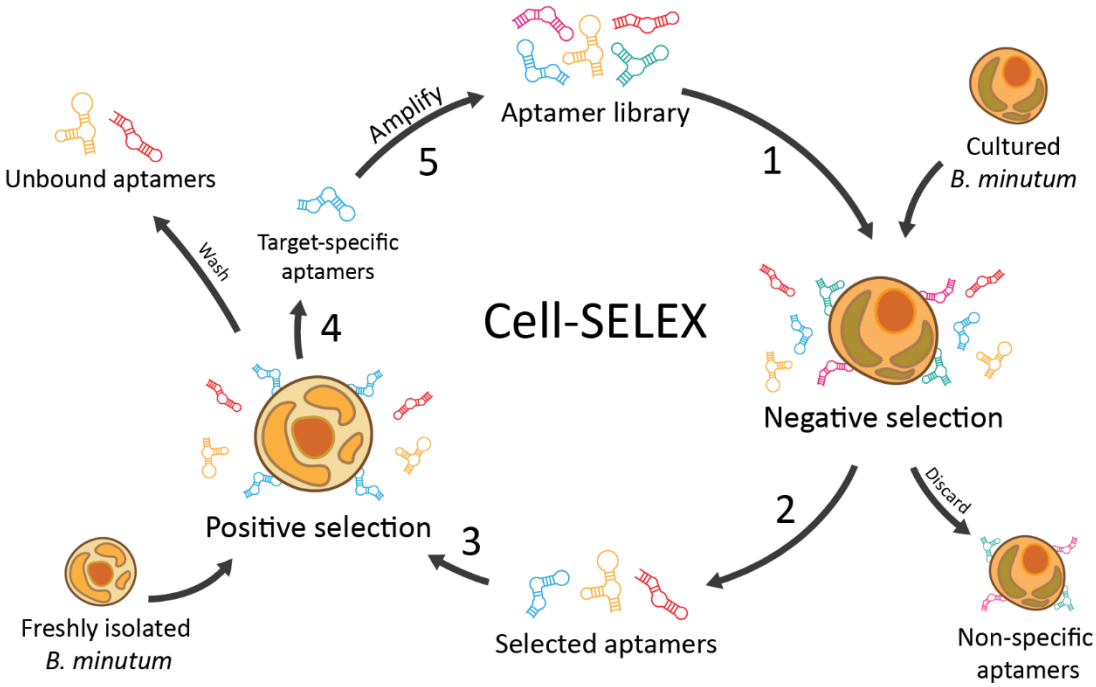

Figure 5.2 – Schematic of the Cell-SELEX process.
Aptamers are self-folding DNA oligonucleotides that bind specifically to targets. (1) The naive aptamer library was first incubated with cultured *Breviolum minutum* to remove non-specific aptamers. (2) Bound aptamers were discarded, and unbound aptamers were collected. (3) Selected aptamers were then bound to freshly isolated *B. minutum* to select for aptamers that are specific to *B. minutum* in the symbiotic state. (4) Target-specific aptamers that bound to freshly isolated *B. minutum* were eluted from the cells and (5) amplified by PCR. A total of six cycles of selection were performed.

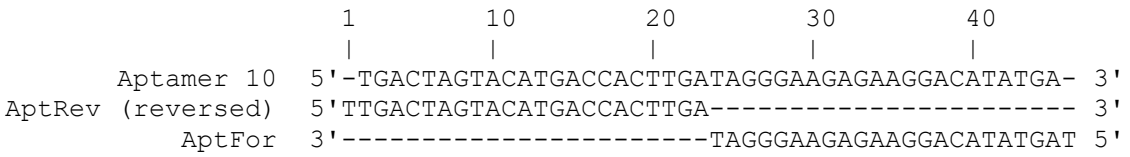

Figure 5.3 – Alignment of aptamer 10 with AptRev and AptFor primers.
Despite strong enrichment over SELEX rounds, aptamer 10 was a PCR artifact and not a functional aptamer.

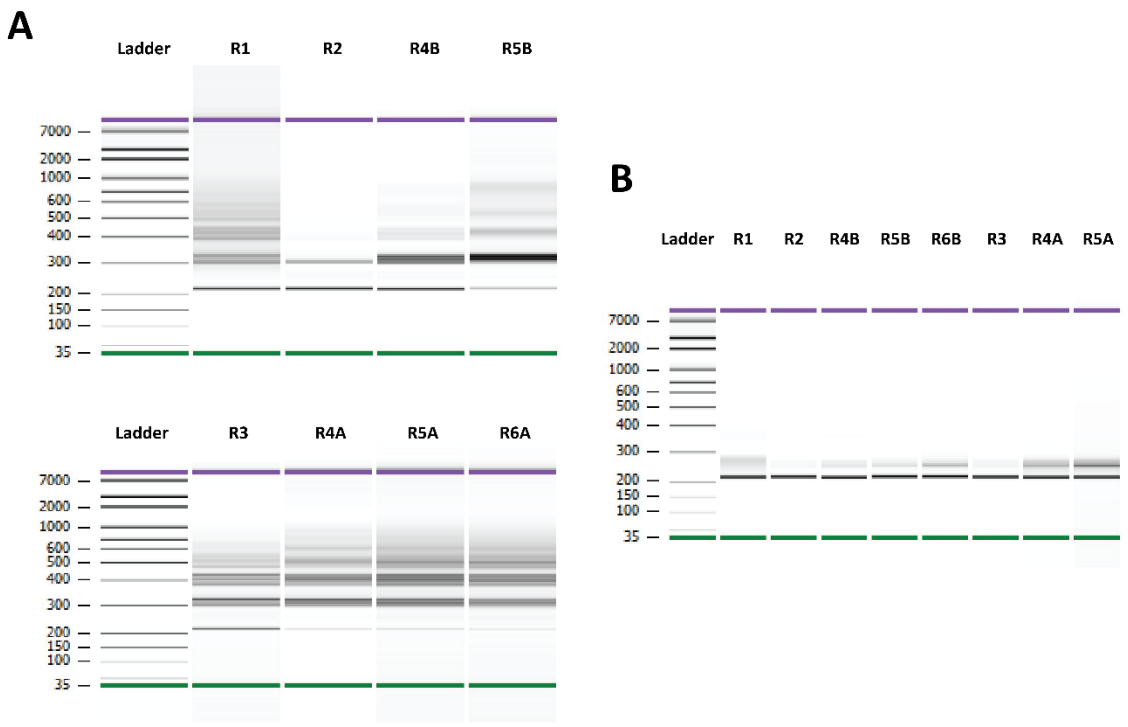

Figure 5.4 – Aptamers produced PCR by-products during preparation of sequencing libraries.
Sequencing libraries were analyzed with an Agilent 2100 Bioanalyzer to determine library size (215 bp expected size). **(A)** PCR by-products were present in the sequencing libraries, with proportionally more by-products in libraries prepared from later rounds of SELEX. **(B)** Size selection using BluePippin was able to recover the aptamer sequencing library. Rounds 6A and 6B are missing from **(B)** and **(A)** respectively, as they were analyzed independently as test samples.

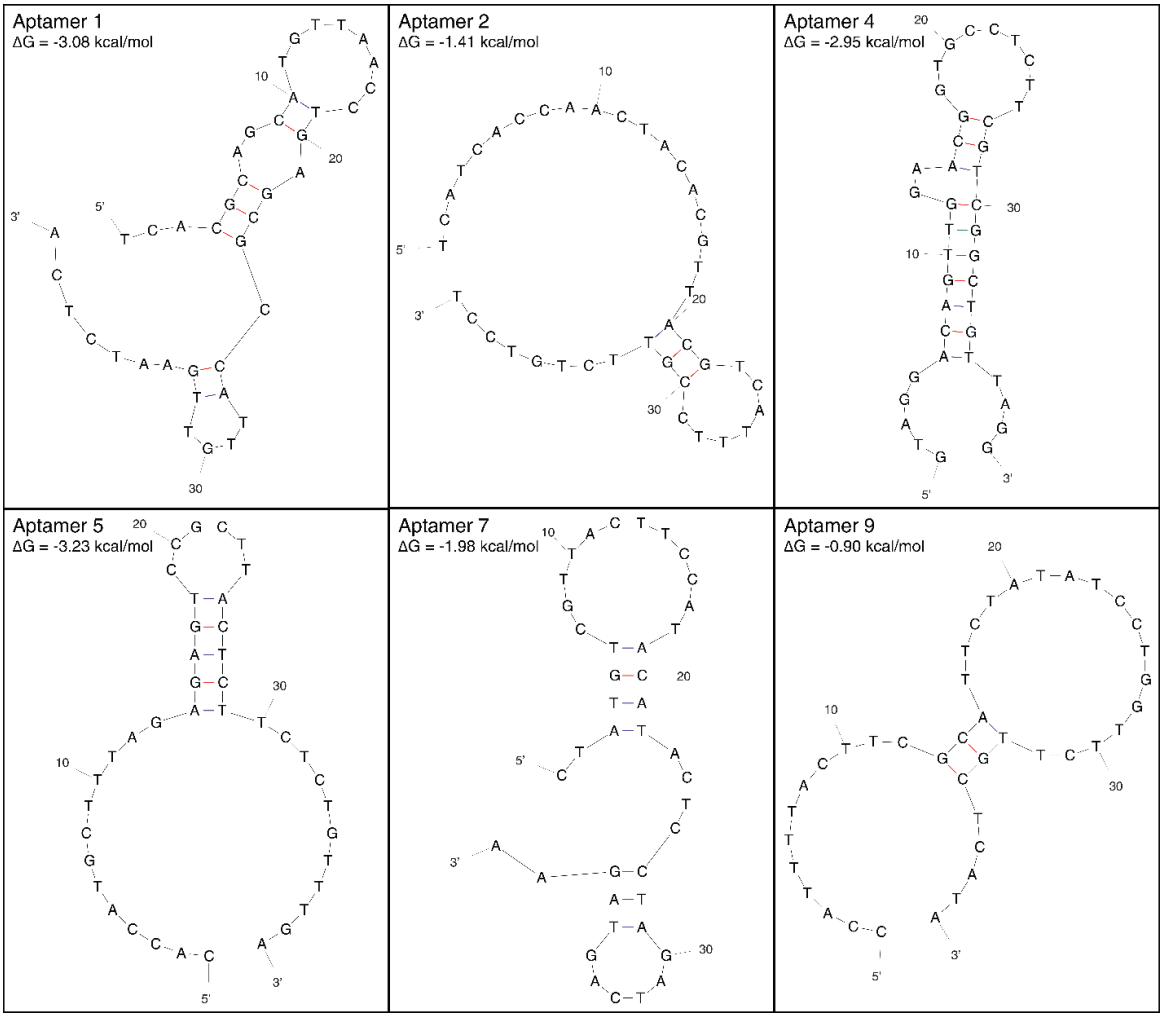

Figure 5.5 – Predicted aptamer secondary structure from mFold.
The secondary structures of select candidate aptamers were analyzed using mFold, with their respective free energies (ΔG) listed. Aptamers varied in their structures, with some using the majority of the sequence (aptamer 4) while others using only a small fraction of the sequence (aptamer 2). Aptamer sequences here do not contain their flanking regions, as they were blocked with oligonucleotides and do not participate in secondary structure formation.

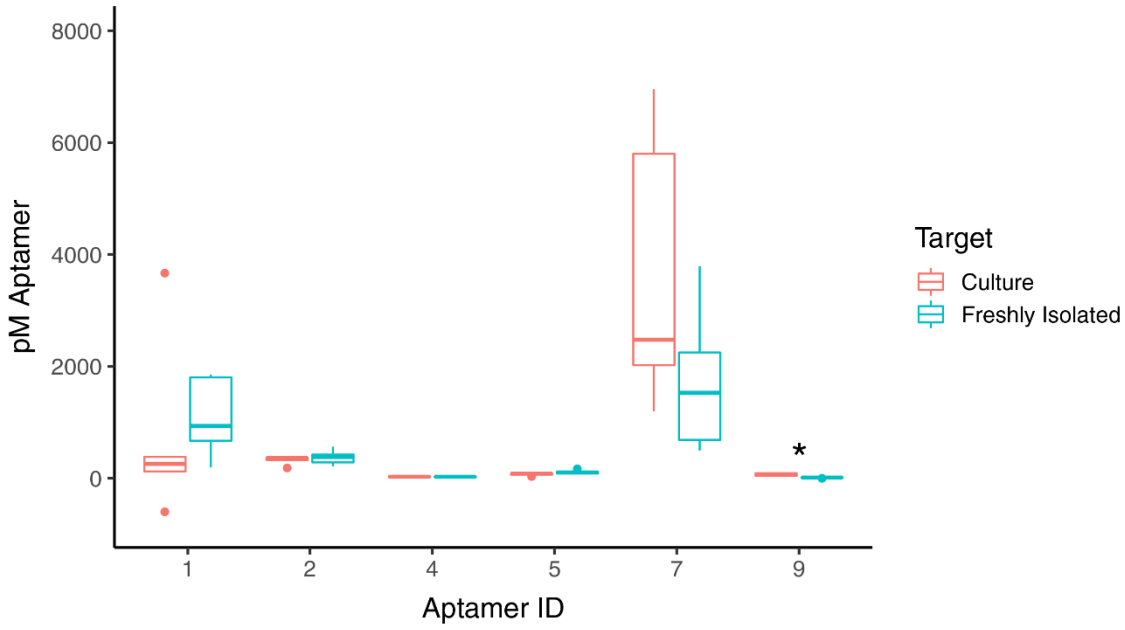

Figure 5.6 – Candidate aptamers failed to specifically target freshly isolated algae. Aptamer candidates were incubated at 200 nM with 100,000 algal cells that were from culture or freshly isolated. Bound aptamer concentrations varied highly between aptamers, but none bound specifically to freshly isolated algae. Aptamer 9 bound better to cultured algae than to freshly isolated algae indicated by a star (n = 5, p = 0.03, Student's t-test).

6. General conclusions and future directions

In this dissertation, I studied the cellular mechanisms governing cnidarian-algal symbiosis. In chapter 2, I found that heat stress of the algal symbiont hinders the re-establishment of symbiosis and shifts the cell-surface glycome of the algal symbiont *Breviolum minutum* to be more like that of non-homologous species of Symbiodiniaceae. In chapter 3, I critically discussed the limitations of using cultured algae for the study of cnidarian-algal symbiosis. In chapter 4, I explored the use of expelled algae in the form of Aiptasia egesta as an alternative to cultured algae to represent the *ex hospite* state of Symbiodiniaceae. In chapter 5, I developed an aptamer cell-SELEX protocol to discover novel symbiosis-specific cell-surface proteins on *B. minutum*.

Algal physiology affects cnidarian-algal symbiosis

Altogether, my work focused on how alga physiology can affect cnidarian-algal symbiosis. In chapter 2, heat-stress was applied only to the algal symbiont, therefore removing the effect of heat-stress on the host during colonization experiments. I found that heat-stress to the algal symbiont alone could hinder the establishment of symbiosis. While I did not provide a direct causal connection between the altered glycome and the hindering of symbiosis establishment, I controlled for factors such as light-induced generation of ROS and algal motility that could all hinder the onset of symbiosis. In addition, there is evidence from other studies that the heat-induced changes in the algal glycome (increase in high-mannose glycans and decrease in galactosylated glycans) are hypothesized to decrease colonization success (Parkinson et al. 2018, Tivey et al. 2020, Tortorelli et al. 2021).

In chapters 3 and 4, I challenged the hypothesis that the host controls nutrient availability to the symbiont as a critical mechanism for the maintenance of symbiosis and symbiont populations (Davy et al. 2012, Xiang et al. 2020). I found through literature review and experimental data using algae from Aiptasia egesta that nutrient availability to the algal symbiont may not be controlled by the host, rather, that nutrients are readily transferred to the symbiont when available (Maruyama and Weis 2021). Therefore, the

limitation of nutrients to the algal symbiont may not be a critical mechanism for the maintenance of symbiosis.

In chapter 4, I examined how algae are released by the hosts as a homeostatic mechanism to control symbiont populations. The algae in this study were released under ambient, healthy conditions, and so is not a result of the breakdown of symbiosis but is instead a necessary mechanism to regulate symbiosis. I found that algal physiology may play a role in the homeostatic release of algae, as the host preferentially expelled dividing algae and released the algae at night – coinciding with when the algae are hypothesized to divide. Algal cell division may therefore signal to the host to release the algae.

Perspective on the use of algal cultures in symbiosis research

In chapter 3 I discussed how cultured algae is not the best representation of the *ex hospite* state of Symbiodiniaceae, particularly in comparative studies against the *in hospite* state. However, there are other aspects of the use of cultured algae in studies that requires critical review. For example, in chapter 2 I explored the algal glycome, and all work was done using cultured algae grown in F/2 algal media. The use of cultured algae in this work was a choice of convenience and logistics – high algal biomasses were needed for experiments - and cultured algae are amenable to experimentation. Symbiodiniaceae in nature, however, do not commonly experience high-nutrient levels found in culture media and so the finding that heat-stress alters the algal glycome in culture is limited to the context of a high-nutrient environment. In addition, algae from egesta were found to decline in health within a few days, and heat-stress treatments lasted for three to seven days in this work, making this experiment difficult to repeat using Aiptasia egesta or even perhaps ecologically irrelevant, if the algae *ex hospite* are predicted to die before heat-stress can alter the algal glycome. Follow-up experiments are necessary to determine if heat stress applied to the holobiont alters the algal glycome *in hospite*, resulting in a release of algae *ex hospite* with a modified glycome.

The development of aptamers using cell-SELEX in chapter 5 also used cultured algae as a representation of algae *ex hospite*. In this comparison, ammonium and nitrate transporters were expected protein targets for aptamers specific to *B. minutum* in the symbiotic state (Maor-Landaw et al. 2020, Xiang et al. 2020). In chapter 4, however, I

found that these targets are not specific to symbiosis and instead are differentially regulated with nutrient availability. Therefore, while cell-SELEX failed to identify symbiosis-specific aptamers, even if it had been successful, the use of culture to represent the *ex hospite* state may have limited the interpretation of the findings.

Applications of aptamer cell-SELEX

Aptamer cell-SELEX could be used in other applications beyond that of identifying symbiosis-specific proteins. The development of aptamers is naïve to its molecular targets and has the potential to identify novel targets specific to certain phenotypes. For example, I found that the algal cell-surface glycome is affected by heat-stress, therefore, aptamer cell-SELEX would be expected to identify other heat or ambient-specific cell surface targets. Indeed, a study on *Breviolum psygmophilum* found that heat stress altered the cell surface proteome (Ricci et al. 2020). Aptamers could also be developed to recognize specific species of algae. This approach could aid in labeling algae when more than one species of Symbiodiniaceae are present in a sample, for example, to visualize symbiont uptake in co-inoculation experiments.

As cnidarian cell culture techniques continue to improve (Chiu et al. 2021, Kawamura et al. 2021, Nowotny et al. 2021), aptamers could be developed to be specific to host cell types. The identification of aptamers specific to phagocytic cells would greatly advance our understanding of cnidarian-algal symbiosis. Currently, it is not known what percentage of the cnidarian gastrodermis cells are capable of phagocytosis and whether the proportion is stable or changes with development or exposure to algal symbionts. Using aptamers to label the phagocytic cells *in vivo* could answer this question. Characterizing the cell-surface proteome of phagocytic cells using aptamers will also aid in describing the molecular processes involved in host-symbiont recognition and signaling cascades involved in phagocytosis.

Studying the host mechanisms involved in the onset and maintenance of symbiosis

While advances are being made in how the algal glycome varies with different species of algae and with heat-stress, there is a comparatively limited understanding of the host lectins involved in symbiont recognition. Few lectins have been characterized

from hosts that recognize symbionts and alter symbiont physiology to favor symbiosis (Jimbo et al. 2000, Kuniya et al. 2015, Zhou et al. 2017) but their role in symbiont recognition is poorly understood. For example, while I found that heat-stress alters the cell-surface glycome, we do not know which host lectins are binding (or failing to bind) to the heat-stressed symbiont. Specifically, I found that heat-stress increases high-mannose glycans, which corroborates previous findings that an increase in high-mannose glycans can hinder symbiosis and that high-mannose glycans are more abundant on non-compatible species of Symbiodininaceae (Tivey et al. 2020, Tortorelli et al. 2021). From this, one could hypothesize that there is a high-mannose binding host lectin that triggers an immune response, resulting in the rejection of algae with a high abundance of high-mannose glycans. There are likely other lectins that are critical for symbiont recognition, phagocytosis, and immune tolerance – such as those binding galactose glycans, as I found that they were more abundant under ambient temperature and previously literature found them to be higher in compatible species of Symbiodiniaceae (Parkinson et al. 2018, Tortorelli et al. 2021).

The host mechanisms governing the homeostatic release of algae is also poorly understood. Algae can be released by host cells through a variety of mechanisms, including host-cell apoptosis, host-cell autophagy, host-cell detachment, intracellular digestion by the host, and through vomocytosis (non-lytic expulsion) (Gates et al. 1992, Dunn et al. 2007, Downs et al. 2013, Bieri et al. 2016, Jacobovitz et al. 2021). I hypothesize that in Aiptasia, under homeostatic conditions, the algae are released through vomocytosis, as I found that algae in egesta were not degraded, and this mechanism has been characterized in Aiptasia as a way for the host cell to release non-compatible species of algae and other microbes after phagocytosis (Jacobovitz et al. 2021). This hypothesis could be investigated by dissociating host tissue and using a cell-sorter to enrich for host cells containing dividing cells based on cell size or DNA content using fluorescent markers. Gene expression could then be analyzed on the host cells containing dividing algae to determine if genes involved in vomocytosis are differentially regulated.

Recent advances have been made in CRISPR-cas9 knockouts in Aiptasia (Cleves, pers. comm) and in corals (Cleves et al. 2018, 2020). The function of specific lectins hypothesized to be involved in symbiont recognition and genes associated with

vomocytosis could be tested using CRISPR-cas9 knockouts. For example, knocking out the function of high-mannose binding lectins may enhance host tolerance for non-compatible symbionts. In turn, knocking out the function of galactose-binding lectins may hinder the establishment of symbiosis.

Effects of the covid-19 pandemic and lockdown on this thesis

During early 2020, stay-at-home lockdowns were mandated around the world to minimize the spread of covid-19. These lockdowns persisted for several months and for a time, entirely prevented physical access to the lab. Gradually, we slowly returned to working in the lab with staggered schedules between lab members to prevent the spread of covid-19. Teaching was conducted remotely until fall of 2021 when vaccines finally became widely available, which at times increased the workload as we developed materials for remote teaching.

This pandemic had significant effects on the progress and trajectory of the thesis. Prior to the pandemic, work on aptamers was nearing its conclusion. Unfortunately, the pandemic dramatically delayed progress on this work by preventing access to the lab, and by preventing access to Oregon State University's sequencing facilities. There were also supply chain issues with sequencing reagents and materials that further delayed progress on this work. There were originally plans to perform proteomics on algae from egesta as well, but this was abandoned due to time constraints conflated by the pandemic. Obtaining the final glycan mass spectrometry data in chapter 2 was also delayed due to the pandemic.

The pandemic, however, provided me with time to think about and write the perspective piece in chapter 3. Writing of this chapter was done entirely during the lockdown period, and work from this chapter shifted the research trajectory for chapter 4. The original focus of chapter 4 was on expelled algae as a source of algal symbionts for new generations of hosts. Instead, the focus of the chapter has shifted on expelled algae as an expermential representation of algae in the *ex hospite* state.

Conclusions

As coral reefs continue to decline due to climate change, there is a dire need for the development of solutions to prevent the continued decline of coral reefs. This effort requires understanding the basic biology of corals and their algal symbionts. My findings have contributed to our understanding of cnidarian-algal symbiosis, and the accumulation of knowledge will inform solutions to coral reef conservation. My contributions include how heat-stress of the algal symbiont alone may alter symbiont recognition by the host, highlighting the importance of both partners for the success of symbiosis. I also brought to attention the additional limitations of using cultured algae, which is largely a concern for experimental studies, but the use of cultured algae to establish heat-evolved strains of Symbiodiniaceae may also have its limitations (Chakravarti and van Oppen 2018, Buerger et al. 2020). As these algae are grown and artificially selected in high-nutrient media, they may not evolve to be suitable partners for their hosts and could partially explain why some heat-evolved strains failed to increase thermal tolerance of the holobiont (Chakravarti and van Oppen 2018, Buerger et al. 2020). Much like how treating human disease requires an understanding of pathogenesis, saving coral reefs will require that we understand the basic biology of corals and their algal symbionts. Nevertheless, the best line of defense for disease and coral reef conservation is prevention, and the panacea for coral decline is the mitigation of anthropogenic climate change. Efforts must continue by global leaders, both for corals and for humanity, to eliminate our reliance on fossil fuels and adopt sustainable sources of energy to halt the release of greenhouse emissions.

6.1 References

Bieri, T., Onishi, M., Xiang, T., Grossman, A.R. & Pringle, J.R. 2016. Relative Contributions of Various Cellular Mechanisms to Loss of Algae during Cnidarian Bleaching. *PLoS One*. 11:e0152693.

Buerger, P., Alvarez-Roa, C., Coppin, C.W., Pearce, S.L., Chakravarti, L.J., Oakeshott, J.G., Edwards, O.R. et al. 2020. Heat-evolved microalgal symbionts increase coral bleaching tolerance. *Sci Adv*. 6:eaba2498.

Chakravarti, L.J. & van Oppen, M.J.H. 2018. Experimental Evolution in Coral Photosymbionts as a Tool to Increase Thermal Tolerance. *Frontiers in Marine Science*. 5.

Chiu, Y.-L., Chang, C.-F. & Shikina, S. 2021. Development of an in vitro tissue culture system for hammer coral (Fimbriaphyllia ancora) ovaries. *Sci. Rep.* 11:24338.

Cleves, P.A., Strader, M.E., Bay, L.K., Pringle, J.R. & Matz, M.V. 2018. CRISPR/Cas9-mediated genome editing in a reef-building coral. *Proc. Natl. Acad. Sci. U. S. A.* 115:5235–40.

Cleves, P.A., Tinoco, A.I., Bradford, J., Perrin, D., Bay, L.K. & Pringle, J.R. 2020. Reduced thermal tolerance in a coral carrying CRISPR-induced mutations in the gene for a heat-shock transcription factor. *Proc. Natl. Acad. Sci. U. S. A.* 117:28899–905.

Davy, S.K., Allemand, D. & Weis, V.M. 2012. Cell biology of cnidarian-dinoflagellate symbiosis. *Microbiol. Mol. Biol. Rev.* 76:229–61.

Downs, C.A., McDougall, K.E., Woodley, C.M., Fauth, J.E., Richmond, R.H., Kushmaro, A., Gibb, S.W. et al. 2013. Heat-stress and light-stress induce different cellular pathologies in the symbiotic dinoflagellate during coral bleaching. *PLoS One*. 8:e77173.

Dunn, S.R., Schnitzler, C.E. & Weis, V.M. 2007. Apoptosis and autophagy as mechanisms of dinoflagellate symbiont release during cnidarian bleaching: every which way you lose. *Proc. Biol. Sci.* 274:3079–85.

Gates, R.D., Baghdasarian, G. & Muscatine, L. 1992. Temperature Stress Causes Host Cell Detachment in Symbiotic Cnidarians: Implications for Coral Bleaching. *Biol. Bull.* 182:324–32.

Jacobovitz, M.R., Rupp, S., Voss, P.A., Maegele, I., Gornik, S.G. & Guse, A. 2021. Dinoflagellate symbionts escape vomocytosis by host cell immune suppression. *Nat Microbiol*. 6:769–82.

Jimbo, M., Yanohara, T., Koike, Kazuhiko, Koike, Kanae, Sakai, R., Muramoto, K. & Kamiya, H. 2000. The d-galactose-binding lectin of the octocoral *Sinularia lochmodes*: characterization and possible relationship to the symbiotic dinoflagellates.

Kawamura, K., Nishitsuji, K., Shoguchi, E., Fujiwara, S. & Satoh, N. 2021. Establishing Sustainable Cell Lines of a Coral, Acropora tenuis. *Mar. Biotechnol.* 23:373–88.

Kuniya, N., Jimbo, M., Tanimoto, F., Yamashita, H., Koike, K., Harii, S., Nakano, Y. et al. 2015. Possible involvement of Tachylectin-2-like lectin from Acropora tenuis in the process of Symbiodinium acquisition. *Fish. Sci.* 81:473–83.

Maor-Landaw, K., van Oppen, M.J.H. & McFadden, G.I. 2020. Symbiotic lifestyle triggers drastic changes in the gene expression of the algal endosymbiont *Breviolum minutum* (Symbiodiniaceae). *Ecol. Evol.* 10:451–66.

Maruyama, S. & Weis, V.M. 2021. Limitations of using cultured algae to study cnidarian-algal symbioses and suggestions for future studies. *J. Phycol.* 57:30–8.

Nowotny, J.D., Connelly, M.T. & Traylor-Knowles, N. 2021. Novel methods to establish whole-body primary cell cultures for the cnidarians *Nematostella vectensis* and *Pocillopora damicornis*. *Sci. Rep.* 11:4086.

Parkinson, J.E., Tivey, T.R., Mandelare, P.E., Adpressa, D.A., Loesgen, S. & Weis, V.M. 2018. Subtle differences in symbiont cell surface glycan profiles do not explain species-specific colonization rates in a model cnidarian-algal symbiosis. *Front. Microbiol.* 9:842.

Ricci, C.A., Kamal, A.H., Chakrabarty, J.K., Ledbetter, B.E., Chowdhury, S.M. & Mydlarz, L.D. 2020. The cell-surface protein composition of a coral symbiont, *Breviolum psygmophilum*, reveals a mechanism for host specificity and displays dynamic regulation during temperature stress. *Mar. Biol.* 167:66.

Tivey, T.R., Parkinson, J.E., Mandelare, P.E., Adpressa, D.A., Peng, W., Dong, X., Mechref, Y. et al. 2020. N-linked surface glycan biosynthesis, composition, inhibition, and function in cnidarian-dinoflagellate symbiosis. *Microb. Ecol.* 80:223–36.

Tortorelli, G., Rautengarten, C., Bacic, A., Segal, G., Ebert, B., Davy, S.K., van Oppen, M.J.H. et al. 2021. Cell surface carbohydrates of symbiotic dinoflagellates and their role in the establishment of cnidarian-dinoflagellate symbiosis. *ISME J.* 16:190–9.

Xiang, T., Lehnert, E., Jinkerson, R.E., Clowez, S., Kim, R.G., DeNofrio, J.C., Pringle, J.R. et al. 2020. Symbiont population control by host-symbiont metabolic interaction in Symbiodiniaceae-cnidarian associations. *Nat. Commun.* 11:108.

Zhou, Z., Yu, X., Tang, J., Zhu, Y., Chen, G., Guo, L. & Huang, B. 2017. Dual recognition activity of a rhamnose-binding lectin to pathogenic bacteria and zooxanthellae in stony coral *Pocillopora damicornis*. *Dev. Comp. Immunol.* 70:88–93.

7. Combined References

Alan Verde, E., Cleveland, A. & Lee, R.W. 2015. Nutritional exchange in a tropical tripartite symbiosis II: direct evidence for the transfer of nutrients from host anemone and zooxanthellae to anemonefish. *Mar. Biol.* 162:2409–29.

Ali, A., Kriefall, N.G., Emery, L.E., Kenkel, C.D., Matz, M.V. & Davies, S.W. 2019. Recruit symbiosis establishment and Symbiodiniaceae composition influenced by adult corals and reef sediment. *Coral Reefs*. 38:405–15.

Al-Moghrabi, S., Goiran, C., Allemand, D., Speziale, N. & Jaubert, J. 1996. Inorganic carbon uptake for photosynthesis by the symbiotic coral-dinoflagellate association II. Mechanisms for bicarbonate uptake. *J. Exp. Mar. Bio. Ecol.* 199:227–48.

Aranda, M., Li, Y., Liew, Y.J., Baumgarten, S., Simakov, O., Wilson, M.C., Piel, J. et al. 2016. Genomes of coral dinoflagellate symbionts highlight evolutionary adaptations conducive to a symbiotic lifestyle. *Sci. Rep.* 6:1–15.

Azzazy, H.M.E. & Highsmith, W.E., Jr 2002. Phage display technology: clinical applications and recent innovations. *Clin. Biochem.* 35:425–45.

Baghdasarian, G. & Muscatine, L. 2000. Preferential expulsion of dividing algal cells as a mechanism for regulating algal-cnidarian symbiosis. *Biol. Bull.* 199:278–86.

Barott, K.L., Venn, A.A., Perez, S.O., Tambutté, S. & Tresguerres, M. 2015. Coral host cells acidify symbiotic algal microenvironment to promote photosynthesis. *Proc. Natl. Acad. Sci. U. S. A.* 112:607–12.

Baumgarten, S., Simakov, O., Esherick, L.Y., Liew, Y.J., Lehnert, E.M., Michell, C.T., Li, Y. et al. 2015. The genome of *Aiptasia*, a sea anemone model for coral symbiosis. *Proc. Natl. Acad. Sci. U. S. A.* 112:201513318.

Bay, L.K., Cumbo, V.R., Abrego, D., Kool, J.T., Ainsworth, T.D. & Willis, B.L. 2011. Infection dynamics vary between *Symbiodinium* types and cell surface treatments during establishment of endosymbiosis with coral larvae. *Diversity* . 3:356–74.

Bellantuono, A.J., Dougan, K.E., Granados-Cifuentes, C. & Rodriguez-Lanetty, M. 2019. Free-living and symbiotic lifestyles of a thermotolerant coral endosymbiont display profoundly distinct transcriptomes under both stable and heat stress conditions. *Mol. Ecol.* 28:5265–81.

Bellantuono, A.J., Granados-Cifuentes, C., Miller, D.J., Hoegh-Guldberg, O. & Rodriguez-Lanetty, M. 2012. Coral thermal tolerance: tuning gene expression to resist thermal stress. *PLoS One*. 7:e50685.

Benedetti, E., Gerstner, N., Pučić-Baković, M., Keser, T., Reiding, K.R., Ruhaak, L.R., Štambuk, T. et al. 2020. Systematic evaluation of normalization methods for glycomics data based on performance of network inference. *Metabolites*. 10.

Berezovski, M.V., Lechmann, M., Musheev, M.U., Mak, T.W. & Krylov, S.N. 2008. Aptamer-facilitated biomarker discovery (AptaBiD). *J. Am. Chem. Soc.* 130:9137–43.

Bertucci, A., Tambutté, E., Tambutté, S., Allemand, D. & Zoccola, D. 2010. Symbiosis-dependent gene expression in coral-dinoflagellate association: cloning and characterization of a P-type H+-ATPase gene. *Proc. Biol. Sci.* 277:87–95.

Bhagooli, R. & Hidaka, M. 2004. Release of zooxanthellae with intact photosynthetic activity by the coral *Galaxea fascicularis* in response to high temperature stress. *Mar. Biol.* 145:329–37.

Bieri, T., Onishi, M., Xiang, T., Grossman, A.R. & Pringle, J.R. 2016. Relative contributions of various cellular mechanisms to loss of algae during cnidarian bleaching. *PLoS One*. 11:e0152693.

Biquand, E., Okubo, N., Aihara, Y., Rolland, V., Hayward, D.C., Hatta, M., Minagawa, J. et al. 2017. Acceptable symbiont cell size differs among cnidarian species and may limit symbiont diversity. *ISME J.* 11:1702–12.

Blackstone, N.W. & Golladay, J.M. 2018. Why Do Corals Bleach? Conflict and Conflict Mediation in a Host/Symbiont Community. *Bioessays*. 40:e1800021.

Buerger, P., Alvarez-Roa, C., Coppin, C.W., Pearce, S.L., Chakravarti, L.J., Oakeshott, J.G., Edwards, O.R. et al. 2020. Heat-evolved microalgal symbionts increase coral bleaching tolerance. *Sci Adv*. 6:eaba2498.

Ceh, J., van Keulen, M. & Bourne, D.G. 2013. Intergenerational transfer of specific bacteria in corals and possible implications for offspring fitness. *Microb. Ecol.* 65:227–31.

Chakravarti, L.J., Beltran, V.H. & van Oppen, M.J.H. 2017. Rapid thermal adaptation in photosymbionts of reef-building corals. *Glob. Chang. Biol.* 23:4675–88.

Chakravarti, L.J. & van Oppen, M.J.H. 2018. Experimental evolution in coral photosymbionts as a tool to increase thermal tolerance. *Frontiers in Marine Science*. 5.

Chandramouli, K. & Qian, P.-Y. 2009. Proteomics: challenges, techniques and possibilities to overcome biological sample complexity. *Hum. Genomics Proteomics*. 2009.

Chen, C.-S., Lin, H.-P., Yeh, C.-C. & Fang, L.-S. 2005. Use of a fluorescent membrane probe to identify zooxanthellae in hospite among dissociated endoderm cell culture from coral. *Protoplasma*. 226:175–9.

Chen, M.-C., Cheng, Y.-M., Sung, P.-J., Kuo, C.-E. & Fang, L.-S. 2003. Molecular identification of Rab7 (ApRab7) in Aiptasia pulchella and its exclusion from phagosomes harboring zooxanthellae. *Biochem. Biophys. Res. Commun.* 308:586–95.

Chiu, Y.-L., Chang, C.-F. & Shikina, S. 2021. Development of an in vitro tissue culture system for hammer coral (*Fimbriaphyllia ancora*) ovaries. *Sci. Rep.* 11:24338.

Cho, B.G., Jiang, P., Goli, M., Gautam, S. & Mechref, Y. 2021. Using micro pillar array columns (μPAC) for the analysis of permethylated glycans. *Analyst*. 146:4374–83.

Cleves, P.A., Krediet, C.J., Lehnert, E.M., Onishi, M. & Pringle, J.R. 2020a. Insights into coral bleaching under heat stress from analysis of gene expression in a sea anemone model system. *Proc. Natl. Acad. Sci. U. S. A.* 117:28906–17.

Cleves, P.A., Strader, M.E., Bay, L.K., Pringle, J.R. & Matz, M.V. 2018. CRISPR/Cas9-mediated genome editing in a reef-building coral. *Proc. Natl. Acad. Sci. U. S. A.* 115:5235–40.

Cleves, P.A., Tinoco, A.I., Bradford, J., Perrin, D., Bay, L.K. & Pringle, J.R. 2020b. Reduced thermal tolerance in a coral carrying CRISPR-induced mutations in the gene for a heat-shock transcription factor. *Proc. Natl. Acad. Sci. U. S. A.* 117:28899–905.

Colley, N. & Trench, R. 1983. Selectivity in phagocytosis and persistence of symbiotic algae by the scyphistoma stage of the jellyfish. *Proceedings of the Royal Society B: Biological Sciences*. 219:61–82.

Cook, C.B., D'Elia, C.F. & Muller-Parker, G. 1988. Host feeding and nutrient sufficiency for zooxanthellae in the sea anemone *Aiptasia pallida*. *Marine Biology*. 262:253–62.

Cui, G., Liew, Y.J., Konciute, M.K., Zhan, Y., Hung, S.-H., Thistle, J., Gastoldi, L. et al. 2022. Nutritional control regulates symbiont proliferation and life history in coral-dinoflagellate symbiosis. *BMC Biol.* 20:103.

Cziesielski, M.J., Liew, Y.J., Cui, G., Schmidt-roach, S., Campana, S., Marondedze, C. & Aranda, M. 2018. Multi-omics analysis of thermal stress response in a zooxanthellate cnidarian reveals the importance of associating with thermotolerant symbionts. *Proceedings of Royal Society B*. 285:20172654.

Dao, P., Hoinka, J., Takahashi, M., Zhou, J., Ho, M., Wang, Y., Costa, F. et al. 2016. AptaTRACE Elucidates RNA Sequence-Structure Motifs from Selection Trends in HT-SELEX Experiments. *Cell Syst*. 3:62–70.

Davy, S.K., Allemand, D. & Weis, V.M. 2012. Cell biology of cnidarian-dinoflagellate symbiosis. *Microbiol. Mol. Biol. Rev.* 76:229–61.

den Haan, J., Huisman, J., Brocke, H.J., Goehlich, H., Latijnhouwers, K.R.W., van Heeringen, S., Honcoop, S.A.S. et al. 2016. Nitrogen and phosphorus uptake rates of different species from a coral reef community after a nutrient pulse. *Sci. Rep.* 6:28821.

Detournay, O., Schnitzler, C.E., Poole, A. & Weis, V.M. 2012. Regulation of cnidarian-dinoflagellate mutualisms: evidence that activation of a host TGFβ innate immune pathway promotes tolerance of the symbiont. *Dev. Comp. Immunol.* 38:525–37.

Dieterle, F., Ross, A., Schlotterbeck, G. & Senn, H. 2006. Probabilistic quotient normalization as robust method to account for dilution of complex biological mixtures. Application in 1H NMR metabonomics. *Anal. Chem.* 78:4281–90.

Dong, X., Zhou, S. & Mechref, Y. 2016. LC-MS/MS analysis of permethylated free oligosaccharides and N-glycans derived from human, bovine, and goat milk samples. *Electrophoresis*. 37:1532–48.

Downs, C.A., McDougall, K.E., Woodley, C.M., Fauth, J.E., Richmond, R.H., Kushmaro, A., Gibb, S.W. et al. 2013. Heat-stress and light-stress induce different cellular pathologies in the symbiotic dinoflagellate during coral bleaching. *PLoS One*. 8:e77173.

Dunn, M.R., Jimenez, R.M. & Chaput, J.C. 2017. Analysis of aptamer discovery and technology. *Nature Reviews Chemistry*. 1:Article number: 0076.

Dunn, S.R., Schnitzler, C.E. & Weis, V.M. 2007. Apoptosis and autophagy as mechanisms of dinoflagellate symbiont release during cnidarian bleaching: every which way you lose. *Proc. Biol. Sci.* 274:3079–85.

Durnford, D.G., Deane, J.A., Tan, S., McFadden, G.I., Gantt, E. & Green, B.R. 1999. A phylogenetic assessment of the eukaryotic light-harvesting antenna proteins, with implications for plastid evolution. *J. Mol. Evol.* 48:59–68.

Dwivedi, H.P., Smiley, R.D. & Jaykus, L.-A. 2013. Selection of DNA aptamers for capture and detection of Salmonella Typhimurium using a whole-cell SELEX

approach in conjunction with cell sorting. *Appl. Microbiol. Biotechnol.* 97:3677–86.

Fadlallah, Y.H. 1983. Sexual reproduction, development and larval biology in scleractinian corals. *Coral Reefs*. 2:129–50.

Falkowski, P.G., Dubinsky, Z., Muscatine, L. & McCloskey, L. 1993. Population control in symbiotic corals. *Bioscience*. 43:606–11.

Ferrier-Pagès, C., Schoelzke, V., Jaubert, J., Muscatine, L. & Hoegh-Guldberg, O. 2001. Response of a scleractinian coral, *Stylophora pistillata*, to iron and nitrate enrichment. *J. Exp. Mar. Bio. Ecol.* 259:249–61.

Fitt, W.K. & Trench, R.K. 1983. The relation of diel patterns of cell division to diel patterns of motility in the symbiotic dinoflagellate *Symbiodinium microadriaticum* Freudenthal in culture. *New Phytol.* 94:421–32.

Flynn, R.A., Pedram, K., Malaker, S.A., Batista, P.J., Smith, B.A.H., Johnson, A.G., George, B.M. et al. 2021. Small RNAs are modified with N-glycans and displayed on the surface of living cells. *Cell*. 184:3109-3124.e22.

Fujise, L., Nitschke, M.R., Frommlet, J.C., Serôdio, J., Woodcock, S., Ralph, P.J. & Suggett, D.J. 2018. Cell cycle dynamics of cultured coral endosymbiotic microalgae (*Symbiodinium*) across different types (species) under alternate light and temperature conditions. *J. Eukaryot. Microbiol.* 65:505–17.

Fujise, L., Suggett, D.J., Stat, M., Kahlke, T., Bunce, M., Gardner, S.G., Goyen, S. et al. 2021. Unlocking the phylogenetic diversity, primary habitats, and abundances of free-living Symbiodiniaceae on a coral reef. *Mol. Ecol.* 30:343–60.

Fujise, L., Yamashita, H., Suzuki, G. & Koike, K. 2013. Expulsion of zooxanthellae (*Symbiodinium*) from several species of scleractinian corals: comparison under non-stress conditions and thermal stress conditions. *Galaxea (Tokyo)*. 15:29–36.

Fujise, L., Yamashita, H., Suzuki, G., Sasaki, K., Liao, L.M. & Koike, K. 2014. Moderate thermal stress causes active and immediate expulsion of photosynthetically damaged zooxanthellae (*Symbiodinium*) from corals. *PLoS One*. 9:1–18.

Gabay, Y., Parkinson, J.E., Wilkinson, S.P., Weis, V.M. & Davy, S.K. 2019. Inter-partner specificity limits the acquisition of thermotolerant symbionts in a model cnidarian-dinoflagellate symbiosis. *ISME J.* 13:2489–99.

Gabay, Y., Weis, V.M. & Davy, S.K. 2018. Symbiont identity influences patterns of symbiosis establishment, host growth, and asexual reproduction in a model cnidarian-dinoflagellate symbiosis. *Biol. Bull.* 234.

Gates, R.D., Baghdasarian, G. & Muscatine, L. 1992. Temperature stress causes host cell detachment in symbiotic cnidarians: Implications for coral bleaching. *Biol. Bull.* 182:324–32.

Gautam, S., Peng, W., Cho, B.G., Huang, Y., Banazadeh, A., Yu, A., Dong, X. et al. 2020. Glucose unit index (GUI) of permethylated glycans for effective identification of glycans and glycan isomers. *Analyst*. 145:6656–67.

Ghosh, S. 2020. Sialic acid and biology of life: An introduction. *In Sialic Acids and Sialoglycoconjugates in the Biology of Life, Health and Disease*. pp. 1–61.

Gilman, V.L. 2012. Methods for identifying nucleic acid ligands.

Godinot, C., Ferrier-Pagès, C. & Grover, R. 2009. Control of phosphate uptake by zooxanthellae and host cells in the scleractinian coral *Stylophora pistillata*. *Limnology and Oceanography*. 54:1627–33.

Goiran, C., Allemand, D. & Galgani, I. 1997. Transient Na+ stress in symbiotic dinoflagellates after isolation from coral-host cells and subsequent immersion in seawater. *Mar. Biol.* 129:581–9.

Goiran, C., Al-moghrabi, S. & Allemand, D. 1996. Inorganic carbon uptake for photosynthesis by the symbiotic coral/dinoflagellate association I. Photosynthetic performances of symbionts and dependence on sea water bicarbonate. *Journal of Experimental Marine Biology and Ecology*. 199:207–25.

Goulet, T.L., Cook, C.B. & Goulet, D. 2005. Effect of short-term exposure to elevated temperatures and light levels on photosynthesis of different host-symbiont combinations in the *Aiptasia pallida-Symbiodinium* symbiosis. *Limnology and Oceanography*. 50:1490–8.

Grawunder, D., Hambleton, E.A., Bucher, M., Wolfowicz, I., Bechtoldt, N. & Guse, A. 2015. Induction of gametogenesis in the cnidarian endosymbiosis model *Aiptasia* sp. *Sci. Rep.* 5:15677.

Grupstra, C.G.B., Lemoine, N.P., Cook, C. & Correa, A.M.S. 2022. Thank you for biting: dispersal of beneficial microbiota through "antagonistic" interactions. *Trends Microbiol.*

Grupstra, C.G.B., Rabbitt, K.M., Howe-Kerr, L.I. & Correa, A.M.S. 2021. Fish predation on corals promotes the dispersal of coral symbionts. *Anim Microbiome*. 3:25.

Hallock, P. & Schlager, W. 1986. Nutrient Excess and the Demise of Coral Reefs and Carbonate Platforms. *Palaios*. 1:389–98.

Hambleton, E.A., Guse, A. & Pringle, J.R. 2014. Similar specificities of symbiont uptake by adults and larvae in an anemone model system for coral biology. *J. Exp. Biol.* 217:1613–9.

Hambleton, E.A., Jones, V.A.S., Maegele, I., Kvaskoff, D., Sachsenheimer, T. & Guse, A. 2019. Sterol transfer by atypical cholesterol-binding NPC2 proteins in coral-algal symbiosis. *Elife*. 8.

Hawkins, T.D., Hagemeyer, J.C.G. & Warner, M.E. 2016. Temperature moderates the infectiousness of two conspecific *Symbiodinium* strains isolated from the same host population. *Environ. Microbiol.* 18:5204–17.

Hernandez-Agreda, A., Gates, R.D. & Ainsworth, T.D. 2017. Defining the core microbiome in corals' microbial soup. *Trends Microbiol.* 25:125–40.

Herrera, M., Klein, S.G., Campana, S., Chen, J.E., Prasanna, A., Duarte, C.M. & Aranda, M. 2021. Temperature transcends partner specificity in the symbiosis establishment of a cnidarian. *ISME J.* 15:141–53.

Hildebrand, M. 2005. Cloning and functional characterization of ammonium transporters from the marine diatom *Cylindrotheca fusiformis* (Bacillariophyceae). *J. Phycol.* 41:105–13.

Hill, R. & Ralph, P.J. 2007. Post-bleaching viability of expelled zooxanthellae from the scleractinian coral *Pocillopora damicornis*. *Mar. Ecol. Prog. Ser.* 352:137–44.

Hoegh-Guldberg, O. 1994. Population dynamics of symbiotic zooxanthellae in the coral *Pocillopora damicornis* exposed to elevated ammonium [(NH4)2 SO4] concentrations. *Pac. Sci.* 48.

Hoegh-Guldberg, O., McCloskey, L.R. & Muscatine, L. 1987. Expulsion of zooxanthellae by symbiotic cnidarians from the Red Sea. *Coral Reefs*. 5:201–4.

Hoegh-Guldberg, O., Poloczanska, E.S., Skirving, W. & Dove, S. 2017. Coral reef ecosystems under climate change and ocean acidification. *Frontiers in Marine Science*. 4:158.

Hoegh-Guldberg, O. & Smith, G.J. 1989. Influence of the population density of zooxanthellae and supply of ammonium on the biomass and metabolic characteristics of the reef corals *Seriatopora hystrix* and *Stylophora pistillata*. *Mar. Ecol. Prog. Ser.*

Hohman, T.C., McNeil, P.L. & Muscatine, L. 1982. Phagosome-lysosome fusion inhibited by algal symbionts of *Hydra viridis*. *J. Cell Biol.* 94:56–63.

Hoinka, J., Backofen, R. & Przytycka, T.M. 2018. AptaSUITE: A Full-Featured Bioinformatics Framework for the Comprehensive Analysis of Aptamers from HT-SELEX Experiments. *Mol. Ther. Nucleic Acids*. 11:515–7.

Hoinka, J., Berezhnoy, A., Sauna, Z.E., Gilboa, E. & Przytycka, T.M. 2014. AptaCluster - A Method to Cluster HT-SELEX Aptamer Pools and Lessons from its Application. *Res. Comput. Mol. Biol.* 8394:115–28.

Hoinka, J. & Przytycka, T. 2016. AptaPLEX - A dedicated, multithreaded demultiplexer for HT-SELEX data. *Methods*. 106:82–5.

Hong, M.C., Huang, Y.S., Song, P.C., Lin, W.W., Fang, L.S. & Chen, M.C. 2009. Cloning and characterization of ApRab4, a recycling rab protein of *Aiptasia pulchella*, and its implication in the symbiosome biogenesis. *Mar. Biotechnol.* 11:771–85.

Hoogenboom, M., Beraud, E. & Ferrier-Pagès, C. 2010. Relationship between symbiont density and photosynthetic carbon acquisition in the temperate coral *Cladocora caespitosa*. *Coral Reefs*. 29:21–9.

Houlbrèque, F., Tambutté, E., Allemand, D. & Ferrier-Pagès, C. 2004. Interactions between zooplankton feeding, photosynthesis and skeletal growth in the scleractinian coral *Stylophora pistillata*. *J. Exp. Biol.* 207:1461–9.

Huang, J., Chen, X., Fu, X., Li, Z., Huang, Y. & Liang, C. 2021. Advances in Aptamer-Based Biomarker Discovery. *Front Cell Dev Biol*. 9:659760.

Huang, K.-J., Huang, Z.-Y., Lin, C.-Y., Wang, L.-H., Chou, P.-H., Chen, C.-S. & Li, H.-H. 2017. Generation of clade- and symbiont-specific antibodies to characterize marker molecules during cnidaria-*Symbiodinium* endosymbiosis. *Sci. Rep.* 7:5488.

Hughes, T.P., Anderson, K.D., Connolly, S.R., Heron, S.F., Kerry, J.T., Lough, J.M., Baird, A.H. et al. 2018a. Spatial and temporal patterns of mass bleaching of corals in the Anthropocene. *Science*. 359:80–3.

Hughes, T.P., Kerry, J.T., Baird, A.H., Connolly, S.R., Dietzel, A., Eakin, C.M., Heron, S.F. et al. 2018b. Global warming transforms coral reef assemblages. *Nature*. 556:492–6.

Irwin, N.A.T., Martin, B.J.E., Young, B.P., Browne, M.J.G., Flaus, A., Loewen, C.J.R., Keeling, P.J. et al. 2018. Viral proteins as a potential driver of histone depletion in dinoflagellates. *Nat. Commun.* 9:1535.

Jacobovitz, M.R., Rupp, S., Voss, P.A., Maegele, I., Gornik, S.G. & Guse, A. 2021. Dinoflagellate symbionts escape vomocytosis by host cell immune suppression. *Nat Microbiol*. 6:769–82.

Jain, P., Chakma, B., Patra, S. & Goswami, P. 2014. Potential biomarkers and their applications for rapid and reliable detection of malaria. *Biomed Res. Int.* 2014:852645.

Jiang, P.-L., Pasaribu, B. & Chen, C.-S. 2014. Nitrogen-deprivation elevates lipid levels in *Symbiodinium* spp. by lipid droplet accumulation: morphological and compositional analyses. *PLoS One*. 9:e87416.

Jimbo, M., Suda, Y., Koike, K., Nakamura-Tsuruta, S., Kominami, J., Kamei, M., Hirabayashi, J. et al. 2013. Possible involvement of glycolipids in lectin-mediated cellular transformation of symbiotic microalgae in corals. *J. Exp. Mar. Bio. Ecol.* 439:129–35.

Jimbo, M., Yamashita, H., Koike, K., Sakai, R. & Kamiya, H. 2010. Effects of lectin in the scleractinian coral *Ctenactis echinata* on symbiotic zooxanthellae. *Fish. Sci.* 76:355–63.

Jimbo, M., Yanohara, T., Koike, Kazuhiko, Koike, Kanae, Sakai, R., Muramoto, K. & Kamiya, H. 2000. The d-galactose-binding lectin of the octocoral *Sinularia lochmodes*: characterization and possible relationship to the symbiotic dinoflagellates.

Jinkerson, R.E., Russo, J.A., Newkirk, C.R., Kirk, A.L., Chi, R.J., Martindale, M.Q., Grossman, A.R. et al. 2022. Cnidarian-Symbiodiniaceae symbiosis establishment is independent of photosynthesis. *Curr. Biol.*

Kang, L.-K., Hwang, S.-P.L., Gong, G.-C., Lin, H.-J., Chen, P.-C. & Chang, J. 2007. Influences of nitrogen deficiency on the transcript levels of ammonium transporter, nitrate transporter and glutamine synthetase genes in *Isochrysis galbana* (Isochrysidales, Haptophyta). *Phycologia*. 46:521–33.

Karako-Lampert, S., Katcoff, D.J., Achituv, Y., Dubinsky, Z. & Stambler, N. 2005. Responses of *Symbiodinium microadriaticum* clade B to different environmental conditions. *J. Exp. Mar. Bio. Ecol.* 318:11–20.

Kaur, S.J., Gilman, V., Duong, M., Asher, D.M. & Gregori, L. 2018. Rapid selection of single-stranded DNA aptamers binding *Staphylococcus epidermidis* in platelet concentrates. *Biotechniques*. 65:331–8.

Kawamura, K., Nishitsuji, K., Shoguchi, E., Fujiwara, S. & Satoh, N. 2021. Establishing sustainable cell lines of a coral, *Acropora tenuis*. *Mar. Biotechnol.* 23:373–88.

Kazandjian, A., Shepherd, V.A., Rodriguez-Lanetty, M., Nordmeier, W., Larkum, A.W.D. & Quinnell, R.G. 2008. Isolation of symbiosomes and the symbiosome membrane complex from the zoanthid *Zoanthus robustus*. *Phycologia*. 47:294–306.

Kim, H.R., Song, M.Y. & Chan Kim, B. 2020. Rapid isolation of bacteria-specific aptamers with a non-SELEX-based method. *Anal. Biochem.* 591:113542.

Kishimoto, M., Baird, A.H., Maruyama, S., Minagawa, J. & Takahashi, S. 2020. Loss of symbiont infectivity following thermal stress can be a factor limiting recovery from bleaching in cnidarians. *ISME J.* 14:3149–52.

Kitchen, S.A., Poole, A.Z. & Weis, V.M. 2017. Sphingolipid metabolism of a sea anemone is altered by the presence of dinoflagellate symbionts. *Biol. Bull.* 233.

Kitchen, S.A. & Weis, V.M. 2017. The sphingosine rheostat is involved in the cnidarian heat stress response but not necessarily in bleaching. *J. Exp. Biol.* 220:1709–20.

Koch, J.C., Verde, E.A. & Weis, V.M. 2020. Carbonic anhydrases are influenced by the size and symbiont identity of the aggregating sea anemone *Anthopleura elegantissima*. *J. Exp. Biol.* 223.

Koike, K., Jimbo, M., Sakai, R., Kaeriyama, M., Muramoto, K., Ogata, T., Maruyama, T. et al. 2004. Octocoral chemical signaling selects and controls dinoflagellate symbionts. *Biol. Bull.* 207:80–6.

Koike, K., Yamashita, H., Oh-Uchi, A., Tamaki, M. & Hayashibara, T. 2007. A quantitative real-time PCR method for monitoring *Symbiodinium* in the water column. *Journal of the Japanese Coral Reef Society*. 9:1–12.

Kolber, Z.S., Prasil, O. & Falkowski, P.G. 1998. Measurements of variable chlorophyll fluorescence using fast repetition rate techniques: defining methodology and experimental protocols. *Biochim. Biophys. Acta*. 1367:88–106.

Krueger, T. 2020. MiCORE Manual. Available At: https://www.researchgate.net/project/The-MiCORE-manual.

Krueger, T. & Gates, R.D. 2012. Cultivating endosymbionts - Host environmental mimics support the survival of *Symbiodinium* C15 *ex hospite*. *Journal of Experimental Marine Biology and Ecology*. 413:169–76.

Kuniya, N., Jimbo, M., Tanimoto, F., Yamashita, H., Koike, K., Harii, S., Nakano, Y. et al. 2015. Possible involvement of Tachylectin-2-like lectin from *Acropora tenuis* in the process of *Symbiodinium* acquisition. *Fish. Sci.* 81:473–83.

Kvennefors, E.C.E., Leggat, W., Hoegh-Guldberg, O., Degnan, B.M. & Barnes, A.C. 2008. An ancient and variable mannose-binding lectin from the coral *Acropora millepora* binds both pathogens and symbionts. *Dev. Comp. Immunol.* 32:1582–92.

LaJeunesse, T.C., Bhagooli, R., Hidaka, M., DeVantier, L., Done, T., Schmidt, G.W., Fitt, W.K. et al. 2004. Closely related *Symbiodinium* spp. differ in relative dominance in coral reef host communities across environmental, latitudinal and biogeographic gradients. *Mar. Ecol. Prog. Ser.* 284:147–61.

LaJeunesse, T.C., Parkinson, J.E., Gabrielson, P.W., Jeong, H.J., Reimer, J.D., Voolstra, C.R. & Santos, S.R. 2018. Systematic revision of Symbiodiniaceae highlights the antiquity and diversity of coral endosymbionts. *Curr. Biol.* 28:2570-2580.e6.

Leggat, W., Yellowlees, D. & Medina, M. 2011. Recent progress in Symbiodinium transcriptomics. *J. Exp. Mar. Bio. Ecol.* 408:120–5.

Lehnert, E.M., Mouchka, M.E., Burriesci, M.S., Gallo, N.D., Schwarz, J.A. & Pringle, J.R. 2014. Extensive differences in gene expression between symbiotic and aposymbiotic cnidarians. 4:277–95.

Lesser, M.P. 1996. Elevated temperatures and ultraviolet radiation cause oxidative stress and inhibit photosynthesis in symbiotic dinoflagellates. *Limnol. Oceanogr.* 41:271–83.

Levin, R.A., Beltran, V.H., Hill, R., Kjelleberg, S., McDougald, D., Steinberg, P.D. & van Oppen, M.J.H. 2016. Sex, scavengers, and chaperones: Transcriptome secrets of divergent *Symbiodinium* thermal tolerances. *Mol. Biol. Evol.* 33:2201–15.

Li, B., Tang, J., Yang, Q., Cui, X., Li, S., Chen, S., Cao, Q. et al. 2016. Performance evaluation and online realization of data-driven normalization methods used in LC/MS based untargeted metabolomics analysis. *Sci. Rep.* 6:38881.

Liew, Y.J., Li, Y., Baumgarten, S., Voolstra, C.R. & Aranda, M. 2017. Condition-specific RNA editing in the coral symbiont Symbiodinium microadriaticum. *PLoS Genet.* 13:e1006619.

Lin, K.-L., Wang, J.-T. & Fang, L.-S. 2000. Participation of glycoproteins on zooxanthellal cell walls in the establishment of a symbiotic relationship with the sea anemone, *Aiptasia pulchella*. *Zoological Studies*. 39:172–8.

Logan, D.D.K., LaFlamme, A.C., Weis, V.M. & Davy, S.K. 2010. Flow-cytometric characterization of the cell-surface glycans of symbiotic dinoflagellates (*Symbiodinium* spp.). *J. Phycol.* 46:525–33.

Mansfield, K.M., Carter, N.M., Nguyen, L., Cleves, P.A., Alshanbayeva, A., Williams, L.M., Crowder, C. et al. 2017. Transcription factor NF-κB is modulated by symbiotic status in a sea anemone model of cnidarian bleaching. *Sci. Rep.* 7:16025.

Mansfield, K.M. & Gilmore, T.D. 2019. Innate immunity and cnidarian-Symbiodiniaceae mutualism. *Dev. Comp. Immunol.* 90:199–209.

Maor-Landaw, K., Karako-Lampert, S., Waldman Ben-Asher, H., Goffredo, S., Falini, G., Dubinsky, Z. & Levy, O. 2014. Gene expression profiles during short-term heat stress in the red sea coral *Stylophora pistillata*. *Glob. Chang. Biol.* 20:3026–35.

Maor-Landaw, K., van Oppen, M.J.H. & McFadden, G.I. 2020. Symbiotic lifestyle triggers drastic changes in the gene expression of the algal endosymbiont *Breviolum minutum* (Symbiodiniaceae). *Ecol. Evol.* 10:451–66.

Marcelino, L.A., Westneat, M.W., Stoyneva, V., Henss, J., Rogers, J.D., Radosevich, A., Turzhitsky, V. et al. 2013. Modulation of light-enhancement to symbiotic algae by light-scattering in corals and evolutionary trends in bleaching. *PLoS One*. 8:e61492.

Markell, D.A. & Wood-Charlson, E.M. 2010. Immunocytochemical evidence that symbiotic algae secrete potential recognition signal molecules in hospite. *Mar. Biol.* 157:1105–11.

Marubini, F. & Davies, P.S. 1996. Nitrate increases zooxanthellae population density and reduces skeletogenesis in corals. *Mar. Biol.* 127:319–28.

Maruyama, S. & Weis, V.M. 2021. Limitations of using cultured algae to study cnidarian-algal symbioses and suggestions for future studies. *J. Phycol.* 57:30–8.

Mathieu-Rivet, E., Scholz, M., Arias, C., Dardelle, F., Schulze, S., Le Mauff, F., Teo, G. et al. 2013. Exploring the N-glycosylation pathway in *Chlamydomonas reinhardtii* unravels novel complex structures. *Mol. Cell. Proteomics*. 12:3160–83.

Matthews, J.L., Crowder, C.M., Oakley, C.A., Lutz, A., Roessner, U., Meyer, E., Grossman, A.R. et al. 2017. Optimal nutrient exchange and immune responses operate in partner specificity in the cnidarian-dinoflagellate symbiosis. *Proc. Natl. Acad. Sci. U. S. A.* 114:13194–9.

Matthews, J.L., Sproles, A.E., Oakley, C.A., Grossman, A.R., Weis, V.M. & Davy, S.K. 2016. Menthol-induced bleaching rapidly and effectively provides experimental aposymbiotic sea anemones (*Aiptasia* sp.) for symbiosis investigations. *J. Exp. Biol.* 219:306–10.

Medrano, E., Merselis, D.G., Bellantuono, A.J. & Rodriguez-Lanetty, M. 2019. Proteomic basis of symbiosis: A heterologous partner fails to duplicate homologous colonization in a novel cnidarian – Symbiodiniaceae mutualism. *Front. Microbiol.* 10:1153.

Merselis, D.G., Lirman, D. & Rodriguez-Lanetty, M. 2018. Symbiotic immuno-suppression: is disease susceptibility the price of bleaching resistance? *PeerJ*. 6:e4494.

Meyer, E. & Weis, V.M. 2012. Study of cnidarian-algal symbiosis in the "omics" age. *Biol. Bull.* 223:44–65.

Mies, M., Voolstra, C.R., Castro, C.B., Pires, D.O., Calderon, E.N. & Sumida, P.Y.G. 2017. Expression of a symbiosis-specific gene in *Symbiodinium* type A1 associated with coral, nudibranch and giant clam larvae. *Royal Society Open Science*. 4:179253.

Miller, R., Wu, G., Deshpande, R.R., Vieler, A., Gärtner, K., Li, X., Moellering, E.R. et al. 2010. Changes in transcript abundance in *Chlamydomonas reinhardtii* following nitrogen deprivation predict diversion of metabolism. *Plant Physiology*. 154:1737–52.

Morelle, W., Faid, V., Chirat, F. & Michalski, J.-C. 2009. Analysis of N- and O-Linked Glycans from Glycoproteins Using MALDI-TOF Mass Spectrometry. *In* Packer, N. H. & Karlsson, N. G. [Eds.] *Glycomics: Methods and Protocols*. Humana Press, Totowa, NJ, pp. 3–21.

Morera, C. & Villanueva, M.A. 2009. Heat treatment and viability assessment by Evans blue in cultured *Symbiodinium kawagutii* cells. *World J. Microbiol. Biotechnol.* 25:1125–8.

Muller-Parker, G., Lee, K.W. & Cook, C.B. 1996. Changes in the ultrastructure of symbiotic zooxanthellae (*Symbiodinium* sp. Dinophyceae) in fed and starved sea anemones maintained under high and low light. *Journal of Phycology*. 32:987–94.

Muller-Parker, G., McCloskey, L.R., Hoegh-Guldberg, O. & McAuley, P.J. 1994. Effect of ammonium enrichment on animal and algal biomass of the coral *Pocillopora damicornis*. *Pac. Sci.*

Muscatine, L., Falkowski, P.G., Dubinskey, Z., Cook, P.A. & McCloskey, L.R. 1989. The effect of external nutrient resources on the population dynamics of zooxanthellae in a reef coral. *Proceedings of the Royal Society London B.* 236:311–24.

Neff, E.P. 2020. The quest for an animal model of coral health and disease. *Lab Anim.* . 49:37–41.

Neubaeur, E.-F., Poole, A.Z., Neubauer, P., Detournay, O., Tan, K., Davy, S.K. & Weis, V.M. 2017. A diverse host thrombospondin-type-1 repeat protein repertoire promotes symbiont colonization during establishment of cnidarian-dinoflagellate symbiosis. *Elife*. 6:e24494.

Neubauer, E.F., Poole, A.Z., Weis, V.M. & Davy, S.K. 2016. The scavenger receptor repertoire in six cnidarian species and its putative role in cnidarian-dinoflagellate symbiosis. *PeerJ*. 4:e2692.

Neves, M.A.D., Reinstein, O., Saad, M. & Johnson, P.E. 2010. Defining the secondary structural requirements of a cocaine-binding aptamer by a thermodynamic and mutation study. *Biophys. Chem.* 153:9–16.

Nitschke, M.R., Craveiro, S.C., Brandão, C., Fidalgo, C., Serôdio, J., Calado, A.J. & Frommlet, J.C. 2020. Description of *Freudenthalidium* gen. nov. and*Halluxium* gen. nov. to formally recognize clades Fr3 and H as genera in the family Symbiodiniaceae (Dinophyceae). *J. Phycol.* 56:923–40.

Nitschke, M.R., Davy, S.K., Cribb, T.H. & Ward, S. 2015. The effect of elevated temperature and substrate on free-living *Symbiodinium* cultures. *Coral Reefs*. 34:161–71.

Nitschke, M.R., Davy, S.K. & Ward, S. 2016. Horizontal transmission of *Symbiodinium* cells between adult and juvenile corals is aided by benthic sediment. *Coral Reefs*. 35:335–44.

Nowotny, J.D., Connelly, M.T. & Traylor-Knowles, N. 2021. Novel methods to establish whole-body primary cell cultures for the cnidarians *Nematostella vectensis* and *Pocillopora damicornis*. *Sci. Rep.* 11:4086.

Oakley, C.A., Ameismeier, M.F., Peng, L., Weis, V.M., Grossman, A.R. & Davy, S.K. 2016. Symbiosis induces widespread changes in the proteome of the model cnidarian Aiptasia. *Cell. Microbiol.* 18:1009–23.

Oakley, C.A. & Davy, S.K. 2018. Cell Biology of Coral Bleaching. *In* van Oppen, M. J. H. & Lough, J. M. [Eds.] *Coral Bleaching: Patterns, Processes, Causes and Consequences*. Springer International Publishing, Cham, pp. 189–211.

Oakley, C.A., Durand, E., Wilkinson, S.P., Peng, L., Weis, V.M., Grossman, A.R. & Davy, S.K. 2017. Thermal shock induces host proteostasis disruption and endoplasmic reticulum stress in the model symbiotic cnidarian Aiptasia. *J. Proteome Res.* 16:2121–34.

Oakley, C.A., Pontasch, S., Fisher, P.L., Wilkinson, S.P., Keyzers, R.A., Krueger, T., Dove, S. et al. 2022. Thylakoid fatty acid composition and response to short-term cold and heat stress in high-latitude Symbiodiniaceae. *Coral Reefs*.

Oltmanns, A., Hoepfner, L., Scholz, M., Zinzius, K., Schulze, S. & Hippler, M. 2019. Novel insights into N-glycan fucosylation and core xylosylation in *C. reinhardtii*. *Front. Plant Sci.* 10:1686.

Ouellet, E., Foley, J.H., Conway, E.M. & Haynes, C. 2015. Hi-Fi SELEX: A high-fidelity digital-PCR based therapeutic aptamer discovery platform. *Biotechnol. Bioeng.* 112:1506–22.

Ouellet, E., Lagally, E.T., Cheung, K.C. & Haynes, C.A. 2014. A simple method for eliminating fixed-region interference of aptamer binding during SELEX. *Biotechnol. Bioeng.* 111:2265–79.

Palincsar, J.S., Jones, W.R. & Palincsar, E.E. 1988. Effects of isolation of the endosymbiont *Symbiodinium microadriaticum* (Dinophyceae) from Its host *Aiptasia pallida* (Anthozoa) on cell wall ultrastructure and mitotic rate. *Trans. Am. Microsc. Soc.* 107:53–66.

Parker, G.M. 1984. Dispersal of zooxanthellae on coral reefs by predators on cnidarians. *Biol. Bull.* 167:159–67.

Parkinson, J.E., Coffroth, M.A. & LaJeunesse, T.C. 2015. New species of Clade B *Symbiodinium* (Dinophyceae) from the greater Caribbean belong to different functional guilds: *S. aenigmaticum* sp. nov., *S. antillogorgium* sp. nov., *S. endomadracis* sp. nov., and *S. pseudominutum* sp. nov. *J. Phycol.* 51:850–8.

Parkinson, J.E., Tivey, T.R., Mandelare, P.E., Adpressa, D.A., Loesgen, S. & Weis, V.M. 2018. Subtle differences in symbiont cell surface glycan profiles do not explain species-specific colonization rates in a model cnidarian-algal symbiosis. 9:1–12.

Pasaribu, B., Li, Y.-S., Kuo, P.-C., Lin, I.-P., Tew, K.S., Tzen, J.T.C., Liao, Y.K. et al. 2016. The effect of temperature and nitrogen deprivation on cell morphology and physiology of Symbiodinium. *Oceanologia*. 58:272–8.

Pasaribu, B., Weng, L.-C., Lin, I.-P., Camargo, E., Tzen, J.T.C., Tsai, H., Ho, S.-L. et al. 2015. Morphological variability and distinct protein profiles of cultured and endosymbiotic *Symbiodinium* cells isolated from *Exaiptasia pulchella*. *Sci. Rep.* 5:15353.

Pasternak, Z., Bachar, A., Abelson, A. & Achituv, Y. 2004. Initiation of symbiosis between the soft coral *Heteroxenia fuscescens* and its zooxanthellae. *Mar. Ecol. Prog. Ser.* 279:113–6.

Peng, S.E., Wang, Y.B., Wang, L.H., Chen, W.N.U., Lu, C.Y., Fang, L.S. & Chen, C.S. 2010. Proteomic analysis of symbiosome membranes in cnidaria-dinoflagellate endosymbiosis. *Proteomics*. 10:1002–16.

Peng, W., Goli, M., Mirzaei, P. & Mechref, Y. 2019. Revealing the biological attributes of N-glycan isomers in breast cancer brain metastasis using porous graphitic carbon (PGC) liquid chromatography-tandem mass spectrometry (LC-MS/MS). *J. Proteome Res.* 18:3731–40.

Perez, S.F., Cook, C.B. & Brooks, W.R. 2001. The role of symbiotic dinoflagellates in the temperature-induced bleaching response of the subtropical sea anemone *Aiptasia pallida*. *Journal of Experimental Marine Biology and Ecology*. 256:1–14.

Petit, D., Teppa, E., Cenci, U., Ball, S. & Harduin-Lepers, A. 2018. Reconstruction of the sialylation pathway in the ancestor of eukaryotes. *Sci. Rep.* 8:2946.

Pietrobono, S. & Stecca, B. 2021. Aberrant sialylation in cancer: Biomarker and potential target for therapeutic intervention? *Cancers*. 13.

Pleiko, K., Saulite, L., Parfejevs, V., Miculis, K., Vjaters, E. & Riekstina, U. 2019. Differential binding cell-SELEX method to identify cell-specific aptamers using high-throughput sequencing. *Sci. Rep.* 9:8142.

Pochon, X. & Gates, R.D. 2010. A new *Symbiodinium* clade (Dinophyceae) from soritid foraminifera in Hawai'i. *Mol. Phylogenet. Evol.* 56:492–7.

Pochon, X. & LaJeunesse, T.C. 2021. Miliolidium n. gen, a new Symbiodiniacean genus whose members associate with soritid foraminifera or are free-living. *J. Eukaryot. Microbiol.* e12856.

Poole, A.Z., Kitchen, S.A. & Weis, V.M. 2016. The role of complement in cnidarian-dinoflagellate symbiosis and immune challenge in the sea anemone *Aiptasia pallida*. *Front. Microbiol.* 7.

Ralph, P.J., Gademann, R. & Larkum, A.W.D. 2001. Zooxanthellae expelled from bleached corals at 33°C are photosynthetically competent. *Mar. Ecol. Prog. Ser.* 220:163–8.

Ricci, C.A., Kamal, A.H., Chakrabarty, J.K., Ledbetter, B.E., Chowdhury, S.M. & Mydlarz, L.D. 2020. The cell-surface protein composition of a coral symbiont, *Breviolum psygmophilum*, reveals a mechanism for host specificity and displays dynamic regulation during temperature stress. *Mar. Biol.* 167:66.

Roberts, C.M., McClean, C.J., Veron, J.E.N., Hawkins, J.P., Allen, G.R., McAllister, D.E., Mittermeier, C.G. et al. 2002. Marine biodiversity hotspots and conservation priorities for tropical reefs. *Science*. 295:1280–4.

Rodriguez-Lanetty, M., Harii, S. & Hoegh-Guldberg, O. 2009. Early molecular responses of coral larvae to hyperthermal stress. *Mol. Ecol.* 18:5101–14.

Rosic, N.N., Pernice, M., Rodriguez-Lanetty, M. & Hoegh-Guldberg, O. 2011. Validation of housekeeping genes for gene expression studies in *Symbiodinium* exposed to thermal and light stress. *Mar. Biotechnol.* 13:355–65.

Rosset, S., D'Angelo, C. & Wiedenmann, J. 2015. Ultrastructural biomarkers in symbiotic algae reflect the availability of dissolved inorganic nutrients and particulate food to the reef coral holobiont. *Frontiers in Marine Science*. 2:103.

Rosset, S., Wiedenmann, J., Reed, A.J. & D'Angelo, C. 2017. Phosphate deficiency promotes coral bleaching and is reflected by the ultrastructure of symbiotic dinoflagellates. *Mar. Pollut. Bull.* 118:180–7.

Rosset, S.L., Oakley, C.A., Ferrier-Pagès, C., Suggett, D.J., Weis, V.M. & Davy, S.K. 2021. The Molecular Language of the Cnidarian-Dinoflagellate Symbiosis. *Trends Microbiol.* 29:320–33.

Rowan, R., Whitney, S.M., Fowler, A. & Yellowlees, D. 1996. Rubisco in marine symbiotic dinoflagellates: form II enzymes in eukaryotic oxygenic phototrophs encoded by a nuclear multigene family. *Plant Cell*. 8:539–53.

Roy, S., Jagus, R. & Morse, D. 2018. Translation and translational control in dinoflagellates. *Microorganisms*. 6.

Santamaria, G., Esposito, C.L., Cerchia, L., Benvenuto, G., Nanjappa, D., Sarno, D., Zingone, A. et al. 2015. Aptamers are an innovative and promising tool for phytoplankton taxonomy and biodiversity research. *Chemistry and Ecology*. 31:92–103.

Santos, S.R., Taylor, D.J. & Coffroth, M.A. 2001. Genetic comparisons of freshly isolated versus cultured symbiotic dinoflagellates: Implications for extrapolating to the intact symbiosis. *J. Phycol.* 37:900–12.

Schwarz, J.A., Weis, V.M. & Potts, D.C. 2002. Feeding behavior and acquisition of zooxanthellae by planula larvae of the sea anemone *Anthopleura elegantissima*. *Mar. biol*. 140:471–8.

Sefah, K., Shangguan, D., Xiong, X., O'Donoghue, M.B. & Tan, W. 2010. Development of DNA aptamers using cell-SELEX. *Nat. Protoc.* 5:1169–85.

Seibt, C. & Schlichter, D. 2001. Compatible intracellular ion composition of the host improves carbon assimilation by zooxanthellae in mutualistic symbioses. *Naturwissenschaften*. 88:382–6.

Seneca, F.O., Forêt, S., Ball, E.E., Smith-Keune, C., Miller, D.J. & van Oppen, M.J.H. 2010. Patterns of gene expression in a scleractinian coral undergoing natural bleaching. *Mar. Biotechnol.* . 12:594–604.

Séveno, M., Bardor, M., Paccalet, T., Gomord, V., Lerouge, P. & Faye, L. 2004. Glycoprotein sialylation in plants?

Shao, K., Ding, W., Wang, F., Li, H., Ma, D. & Wang, H. 2011. Emulsion PCR: a high efficient way of PCR amplification of random DNA libraries in aptamer selection. *PLoS One*. 6:e24910.

Shoguchi, E., Shinzato, C., Kawashima, T., Gyoja, F., Mungpakdee, S., Koyanagi, R., Takeuchi, T. et al. 2013. Draft assembly of the *Symbiodinium minutum* nuclear genome reveals dinoflagellate gene structure. *Curr. Biol.* 23:1399–408.

Smith, G.J. & Muscatine, L. 1999a. Cell cycle of symbiotic dinoagellates : variation in G_1 phase-duration with anemone nutritional status and macronutrient supply in the *Aiptasia pulchella-Symbiodinium pulchrorum* symbiosis. *Marine Biology*. 134:405–18.

Smith, G.J. & Muscatine, L. 1999b. Cell cycle of symbiotic dinoflagellates: variation in G1 phase-duration with anemone nutritional status and macronutrient supply in the *Aiptasia pulchella–Symbiodinium pulchrorum* symbiosis. *Mar. Biol.* 134:405–18.

Sproles, A.E., Oakley, C.A., Krueger, T., Grossman, A.R., Weis, V.M., Meibom, A. & Davy, S.K. 2020. Sub-cellular imaging shows reduced photosynthetic carbon and increased nitrogen assimilation by the non-native endosymbiont *Durusdinium trenchii* in the model cnidarian Aiptasia. *Environ. Microbiol.* 22:3741–53.

Stambler, N., Popper, N., Dubinsky, Z.V.Y. & Stimson, J. 1991. Effects of nutrient enrichment and water motion on the coral *Pocillopora damicornis*. *Pacific Science*. 45:299–307.

Steele, R.D. 1975. Stages in the life history of a symbiotic zooxanthella in pellets extruded by its host *Aiptasia tagetes* (Duch and Mich.) (Coelenterata, Anthozoa). *Biol. Bull.* 149:590–600.

Stimson, J. & Kinzie, R.A. 1991. The temporal pattern and rate of release of zooxanthellae from the reef coral *Pocillopora damicornis* (Linnaeus) under nitrogen-enrichment and control conditions. *J. Exp. Mar. Bio. Ecol.* 153:63–74.

Stochaj, W.R. & Grossman, A.R. 1997. Differences in the protein profiles of cultured and endosymbiotic *Symbiodinium* sp. (Pyrrophyta) from the anemone *Aiptasia pallida* (Anthozoa). *J. Phycol.* 33:44–53.

Strasser, R. 2016. Plant protein glycosylation. *Glycobiology*. 26:926–39.

Suggett, D.J., Warner, M.E., Smith, D.J., Davey, P., Hennige, S. & Baker, N.R. 2008. Photosynthesis and production of hydrogen peroxide by *Symbiodinium* (Pyrrhophyta) phylotypes with different thermal tolerances. *J. Phycol.* 44:948–56.

Sunagawa, S., Wilson, E.C., Thaler, M., Smith, M.L., Caruso, C., Pringle, J.R., Weis, V.M. et al. 2009. Generation and analysis of transcriptomic resources for a model system on the rise: The sea anemone *Aiptasia pallida* and its dinoflagellate endosymbiont. *BMC Genomics*. 10:1–10.

Takahashi, M., Wu, X., Ho, M., Chomchan, P., Rossi, J.J., Burnett, J.C. & Zhou, J. 2016. High throughput sequencing analysis of RNA libraries reveals the influences of initial library and PCR methods on SELEX efficiency. *Sci. Rep.* 6:33697.

Takeuchi, R., Jimbo, M., Tanimoto, F., Tanaka, C., Harii, S., Nakano, Y., Yasumoto, K. et al. 2017. Establishment of a model for chemoattraction of *Symbiodinium* and characterization of chemotactic compounds in *Acropora tenuis*. *Fish. Sci.* 83:479–87.

Tansik, A.L., Fitt, W.K. & Hopkinson, B.M. 2017. Inorganic carbon is scarce for symbionts in scleractinian corals. *Limnol. Oceanogr.*

Tchernov, D., Gorbunov, M.Y., de Vargas, C., Narayan Yadav, S., Milligan, A.J., Häggblom, M. & Falkowski, P.G. 2004. Membrane lipids of symbiotic algae are

diagnostic of sensitivity to thermal bleaching in corals. *Proc. Natl. Acad. Sci. U. S. A.* 101:13531–5.

Thornhill, D.J., Howells, E.J., Wham, D.C., Steury, T.D. & Santos, S.R. 2017. Population genetics of reef coral endosymbionts (*Symbiodinium*, Dinophyceae). *Mol. Ecol.* 26:2640–59.

Thornhill, D.J., Xiang, Y., Pettay, D.T., Zhong, M. & Santos, S.R. 2013. Population genetic data of a model symbiotic cnidarian system reveal remarkable symbiotic specificity and vectored introductions across ocean basins. *Mol. Ecol.* 22:4499–515.

Tivey, T.R., Parkinson, J.E., Mandelare, P.E., Adpressa, D.A., Peng, W., Dong, X., Mechref, Y. et al. 2020a. N-linked surface glycan biosynthesis, composition, inhibition, and function in cnidarian-dinoflagellate symbiosis. *Microb. Ecol.* 80:223–36.

Tivey, T.R., Parkinson, J.E. & Weis, V.M. 2020b. Host and symbiont cell cycle coordination is mediated by symbiotic state, nutrition, and partner identity in a model cnidarian-dinoflagellate symbiosis. *MBio*. 11:e02626-19.

Tolle, F., Wilke, J., Wengel, J. & Mayer, G. 2014. By-product formation in repetitive PCR amplification of DNA libraries during SELEX. *PLoS One*. 9:e114693.

Tonelli, R.R., Colli, W. & Alves, M.J.M. 2012. Selection of binding targets in parasites using phage-display and aptamer libraries in vivo and in vitro. *Front. Immunol.* 3:1–16.

Tortorelli, G., Rautengarten, C., Bacic, A., Segal, G., Ebert, B., Davy, S.K., van Oppen, M.J.H. et al. 2021. Cell surface carbohydrates of symbiotic dinoflagellates and their role in the establishment of cnidarian-dinoflagellate symbiosis. *ISME J.* 16:190–9.

Umeki, M., Yamashita, H., Suzuki, G., Sato, T., Ohara, S. & Koike, K. 2020. Fecal pellets of giant clams as a route for transporting Symbiodiniaceae to corals. *PLoS One*. 15:e0243087.

van Oppen, M.J.H. & Lough, J.M. (Eds.) 2018. Coral Bleaching: Patterns, Processes, Causes and Consequences. Springer, Cham.

van Ree, R., Cabanes-Macheteau, M., Akkerdaas, J., Milazzo, J.P., Loutelier-Bourhis, C., Rayon, C., Villalba, M. et al. 2000. Beta(1,2)-xylose and alpha(1,3)-fucose residues have a strong contribution in IgE binding to plant glycoallergens. *J. Biol. Chem.* 275:11451–8.

Varki, A. 2017. Biological roles of glycans. *Glycobiology*. 27:3–49.

Varki, A., Cummings, R.D., Esko, J.D., Stanley, P., Hart, G.W., Aebi, M., Darvill, A.G. et al. (Eds.) 2016. Essentials of Glycobiology. Cold Spring Harbor Laboratory Press, Cold Spring Harbor (NY).

Vidal-Dupiol, J., Adjeroud, M., Roger, E., Foure, L., Duval, D., Mone, Y., Ferrier-Pages, C. et al. 2009. Coral bleaching under thermal stress: putative involvement of host/symbiont recognition mechanisms. *BMC Physiol.* 9:14.

Wakefield, T.S., Farmer, M.A. & Kempf, S.C. 2000. Revised description of the fine structure of *in situ* zooxanthellae genus *Symbiodinium*. *Biological Bulletin*. 199:76–84.

Wang, L.-H., Chen, H.-K., Jhu, C.-S., Cheng, J.-O., Fang, L.-S. & Chen, C.-S. 2015. Different strategies of energy storage in cultured and freshly isolated *Symbiodinium* sp. *J. Phycol.* 51:1127–36.

Wang, T., Cai, Z.P., Gu, X.Q., Ma, H.Y., Du, Y.M., Huang, K., Voglmeir, J. et al. 2014. Discovery and characterization of a novel extremely acidic bacterial N-glycanase with combined advantages of PNGase F and A. *Biosci. Rep.* 34:e00149.

Weis, V.M. 2019. Cell biology of coral symbiosis: Foundational study can inform solutions to the coral reef crisis. *Integr. Comp. Biol.* 59:845–55.

Weis, V.M., Davy, S.K., Hoegh-guldberg, O., Rodriguez-lanetty, M. & Pringle, J.R. 2008. Cell biology in model systems as the key to understanding corals. *Trends Ecol. Evol.* 23:369–76.

Weng, L.-C., Pasaribu, B., -Ping Lin, I., Tsai, C.-H., Chen, C.-S. & Jiang, P.-L. 2014. Nitrogen deprivation induces lipid droplet accumulation and alters fatty acid metabolism in symbiotic dinoflagellates isolated from *Aiptasia pulchella*. *Sci. Rep.* 4:1–8.

Williams, L.M., Fuess, L.E., Brennan, J.J., Mansfield, K.M., Salas-Rodriguez, E., Welsh, J., Awtry, J. et al. 2018. A conserved Toll-like receptor-to-NF-κB signaling pathway in the endangered coral *Orbicella faveolata*. *Dev. Comp. Immunol.* 79:128–36.

Wood-Charlson, E.M., Hollingsworth, L.L., Krupp, D.A. & Weis, V.M. 2006. Lectin/glycan interactions play a role in recognition in a coral/dinoflagellate symbiosis. *Cell. Microbiol.* 8:1985–93.

Xiang, T., Lehnert, E., Jinkerson, R.E., Clowez, S., Kim, R.G., DeNofrio, J.C., Pringle, J.R. et al. 2020. Symbiont population control by host-symbiont metabolic interaction in Symbiodiniaceae-cnidarian associations. *Nat. Commun.* 11:108.

Xiang, T., Nelson, W., Rodriguez, J., Tolleter, D. & Grossman, A.R. 2015. *Symbiodinium* transcriptome and global responses of cells to immediate changes in light intensity when grown under autotrophic or mixotrophic conditions. *Plant J.* 82:67–80.

Yacobovitch, T., Benayahu, Y. & Weis, V.M. 2004. Motility of zooxanthellae isolated from the Red Sea soft coral *Heteroxenia fuscescens* (Cnidaria). *J. Exp. Mar. Bio. Ecol.* 298:35–48.

Yamashita, H. & Koike, K. 2016. Motility and cell division patterns among several strains of *Symbiodinium*. *Galaxea, Journal of Coral Reef Studies*. 18:13–9.

Yarden, Y. & Sliwkowski, M.X. 2001. Untangling the ErbB signalling network. *Nat. Rev. Mol. Cell Biol.* 2:127–37.

Zeleny, R., Kolarich, D., Strasser, R. & Altmann, F. 2006. Sialic acid concentrations in plants are in the range of inadvertent contamination. *Planta*. 224:222–7.

Zhou, Z., Yu, X., Tang, J., Zhu, Y., Chen, G., Guo, L. & Huang, B. 2017. Dual recognition activity of a rhamnose-binding lectin to pathogenic bacteria and zooxanthellae in stony coral *Pocillopora damicornis*. *Dev. Comp. Immunol.* 70:88–93.

Zhou, Z., Zhao, S., Ni, J., Su, Y., Wang, L. & Xu, Y. 2018. Effects of environmental factors on C-type lectin recognition to zooxanthellae in the stony coral *Pocillopora damicornis*. *Fish Shellfish Immunol.* 79:228–33.

Zuker, M. 2003. Mfold web server for nucleic acid folding and hybridization prediction. *Nucleic Acids Res.* 31:3406–15.

8. Appendices

8.1 Appendix A – Supplementary Material for Chapter 2

Supplementary Methods A1

Inoculation experiments were conducted with *Cladocopium goreaui* (culture ID: LHI-33) and *Durusdinium trenchii* (culture id: D1a Ap2) in *Acropora tenuis* larvae. Algal cultures of each species were kept in sealed 30 mL glass vials in 6 mL of F/2 algal media at a density of 1 x 10^6 cells/mL. Vials containing algae were then placed in a heated water bath, either at 25 °C or 32 °C for 3 days. LED full-spectrum lights were set to 12h:12h light:dark cycle at 30 μmol photons/m^2/s over the water bath.

After heat treatment, cultures were spun down at 1 000 x g for 5 minutes and washed with filtered seawater. Half of the culture was used in inoculation experiments while the other was immediately fixed in 4% paraformaldehyde for later lectin-staining experiments.

Fifteen *Acropora tenuis* larvae 10 days post-fertilization were inoculated with 250 000 cells/mL of respective algal cultures in a 1 mL volume of filtered seawater in wells of a 24 well plate (n=3). Larvae were immediately fed 5 μL of BSE. After 12 hours of inoculation, larvae were rinsed in filtered seawater and fixed in 4% paraformaldehyde. All larvae from each inoculation sample was imaged manually under a fluorescent microscope and the number of algae recorded as alga/larvae.

Paraformaldehyde fixed cultures of *C. goreaui* and *D. trenchii* were washed with 3.3X PBS and 250 000 cells stained with 5 μg/mL of phycoerythrin conjugated CVN lectin in 200 μL total volume for 2 hours in the dark with three staining replicates. After staining, algae were washed twice with 3.3X PBS and then resuspended in 1 mL of 3.3X PBS. Samples were then run on a CytoFLEX flow cytometer and data analyzed using FlowJo software. Algal cell populations were identified with forward and side scatter, and positive chlorophyll autofluorescence signals were confirmed by 488 nm excitation and detection in the PerCP channel (690/50 band pass). Median fluorescence intensities (MFI) of the PE signal were obtained from the total algal cell population by excitation at 561 nm and capture in channel PE (585/42 band pass). Unstained cells were used as blank controls, and the MFI of stained cells were subtracted by the MFI of unstained cells.

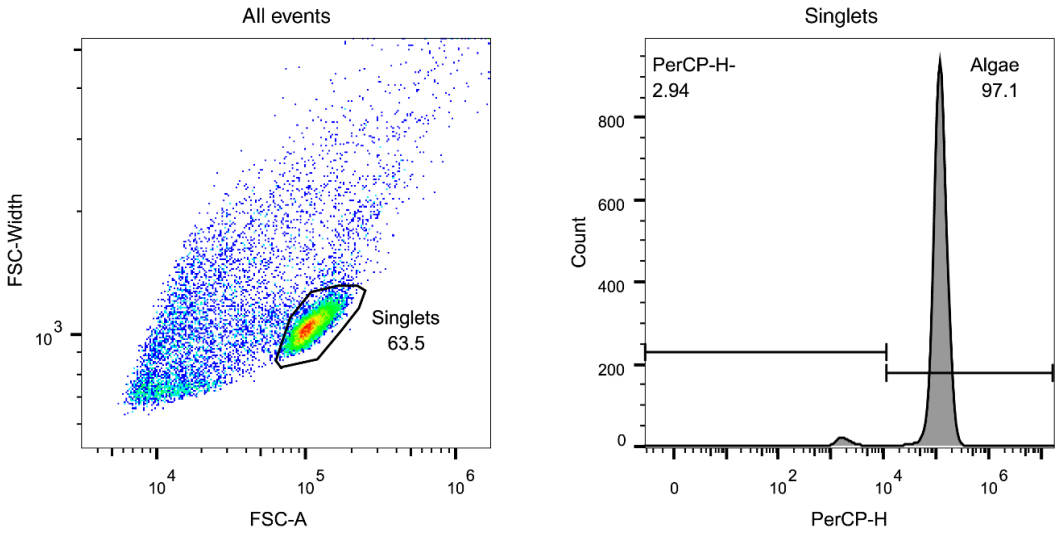

Supplementary Figure A1 – **Representative cytogram of unstained ambient temperature algal cells.**
First, singlets were determined by FSC-Width vs FSC-A plots. Then live algal cells were determined using the PerCP channel to detect chlorophyll autofluorescence. Gating strategies were determined using unstained cells and applied to all corresponding lectin-stained samples.

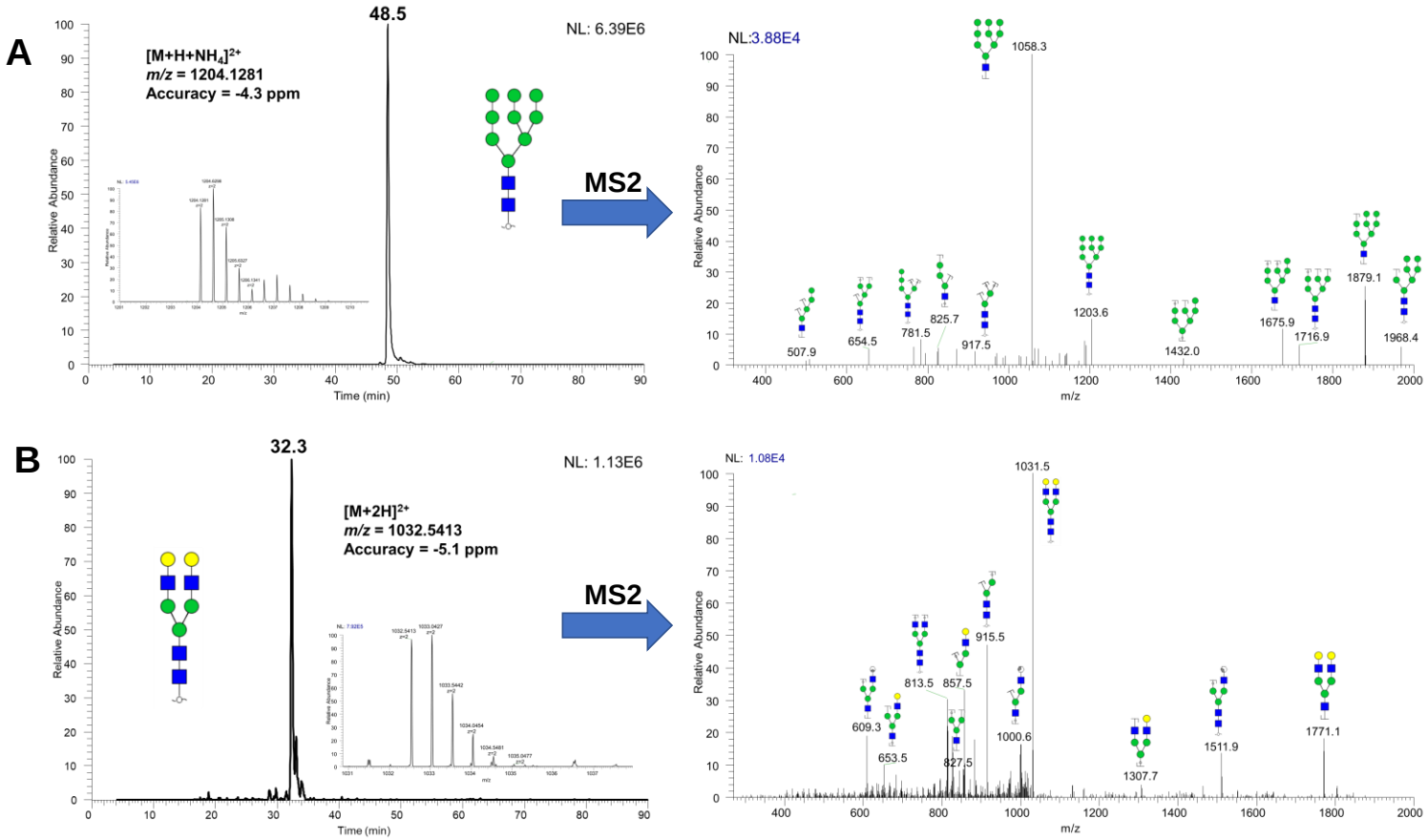

Supplementary Figure A2 – Illustration of N-glycan structure annotation for (A) high-mannose and (B) complex glycans, respectively.

The insets are corresponding full MS spectra which represent the monoisotopic m/z values and isotopic distributions of the glycans under the LC peak. The fragments in the MS2 spectra can match the putative N-glycan structures, confirming the structural annotation. Symbols: blue square represents N-acetylglucosamine (GlcNAc); green circle represents mannose (Man); yellow circle represents galactose (Gal).

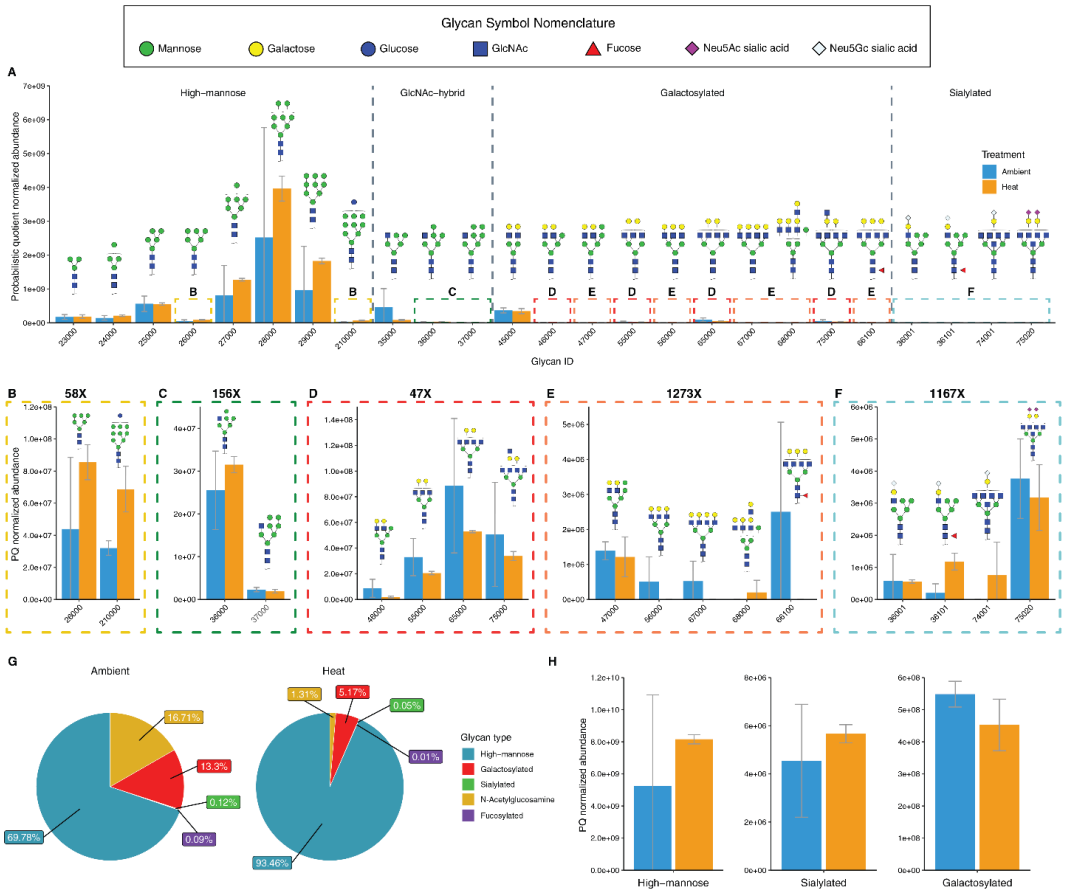

Supplementary Figure A3 – Abundance of glycans from *Breviolum minutum* crude extract.
(A) Probabilistic quotient normalized abundance of individual glycans separated into different categories based on their terminal residues. Boxed sections **(B)-(D)** are zoomed in graphs of corresponding boxes in **(A)**. **(G)** The relative abundance of glycans separated by type. “Fucosylated” category was separated from “Sialylated” and “Galactosylated” glycan groups. **(H)** Probabilistic quotient normalized abundance of glycans separated by type.

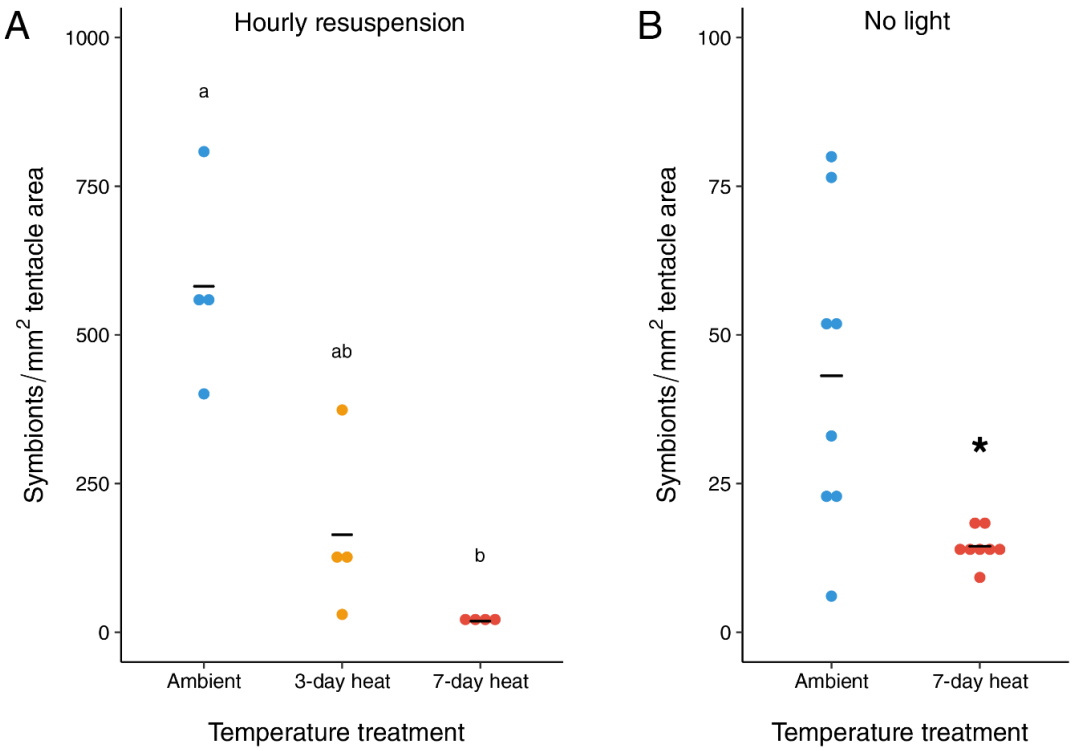

Supplementary Figure A4 – Colonization with hourly resuspension or done in the darkness still caused a heat-stress associated decline in colonization.
(A) Algae were resuspended every hour during the light period of inoculation to control for the effect of heat stress on algal motility. **(B)** Inoculations were conducted in the dark to minimize the effect of light-induced oxidative stress that would result from heat stressing the algae, but heat still reduced colonization. 3 day heat stressed algae were not included in this experiment. Letters indicate statistically significant differences ($p \leq 0.05$) as determined by Kruskal-Wallis and post-hoc Dunn Tests. Stars indicate significant differences ($p \leq 0.05$) as determined by Welch's t-test.

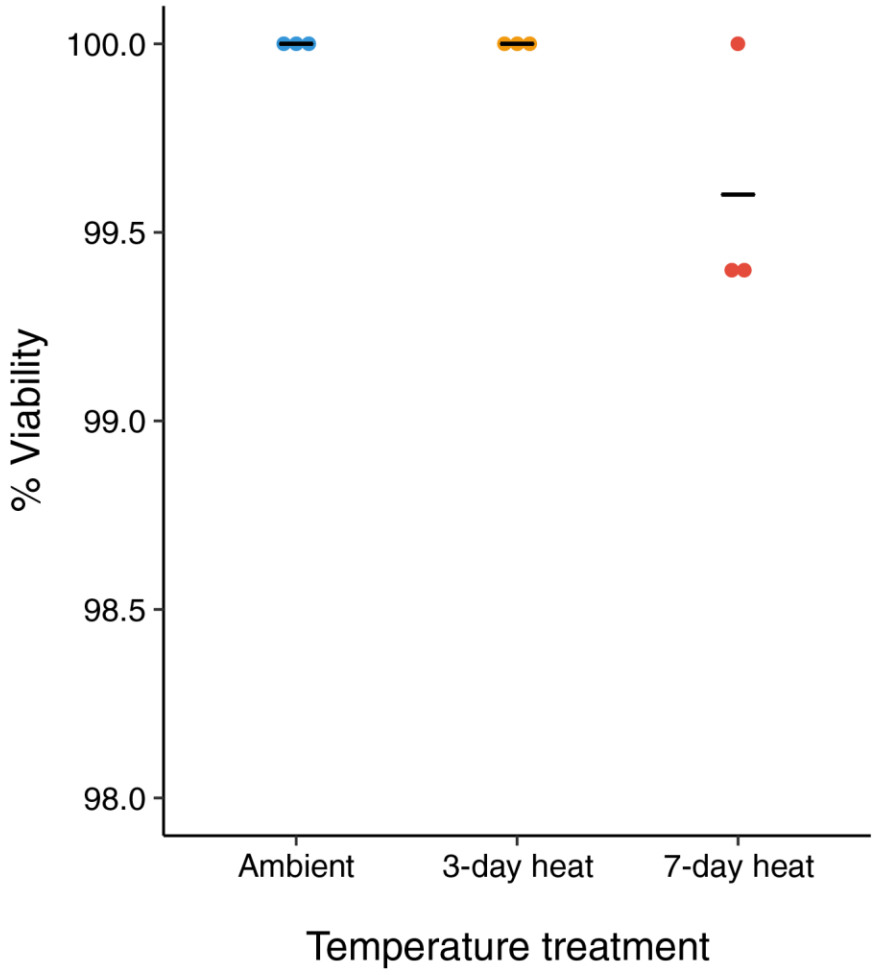

Supplementary Figure A5 – Algae were stained with Evans Blue dye after heat stress to test cell viability.
Heat stress caused a very small decline in cell viability that was not statistically significant.

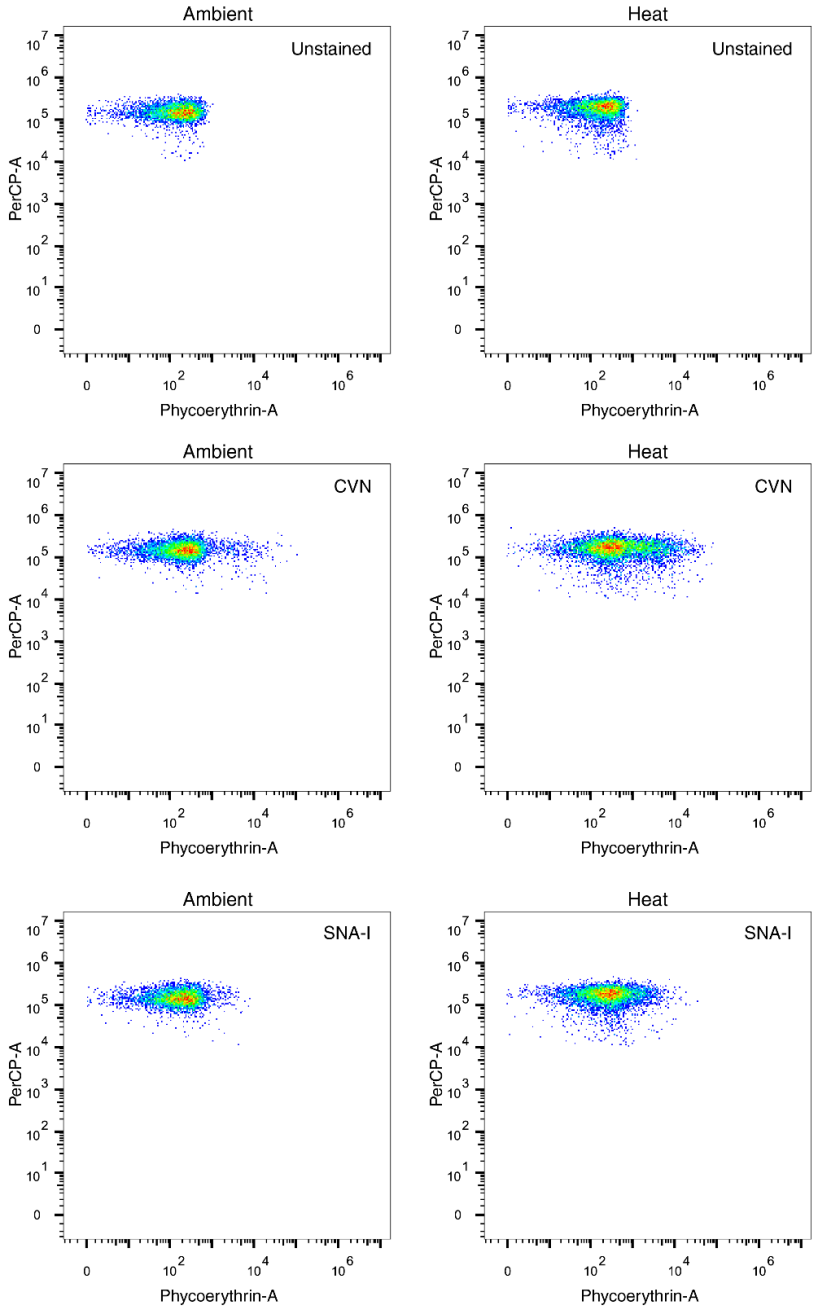

Supplementary Figure A6 – Representative flow cytograms from one replicate each. The PerCP channel detected chlorophyll fluorescence and was used to gate live cells. The phycoerythrin channel detected the PE-labeled lectins, CVN and SNA-I. Unstained cells were used as blank controls and MFI values obtained from lectin labeled cells were corrected with MFI from the unstained cells.

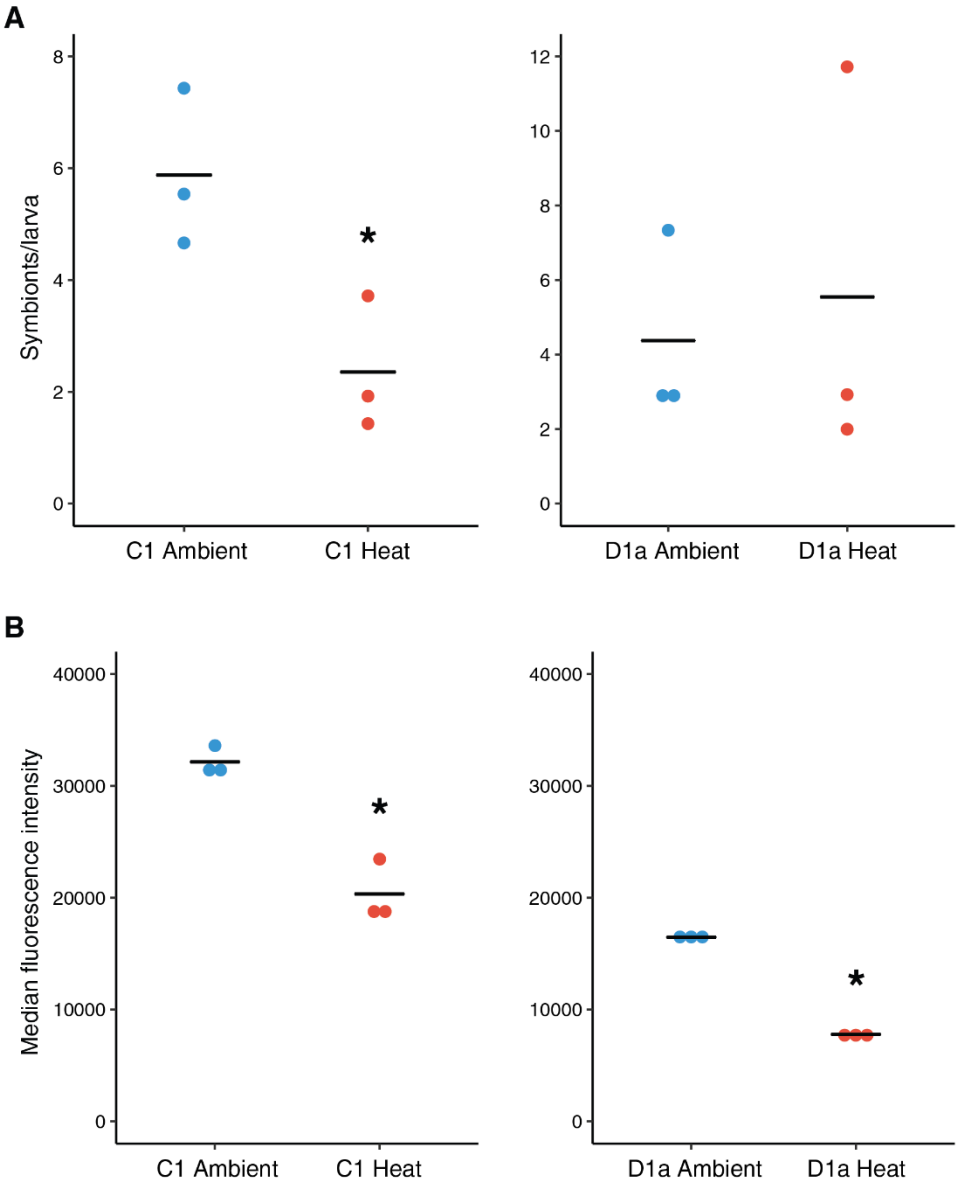

Supplementary Figure A7 – The effect of heat-stress on coral symbionts.
(A) *Acropora tenuis* larvae were inoculated with ambient and heat stressed cultures of *Cladocoopium goreaui* (C1) or *Durusdinium trenchii* (D1a). Heat stress caused a decline in colonization in *C. goreaui* but not in *D. trenchii*. **(B)** Paraformaldehyde fixed cells were stained with PE conjugated CVN lectin and fluorescence detected with flow cytometry. Heat caused a decline in CVN labeling in both *C. goreaui* and *D. trenchii*. Stars indicate statistical differences ($p \leq 0.05$) as determined by Student's t-tests.

8.2 Appendix B – Supplementary Material for Chapter 4

transcript ID	Gene Annotation	Forward primer	Reverse Primer	Primer Efficiency
s6_38207	AMT1-related	AGATGAAGCTAGTCATGAAG	TGTGGAATGCAACTCTGATG	91%
s6_422	Nitrate transporter	TGTTTGCACATCAGGAAC	AAATCGCTCCAACAATGTG	91%
s6_27894	Purine nucleoside permease	AGCTGACTCATATGGTAAG	TGATGGGCATTTTGTCGAAC	117%
s6_34	Nitrate reductase	TGATGATGTATTCGGGTTTG	TCAGACAAGCCTTCGGAAAATC	99%
s6_5551	Glutamine synthetase	TCGCTGAGTATGTATGGTTG	GTTCCAAGTACGAAGACCTT	92%
psbA	Photosystem II protein D1 precursor	TCAGCACCTGTTGTTGCAG	AATACTCCAGCTACTCCTAG	101%
s6_35311	SWEET 1	GTAATGTTCTGAGCATTGCC	AATCCGACTGAGAGGTAGAA	103%
Cyclophilin	Cyclophilin	TGCTTGAGGGTAAAGTTCTC	CAACCCCTTCATTTCAAAGG	93%

Table B1 Primer sequences and their primer efficiencies used in qPCR experiments.